TRAFFIC CONTROL STRATEGY FORMULATION AND OPTIMIZATION ENABLED BY HOMOGENOUS CONNECTED AND AUTONOMOUS VEHICLE SYSTEMS

A DISSERTATION SUBMITTED TO THE GRADUATE DIVISION OF THE UNIVERSITY OF HAWAIʻI AT MĀNOA IN PARTIAL FULFILLMENT OF THE REQUIREMENTS FOR THE DEGREE OF

DOCTOR OF PHILOSOPHY

IN

CIVIL ENGINEERING

DECEMBER 2017

By

Qiong Wu

Dissertation Committee:

Guohui Zhang, Chairperson
Panos D. Prevedouros
A. Ricardo Archilla
Zong Z. Tian
Yingfei Dong

ACKNOWLEDGEMENTS

I would like to express my sincere gratitude to my advisor, Dr. Guohui Zhang, for his enthusiastic encouragement, continuous professional and generous support through my entire Ph.D. study. It has been my great honor to work with Dr. Guohui Zhang, and I benefited a lot from his insightful advice not only on my scientific research and career development in the field of transportation but also outlook on life. His guidance and professional style will remain with me as I continue my career.

I would like to express my sincere thanks to Dr. Panos D. Prevedouros, a member of doctoral committee for his detailed comments on my dissertation draft. I greatly appreciate his consistent support for my various scholarship applications as well as my Ph.D. study.

I am also thankful to Dr. A. Ricardo Archilla, Dr. Zong Z. Tian and Dr. Yingfei Dong, for their instrumental recommendation on my dissertation and for serving on my dissertation committee. I benefited a lot from their valuable instructions provided in the completion of my dissertation.

Special thanks to my supervisors at SSFM International Inc., Ms. Susan LeBrun and Ms. Juanita Wolfgramm, and my colleague Ms. Lulu Chen, for their advice during my internship there, giving me valuable experience in the field of transportation industry and enlightening me that the industry is ideal to develop my career.

I wish to express my thanks to my friends in the Department of Civil Engineering, University of New Mexico, and the Department of Civil and Environmental Engineering, University of Hawaii at Manoa, for their strong support in life. Special thanks firstly go to Dr. Jielin Pan, Dr. Su Zhang, Dr. Susan Bogus Halter, for their advice and support during my Ph.D. study in New

Mexico. I am grateful to my friend, Dr. Liang Shi, who provided me great support during my relocation to Hawaii. I particularly acknowledge Mr. Zhenning Li, Dr. Hao Yu, Mr. Cheng Wang and Dr. Shu Yang for their extensive contributions to my knowledge of intersection control systems and VISSIM-based simulation platform development. Their constructive advice is indispensable to the completion of my dissertation. I am also grateful to my friends, Jialin Wang, Wenqian Gu, Hongji Du, Qian Zhang, and Juan Qin for their generous support.

I would like to express my appreciation to my parents and my little brother for their invaluable support and love. Finally, but definitely the most, I am extremely grateful to my husband, Dr. Cong Chen, for his persistent support all the time.

ABSTRACT

Traffic congestion has become a serious issue all over the world due to the rapid increase in population and traffic demands. The advances in Connected and Autonomous Vehicles (CAVs) have demonstrated a potential to improve traffic mobility and safety performance at intersections. An advanced intersection control system, CAV-enabled Intersection Management Mechanism (CAVIMM), was developed to ensure traffic safety and operation efficiency at intersections without using any traditional traffic signals. CAVIMM releases vehicle movement restrictions of dedicated turning lanes in traditional signalized intersections by enabling left-turn, straight and right-turn movements from any lane of each approach. CAVs approaching intersections are controlled by an Intersection Control Center (ICC) using communication between vehicles and intersection infrastructures (V2I).

Due to the increasing number of potential conflict areas introduced by CAVIMM, there is a need for a precise vehicle trajectory model, which helps the ICC to better control CAVs passing through the intersection. A trajectory coordination model, Temporal-Spatial Dimension Extension-based Trajectory Coordination Model (TSDTCM), was developed to account for CAV widths and lengths. Based on vehicle trajectory formulation, various algorithms for determining conflicting CAVs passing sequences were developed. The First-Come-First-Serve (FCFS) algorithm is the most widely used one due to its simplicity; however, it may not be the optimal one in terms of minimizing total intersection delay or maximizing overall throughput. Therefore, two CAVIMM systems using FCFS and an optimal algorithm, Discrete Forward-Rolling Optimal Control (DFROC) algorithm, were developed in this study.

The performance comparisons between CAVIMM systems and traditional signal control were conducted at a 4-leg intersection through VISSIM-based simulations. Their performance under

different scenarios with various traffic volumes and intersection configurations were evaluated. Experimental results indicated that the CAVIMM system outperformed traditional traffic signals in terms of reducing total traffic delay at intersections. At the 100% level of volume, the total traffic delay was reduced by more than 90% for all scenarios of CAVIMM system. Several factors, including intersection configurations, traffic volumes, algorithms of determining CAVs' passing sequences and the sizes of buffer zone, directly affected the CAVIMM performance with respect to the reduction of the total traffic delay.

TABLE OF CONTENTS

LIST OF TABLES

LIST OF FIGURES

CHAPTER 1. INTRODUCTION

1.1 Background

Traffic congestion due to rapid increase of population and traffic demand has become a serious issue affecting the standard of living in urban settings. According to Texas A&M Transportation Institute (TTI) (2013), the people living in 498 urban areas in the U.S. traveled 5.5 billion more hours and purchased 2.9 billion extra gallons of fuel for a congestion cost of $121 billion. Among several main causes of congestion, delay at intersections with signals accounts for an estimated 5% to 10% of all traffic delay or 295 million vehicle-hours of delay on major roadways alone (Federal Highway Administration, 2012). The most common traffic control measure at intersections is signal control, which may manage the movement of as many as 100,000 vehicles per day at a busy intersection in a typical urban area (FHWA, 2008). Therefore, improvement in traffic signal control at intersections can significantly benefit the overall transportation network especially for urban areas.

One source of delay at signalized intersections is driver reaction-related delay. In terms of traffic safety, 90% roadway crashes are caused by human errors (NHTSA, 2012). Autonomous vehicles (AVs), which are partially or fully self-operated without human intervention, have the potential to reduce the negative impacts of human errors on traffic delay and safety at intersections. AVs are capable of self-driving in real-world highway systems and performing complex tasks such as merging, weaving, and driving through intersections (Li et al., 2013b). According to the U.S. Department of Transportation (USDOT) Research and Innovative Technology Administration (RITA), 81% of all vehicle-involved crashes can be avoided or mitigated based on connected vehicle technologies. AVs can be partially or fully self-driven, and have attracted significant research attention recently. By assisting and making decisions for drivers and allowing communications among AVs as well as between AVs and transportation infrastructure, the application of AVs can has the potential to maximize the efficiency of intersections and thus improve traffic mobility by providing smooth traffic flow as well as reducing intersection-related crash rates simultaneously. Although the benefits of AVs can be expected, maximizing performance of AVs requires increasing efforts in order to take fully advantage of AV capabilities.

Connected Vehicle (CV) technology enables communication and information exchange among vehicles (V2V) and between vehicles and infrastructure (V2I) to provide a safer, higher mobility and greener driving environment (Genders et al., 2015). However, human factors are still posing significant influence in such driving environment by adjusting behaviors according to communication among vehicles, which may compromise the benefit of CV technology. AVs were proposed to minimize the negative influence of human factors (Alonso et al., 2011). With the help of CV techniques, AVs enable smarter self-driving which benefit the entire transportation system. Based on seamless V2V and V2I communications as well as autonomous driving technologies, traffic management and control could be revolutionized. The CAV-enabled traffic system has demonstrated great potential to mitigate congestion, reduce travel delay, and improve traffic mobility and safety performance. Existing studies (TTI, 2013) indicate that traffic lights will be eliminated and 75% of vehicles will be AVs by 2040. However, one should note that the current research regarding CAV-enabled system management and control is still at an early stage.

1.2 Problem Statement and Research Objectives

In the previous studies, many intersection management strategies of CAVs have been proposed and verified to be more effective in improving the efficiency of intersection than existing traffic signal through simulation (e.g. Alonso et al., 2011; Carlino et al., 2013; Dresner and Stone, 2005; Yan et al., 2014). For example, the reservation-based system, Autonomous Intersection Management (AIM), which was first proposed by Dresner and Stone (2005), is widely used to manage CAVs at intersections. Vehicles and intersections are viewed as agents in a multi-agent system. Vehicles are controlled by a virtual intersection manager, which assigns right-of-way for each vehicle to avoid any collision between them. This helps significantly reduce traffic delay. However, the whole intersection is reserved for conflicting vehicles passing through in sequences without conflicts. Thus, the intersection area is not efficiently utilized. Kamal et al.(2015) presented a coordination scheme of AVs at intersections without using any traffic signals, which was evaluated through numerical simulation under different traffic flow at a test intersection consist of both multiple-lane and single-lane approaches. The results showed that the proposed coordination scheme significantly improved intersection performance compared with the traditional traffic signal. However, the proposed scheme could only coordinate two conflicting vehicles from each lane at a time when the two vehicles were already very close to the intersection, which is impractical for analyzing busy traffic. Although the performance of the reservation-based system and correlated policies at intersections are better than other types of traffic control schemes (Wu et al., 2010), starvation issues still exist when the traffic demand is fluctuating (Li et al., 2013a). Therefore, the management of CAVs around intersections still needs further investigation in terms of improving the mobility and reducing traffic delay.

The goal of an advanced intersection management system is to allow vehicles to pass through the intersection safely and smoothly. With V2V and V2I communications, information of all CAVs, including speed, acceleration/deceleration rate, location and movements within the intersection, can be easily obtained before vehicles entering the intersection. Trajectories of all approaching vehicles can be predicted before entering the intersection based on the obtained vehicle information, helping identify potential collisions among all approaching vehicles.

Therefore, to improve traffic mobility by providing smooth traffic flow as well as reducing intersection-related crash risk, the CAV-enabled Intersection Management Mechanism (CAVIMM) was proposed in this study. It developed based on a precise vehicle trajectory formulation model, Temporal-Spatial Dimension Extension-based Trajectory Coordination Model (TSDTCM), with vehicle width and length elements taken into account, helping better use limited intersection temporal and spatial resources. Then the order of the assignment of intersection temporal and special resources (right-of-way) was addressed by the Discrete Forward-Rolling Optimal Control (DFROC) model to maximizing intersection capacity and operational efficiency.

1.2.1 Trajectory coordination model

With the above definitions and statements, the safety issue can be addressed by identifying the potential conflict area for any two approaching vehicles and preventing conflicting vehicles arriving in this area at the same time. Intersection temporal and spatial resources are not fully utilized through traditional intersection control methods, including signals, stop signs, and yield signs. In most previous studies about CAV-enabled intersection management (e.g., Au et al., 2015; Azimi et al., 2014; Wuthishuwong and Traechtler, 2013), trajectory-based approaches were used, where certain time-space resources of the intersection was reserved for vehicles to cross the intersection based on the predicted vehicle trajectories. The safety issue can be addressed by avoiding potential collisions through coordinating all predicted trajectories. In the analyses of trajectory prediction in the previous studies, vehicles were considered as points without taking vehicle width and length into consideration, making the process of vehicle crossing intersection imprecise. Moreover, it should be noted that none of these previous studies included systematically formulated model to identify potential collisions in the intersections. Therefore, a more precise trajectory prediction system with consideration of vehicle widths and lengths is needed to make better utilization of limited intersection temporal and spatial resources.

1.2.2 Passing sequence optimization algorithm

The passing sequence of conflicting vehicles has significant impacts on intersection resource utilization and affects intersection operation efficiency. Based on vehicle trajectory formulation, various CAV intersection control strategies have been developed. The First-Come-First-Serve (FCFS) is the most widely used strategy in CAV-enabled management due to its simplicity and interpretability. In a FCFS-controlled intersection system, the passing sequence is conducted by the Intersection Control Center (ICC) according to the sequence of approaching vehicles. However, FCFS may not always provide the best passing sequence of conflicting CAVs for minimizing intersection total delay or maximizing overall throughput. Therefore, many previous studies have been conducted for developing an optimal algorithm to achieve specified goals, such as minimizing total traffic delay or the number of stops. In this study, an algorithm was also proposed aimed at reducing total intersection traffic delay through the coordination of predicted CAV trajectories.

1.2.3 Performance evaluation

Due to the complexity of field implementation, most researchers used traffic simulations to validate their developed strategies for management of CAVs at intersections (Li et al., 2013a). Simulation-based investigation on traffic system operations provides a cost-effective and risk-free means of exploring optimal management strategies, identifying potential problems, and evaluating various alternatives. In terms of performance evaluation, most previous studies used independently developed simulation software. Results from different studies cannot be easily compared to each other if there is no uniformed platform for evaluation.

This study developed a VISSIM-based simulation platform to enable an innovative autonomous intersection control mechanism and optimize CAV operations at intersections without signal lights. Five objectives in this research are:

1) Proposing an advanced intersection management mechanism
2) Formulating intersection temporal and spatial resources
3) Developing CAV trajectory coordination models
4) Proposing optimization algorithm for CAV passing sequences
5) Developing a standard platform for performance evaluation of the proposed intersection management mechanism

1.3 Dissertation Organization

The remainder of this dissertation is organized in the following manner. Chapter 2 presents a comprehensive review of previous studies that are relevant to this dissertation. First, traffic safety and operation efficiency issues at intersections are introduced and the popular methods to address those issues are summarized. Then, contemporary applications of CVs, AVs, and CAVs in the real world and their impacts on current transportation system are introduced. Third, the significant changes of intersection management due to CAV implementation are comprehensively examined. In this Chapter, various intersection management strategies to alleviate traffic congestion are summarized, including pre-timed signal control, actuated signal control, the CAV-enable intersection control, as well as other related control schemes. In terms of CAV-enable intersection control, the most widely used control systems are reviewed, including centralized and decentralized intersection control systems. The fundamental system structures of different intersection control systems are analyzed and compared, and the major issues regarding vehicle trajectory formulation in previous studies are identified. Additionally, the peer methods of intersection operation efficiency optimization under CAV environment are evaluated, including FCFS, discrete event dynamic system, and various optimization algorithms. Finally, the methods of evaluating performance of intersection control strategy are examined and summarized, and the major issue regarding the need of a standard evaluation platform for conducting comparisons among various intersection control strategies is identified.

Chapter 3 presents the methodological framework logic, design and specifications of the CAV-enabled Intersection Management Mechanism (CAVIMM) proposed in this dissertation. The major aim of this CAVIMM is to act as an advanced intersection control system to lead CAVs to pass through the intersection safely and smoothly. CAVIMM is a centralized intersection control system where all movements of approaching CAVs are globally controlled by an Intersection Control Center (ICC). The area around intersections under the control of the ICC is defined in this Chapter. Based on the assumptions made for CAVIMM development, the temporal and spatial resources of a 4-leg intersection with three lanes for each approach are formulated. By releasing vehicle movement restriction by dedicated turning lanes in traditional intersection configurations, the CAVIMM system enable both going straight and turning movements at any lane through four approaches.

Using the intersection formulation model proposed in Chapter 3, the traffic safety and operation efficiency issues are addressed in Chapters 4 and 5. Chapter 4 shows the development of a trajectory coordination model, TSDTCM, to precisely formulate real vehicle trajectories with consideration of vehicle width and length information. Different from the previous studies where vehicle trajectories were predicted as lines or chains of cubes within intersections, in this dissertation, all CAV trajectories are formulated in a 3-dimention domain with the addition of travel time as the third axis. Then, the conflicting trajectories within intersections are identified for any two approaching CAVs. A case study of two potentially conflicting CAVs in a 4-leg intersection is illustrated through TSDTCM. The issue of traffic safety can be addressed by ensuring any conflicting CAVs arrive at potential conflict areas successively, which is also defined as the set of constraints for operation efficiency optimization of the intersection.

Chapter 5 presents the development of algorithms for determining the passing sequence of conflicting CAVs at intersections. The FCFS algorithm is employed based on TSDTCM in CAVIMM, which is the most widely used algorithm in the previous intersection management systems, due to its advantage in logic simplicity and interpretability. The logic of FCFS and its implementation in CAVIMM are discussed. However, FCFS may not be the best approach in terms of minimizing total intersection delay. Then an algorithm, Discrete Forward-Rolling Optimal Control (DFROC), is developed in this study, aiming to reduce the total intersection traffic delay by using the TSDTCM developed in Chapter 4.

Chapter 6 presents the development of a VISSIM-based simulation platform for CAVIMM performance assessment in terms of improving intersection operation efficiency. The proposed CAVIMM is evaluated at a 4-leg intersection with three lanes for each approach, and compared with actuated signal control in the same intersection geometric layout. Due to the different intersection configurations between the signalized intersection and CAVIMM controlled intersection, a new CAVIMM-based model, CAVIMM-EC, is developed using the same configuration as the signalized intersection. The potential conflict areas in CAVIMM-EC are identified and summarized using TSDTCM. All intersection control systems with different configurations are developed using FCFS and DFROC under different sizes of buffer zone, respectively. All control mechanisms are evaluated in the developed VISSIM-based simulation platform under different traffic volume scenarios. Evaluation criteria proposed in Highway Capacity Manual (HCM) are introduced. The comparison among different mechanisms are conducted and discussed in this Chapter.

Finally, Chapter 7 presents the conclusions of this dissertation and the recommendations for future research.

CHAPTER 2. LITERATURE REVIEW

2.1 Intersection-Related Problems in Traffic Safety and Operation Efficiency

Intersection-related traffic delay accounts for nearly 5% to 10% of total delay on major roadways (FHWA, 2012). In addition, due to control interruptions to traffic flow progression by intersections, crashes involving two or more vehicles, such as right-angle and rear-end crashes, are more likely to happen around intersections.

As shown in the statistics released by the Centers for Disease Control and Prevention (2010), traffic crashes have become the leading cause of death for the age group encompassing 4 year-old to 34 year-old in the U.S.. Two-thirds of urban Vehicle Mile Traveled (VMTs) are on signalized roadways (Federal Highway Administration, 2010). Intersection-related crashes, including right-angle, rear-end, and left turn crashes, have resulted in significant injuries and fatalities (Chen et al., 2015; Werneke and Vollrath, 2012). Therefore, a great research effort have been made on identifying the contributing factors on intersection-related crash frequency and severity, including roadway geometric characteristics, control interruptions and human factors, etc. (Abdel-Aty and Keller, 2005; Chen et al., 2016; National Highway Traffic Safety Administration, 2010; National Safety Council, 2011; Retting et al., 2003). Obeng (2008) analyzed contributing factors for crashes occurring at intersections with signal control and found that using three-point seatbelt can significantly reduce injury severities. Zhang et al. (2014) identified a variety of factors, including driver gender and age, vehicle types, and traffic situations, having significant impacts on intersection-related crash severity. Bédard et al. (2002) found that vehicle turning and crossing movements have the potential to result in crashes leading to severe injuries. Moore et al. (2011) developed a mixed logit model to analyze contributing factors affecting injury serveries at intersections. Due to the underestimation of complex traffic situation, drivers are more likely to result in more severe injuries at intersections. Wu et al. (2015) estimated two multinomial logit models for teenage and adult drivers, respectively, to analyze injury severities in crashes occurring at and influenced by intersections in New Mexico. Chen et al. (2012) analyzed the severity levels of intersection-related crashes using Logistic regression models. Zhang et al. (2014) employed ordered Probit models for crashes occurring at intersections in the U.S.. Wu and Zhang (2016) quantified the impacts of alcohol and non-alcohol influenced driver behavior as well as geometric and environmental characteristics on driver injury severities at intersections. The previous studies identified a variety of human errors as the contributing factors for intersection-related crashes.

Furthermore, as reported in Traffic Safety Facts (NHTSA, 2015), a total of 48,923 vehicles got involved in crashes resulting in fatalities in 2015 in the U. S., of which 13,846 vehicles (28%) were involved in crashes occurring at or influenced by intersections. Intersections experience much higher crash rates than roadway segments in the transportation network. Crash rates increase as the total number of intersections per mile along an arterial increases (Chen et al., 2017). Therefore, it is of importance to investigate the significant causal factors for intersection-related crashes so that cost-effective countermeasures can be proposed to reduce intersection-related crash rates. Retting et al. (2003) investigated crashes occurring at intersections with stop signs, and it was found that about two-thirds of stop sign violation crashes were caused by inability or failure to see approaching traffic. Countermeasures including changing intersection design and improving intersection sight distance were recommended to improve safety performance of intersections with stop sign. Poch and Mannering (1996) identified crash risk at signalized and un-signalized intersections through negative binomial models. Their results were helpful for intersection risk reviewers to locate the intersection approach where the elements known to increase crashes presented, and to determine the feasibility of revising the approach.

2.2 General CAV Analysis at Intersections

2.2.1. Connected vehicle

CV research is sponsored by USDOT to leverage the potentially transformative capabilities of wireless technology to make ground transportation safer, smarter and greener. If successful, CVs could enhance the mobility and quality of the way Americans travel and help to reduce the negative environmental impacts of ground transportation (USDOT, 2011). CV technologies aim to tackle some of the biggest challenges in ground transportation industry (USDOT, 2011):

1) Safety: According to the NHTSA, there were 5.6 million crashes in 2013. The number of traffic crash fatalities was falling but still accounted for 32,719 deaths. CV technologies have the potential to provide drivers more accurate alternatives to alleviate crash potential, and to significantly reduce the number of lives lost each year.
2) Mobility: According to the TTI (2013), U.S. highway users wasted 6.9 billion hours stuck in traffic in 2014. CV mobility applications will enable system users and system operators to make smart choices that reduce travel delay.
3) Environment: According to TTI (2013), the total amount of wasted fuel topped 3.1 billion gallons in 2014. CV environmental applications could give motorists the real-time information they need to make “green” transportation choices.

In August 2014, NHTSA announced that it would begin taking steps to enable V2V communication technology for light vehicles and is now working on corresponding regulations demanding its mass installation in all new light vehicles in the coming years (Ilgin Guler et al., 2014). In May 2015, the USDOT announced to accelerate the deployment of CVs. In 2015, the FHWA released a V2I guidance document to assist transportation managers and operators interested in adapting their traffic signals and other roadside devices so they are compatible with the new CVs (FHWA, 2014). In December 2016, USDOT issued a proposed rule that would advances deployment of V2V technology to prevent crashes by enabling V2V communication technology on all new light-duty vehicles (NHTSA, 2016).

2.2.2. Autonomous vehicle

An AV, also known as driverless car, self-driving car and robotic car, is capable of fulfilling the main transportation capabilities of a traditional car. It is capable of sensing its environment and navigating without human input (Durbin, 2015). Advanced control systems interpret sensory information, which is obtained with the help of Radar, LIDAR, GPS, and computer techniques (Pavlic and Passino, 2009), to identify appropriate navigation paths, as well as obstacles and relevant signage (Martínez-Barberá and Herrero-Pérez, 2014).

The field of intelligent vehicles is rapidly growing all over the world in the diversity of both applications and research. In the U.S., autonomous driving is under extensive study for safety and energy-saving purposes among governmental agencies, universities and industrial firms.

2.2.3. Connected and Autonomous Vehicle (CAV)

Enabling V2V and V2I communications has been expected to provide a safer, higher mobility and greener driving environment (Genders et al., 2015). However, human factors are still posing significant influence in such driving environment, which may compromise the benefit of connected vehicles. AVs were proposed to minimize the negative influence of humans (Alonso et al., 2011). With the help of CV technique, AVs enable smarter self-driving which could benefit the entire transportation system.

With the increased implementation of communication technology and development of the AVs, CAV-enabled traffic systems have attracted a growing attention to tackle traffic congestion problems. Based on seamless V2V and V2I communication as well as autonomous driving technologies, and with the recent advancement in CV/AV research and regulations, traffic management and control may be revolutionized.

2.3 Intersection Management

2.3.1. Centralized and decentralized intersection control system

Based on existing approaches of vehicle right-of-way assignment, two major traffic management strategies have been investigated for CAV-enabled traffic system: centralized control system and decentralized control system.

1) Centralized intersection control system

For the centralized control mechanism, there is an intersection management center to manage the whole intersection, and all vehicles travel through intersections under the control of this center. Dresner and Stone (2005b) developed a multi-agent system to regulate AVs at intersections. It is a reservation-based centralized control approach, where all approaching vehicles sent requests to the intersection management center to reserve specific time-space resources of the intersection for traveling through it safely. The center decided if the requests should be approved or not based on intersection occupancy status. If the intersection was occupied by vehicles with pre-approved requests, the requests of new approaching vehicles were denied. In further study by Dresner and Stone (2008), they improved this system to a more comprehensive one and the performance was evaluated under different scenarios by their self-developed simulator. The results showed that revised AIM was effective in reducing delay. Similarly, Fajardo et al. (2012) explored an Automated Intersection Control protocol which was also based on a reservation system. The performance of this system was evaluated through microscopic simulation. The experimental results indicated significant improvements in respect to reducing total delay compared with a traditional traffic signal. In addition, Zohdy et al. (2012) proposed a new tool, Intersection Management using Cooperative Adaptive Cruise Control (iCACC), to manage vehicle trajectories so that vehicles can cross intersection safely with minimized delay. A vehicle trajectory is divided into three parts: Zone 1, Zone 2 and Intersection Box. All vehicles accelerate to the maximum speed when they reach the end of Zone 1. Then the iCACC system manages the speed profile of each vehicle in Zone 2 so that they can traverse the Intersection Box using the maximum speed without any conflicts with the other vehicles. Therefore, the main objective of iCACC is to minimize the speed changing time in Zone 2. The effectiveness of this algorithm is tested by simulating a single 4-legged intersection under 16 scenarios, and the results show that the saving in delay is in the range of 91 and 82 percent compared with traditional signal control.

2) Decentralized intersection control system

Rather than centralized intersection control system, other studies focused on control mechanisms enabling information communication and right-of-way negotiation between vehicles. If vehicles are self-controlled by communications with other AVs (Lückel et al., 1999; Naumann et al., 1998), it is named as decentralized control system (Carlino et al., 2013; Makarem and Gillet, 2013; Neuendorf and Bruns, 2004). All vehicles are managed by proposed protocols based on communications among vehicles instead of between vehicles and a control manager.

For example, VanMiddlesworth et al. (2008) proposed an intersection mechanism based on peer-to-peer communication for low-traffic intersections. They found that the proposed mechanism significantly outperformed traditional stop signs in terms of vehicle waiting time. In the study of Dresner and Stone (2005b), a control mechanism of AVs at intersections was developed allowing vehicles to traverse intersections without surrendering control to any centralized management center. Carlino et al. (2013) proposed a market-based pricing mechanism which allowed vehicles to be self-organized in a way that prioritized higher-valued trips. By introducing intersection auctions in a micro simulator framework, drivers were enabled to express their preferences of time and cost.

Both centralized and decentralized control systems were found effective in reducing traffic delay and improving traffic mobility at intersections compared to traditional signal control under different scenarios. In the study of Wu et al. (2010), a reservation-based centralized control system was found to be superior to a decentralized one by taking more advantage of intersection capability after simulating both control systems in their self-developed simulator. Therefore, a centralized control mechanism was employed in this study to lead CAVs travel through an isolated intersection.

2.3.2. Collision avoidance system

The two major objectives of an advanced intersection management system are ensuring safety and improving operational efficiency. In previous studies, the safety issue could be addressed by predicting vehicle trajectories to identify the potential collision. The levels of intersection time-space resource utilization partially affect intersection efficiency. Based on the movement information sent to the intersection control center by approaching vehicles, the time and space a vehicle needs to travel through the intersection can be predicted. If there are no other vehicles traversing the same space at the same time (or within a limited time period), the vehicle is free to cross the intersection. Otherwise, certain countermeasures should be implemented to avoid collision.

A significant amount of intersection time-space division methods have been developed:

1) Grid-based trajectory prediction

In this method, the intersection is divided into an *n* by *n* grid of tiles, where *n* is the granularity of the proposed control strategy, as shown in Figure 2.1. When a vehicle approaches the intersection, the driver agent (robot) representing the vehicle communicates with the intersection manager. The basic mechanism of autonomous intersection management (AIM) is that the driver agent sends requests to the intersection manager to reserve certain time-space resource for traversing the intersection based on the vehicle's estimated arrival and departure time. The intersection manager checks what and how many resource (tiles) will be occupied by the requesting vehicle, and identifies whether these requested tiles have already been reserved by other vehicles. If the tiles are already reserved, the request is rejected; otherwise, the request is approved and the reservation is made. The vehicle agent is notified by the intersection manager regarding the final decision of the request. The instruction of travel is sent to the vehicle agent by the intersection manager with the approval notice (Au et al., 2015, 2012a; Azimi et al., 2014; Dresner and Stone, 2008, 2005a, 2004; Jin et al., 2012a; Li et al., 2013b).

This trajectory prediction method was the first attempt to better utilize space resources of an intersection. However, it fails to consider the time-related feature along with the space. For example, no matter how long the previous vehicles use the reserved space, this approach does not allow a conflicting vehicle to make a reservation until the previous vehicles with approved request passing the intersection, indicating that the resources of the intersection are not fully utilized. Therefore, many studies (Abdelhameed et al., 2014; Ammoun and Nashashibi, 2009; C. Wuthishuwong and Traechtler, 2013) further formulated trajectories through a three-dimension model.

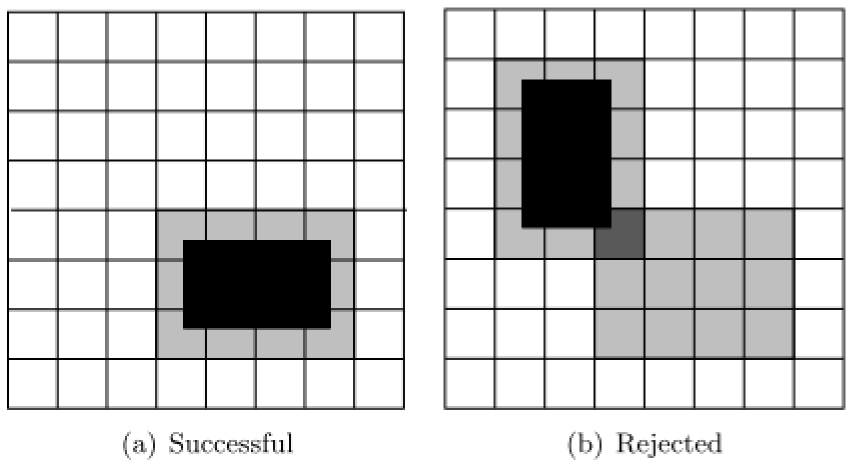

Figure 2.1 Grid-based Collision Avoidance System (Dresner and Stone, 2008)

2) *Time-space-based linear trajectory prediction*

Other studies further implemented a three-dimension space to identify potential collisions at intersections (Abdelhameed et al., 2014; Ammoun and Nashashibi, 2009; C. a Wuthishuwong and Traechtler, 2013). The space of an intersection is defined on the horizontal plane, and the third dimension represents time. Then the vehicle trajectories can be illustrated by curves (turning movements) or lines (straight movements) in three-dimension space, and there will be a collision if any two trajectories intersect within a limited space (safety buffer zone). This approach allows vehicles to reserve the same space at different time periods, and therefore better utilizes intersection resources than the grid-based method above (Abdelhameed et al., 2014; Bento et al., 2013).

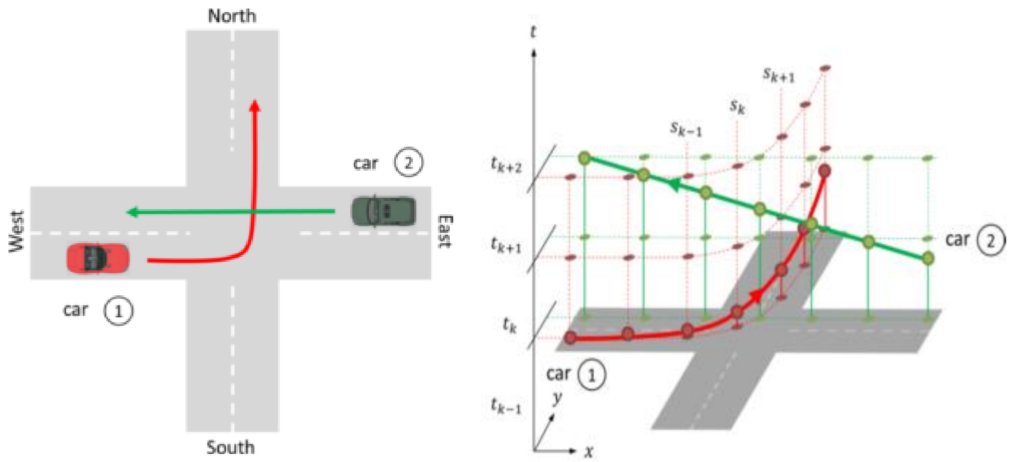

Figure 2.2 3D View of Time-Space Based Collision Avoidance System (C. Wuthishuwong and Traechtler, 2013)

3) Time-space- based grid trajectory prediction

Several studies combined these two methods and proposed a three-dimension grid-based approach for collision check (Azimi et al., 2014; Bento et al., 2012; Fang et al., 2013), where the space of intersection is represented by the *n* by *n* grid of tiles on the horizontal plane and the vertical axis represents time (Figure 2.3). Then the trajectories are illustrated as a chain of cubes instead of curves or lines in the second approach. If a time-space trajectory passes through a time-space cube, this cube is called a used time-space cube; otherwise, it is called an unused time-space cube.

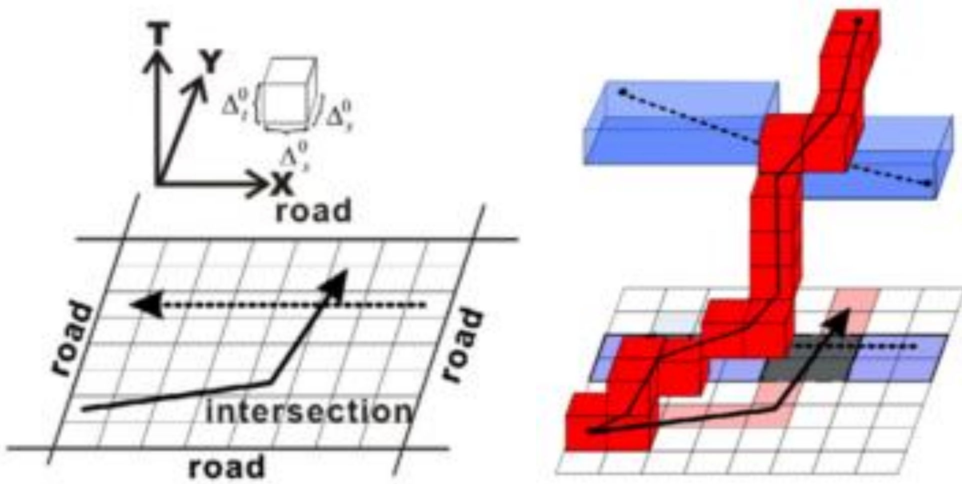

Figure 2.3 3D View of Time-Space Based Collision Avoidance System (Fang et al., 2013)

4) Other methods

A few studies focused on CV techniques such as sensor detection in a decentralized intersection control system (Alonso et al., 2011; Au et al., 2012a; Hu et al., 2004). Vehicles equipped with sensors and actuators could be autonomously driven using a decision algorithm, which is designed for solving priority conflict resolution at the intersection. The intersection control center is no longer needed in this kind of control systems. However, this method can only detect surrounding environment and potential conflicts are identified when vehicles nearly arrive at the conflicting areas.

All approaches mentioned above failed to formulate vehicle trajectories as a smooth series of movements (not a chain of cubes) and also doesn't consider vehicle length or width (not an arc or a line). In order to fill this research gap, a three-dimension based autonomous intersection control model is proposed for trajectory prediction formulation.

2.3.3. Intersection control mechanism

Nearly 5% to 10% of total delay on major roadways is intersection-related traffic delay (FHWA, 2012). In addition, crashes involving two or more vehicles, such as right-angle and rear-end accidents, are more likely to happen around intersections. In the past decades, a great many studies have been conducted to explore methods for intersection management improvement to provide smooth traffic flow as well as reducing intersection-related crash rates. According to the level of automation in vehicle composition, traffic control strategies at intersections can be classified into three categories:

1) Traditional intersection control

The traffic signal, which is the main traffic control that has been implemented worldwide, was first developed in the early 1900s with the goal to prevent crashes and improve traffic mobility by alternatively assigning right-of-way (Federal Highway Administration, 2008). The detailed control methods can be largely classified into time-of-day, fixed-time control and actuated control methods (Chang and Park, 2013). Fixed-time signal control, which utilized a signal timing plan set by an administrator, is a major signal control method since it is easy to implement (Gordon et al., 2005). Guberinic and Senborn (1978) proposed a method to determine the optimal sequences of fixed-time signal plans in order to decrease traffic delay. The implementation of traffic detectors at intersections has attracted abundant research to improve signalized intersection efficiency by dynamically adapting traffic signals based on real-time traffic (actuated signal control). Compared to fixed-time signals, actuated signal plans have demonstrated great improvement to reduce traffic delay at signalized intersections. Shi et al. (2015) proposed an optimization algorithm of real-timing signal control by adjusting average utilization rate of green time automatically, and simulation results indicated that the proposed algorithm outperformed the fixed timing plan in terms of reducing average delay and queue lengths. Lee et al. (2005) used genetic algorithms to optimize real-time adaptive signals, and the results showed that the proposed genetic control outperformed fixed-time signal plans in all scenarios in terms of total delay. Bari et al. (2003) developed a real-time optimization model for two coordinated signalized intersections considering traffic scenarios with different types of vehicles, and the proposed model could help to minimize the vehicle queue lengths in urban areas.

2) New adjusted intersection control

In a conceptual Intelligent Transportation System (ITS), vehicles are progressed through signalized intersections under the automatic control of road-side and in-vehicle infrastructure (Au et al., 2015; Bento et al., 2013; Clement et al., 2004; Glaser et al., 2010; Ilgin Guler et al., 2014; Li et al., 2014). If a proportion of traveling vehicles are CVs or AVs, the coordination of vehicles with new techniques and the advanced signal control plans considering 'smart vehicles' are also analyzed (Li et al., 2014; Onieva et al., 2015). Agbolosu-Amison et al. (2012) investigated the benefits of a dynamic gap-out feature at an actuated signalized intersection under the CV environment. If a CV was approaching the intersection, the gap-out would dynamically applied based on the arrival time sent by the CV. The performance of this system with 100% penetration rate of CV deployment was examined using a simulation-based test-bed, and the results indicated that this dynamic gap-out actuated signalized intersection control system reduced approximately 12.5% of total delay compared to existing regular gap-out.

3) Autonomous intersection control

In this scenario, all vehicles crossing the intersections are assumed to be CVs, AVs or CAVs. As mentioned in the section of 2.3.1, according to the means of assigning right-of-way to approaching vehicles, autonomous intersection control was classified into two major strategies: centralized in control system (Dresner and Stone, 2005a, 2004; Zohdy et al., 2012) and decentralized control system (Alonso et al., 2011; Carlino et al., 2012; Wu et al., 2010).

2.3.4. Passing sequence algorithm

1) First-Come-First-Serve algorithm

The First-Come-First-Serve queueing algorithm has overcome some operational issues identified in previous studies (Au et al., 2011), and it has been widely used in AV's Intersection Management (Dresner and Stone, 2008; Li et al., 2013a). The major concept of FCFS is that each CAV sends a request to the intersection control center for passing through the intersection. The intersection control center decides if the request should be approved according to their arrival time. If two conflicting CAVs sent the requests, the one which arrives at the intersection area earlier has higher priority to pass through the intersection (Zohdy and Rakha, 2014). In the study of Fajardo et al. (2012), the performance of a simulated intersection in two scenarios: a FCFS control and a traditional signal control were evaluated using Synchro. They concluded that compared with traditional signal control, the FCFS control dramatically reduces the traffic delay. Some studies developed dynamic systems based on FCFS algorithm. Discrete Event Dynamic Systems (DEDS) were modeled in the study of Abbas-Turki et al. (2012). DEDS employed Petri Nets (PN), which mathematical equations were derived, to describe the dynamic of the studied system. Dioid algebra was used for analyzing and controlling DEDS based on FCFS. The simulation results showed that DEDS was efficient for an isolated intersection.

2) Optimization algorithm

Many algorithms have been developed with different objectives, such as minimizing total delay or minimizing total number of stops, and the optimization results can be calculated to maximize intersection efficiency. Jin et al. (2012b) optimized the scheduling of vehicle departure time in their study. In the study of Ilgin Guler et al. (2014), the objective function would have solutions when the delay and the number of stops were minimal. Minimum overlap of vehicular trajectories was set as the objective function in many previous studies (Lee et al., 2013; Lee and Park, 2012; Makarem and Gillet, 2013). A two-tier hybrid multi-objective optimization algorithm was proposed to plan vehicle and pedestrian turning movement directions in some studies (Fang et al., 2013). Zhu and Ukkusuri (2015) developed a linear programming formulation for autonomous intersection control optimization by relaxing the nonlinear constraints with a set of linear inequalities.

Those techniques are sequentially invoked to solve the problem in the control logic. Note that the optimization techniques do not always find feasible solutions, in which case there must be a special mode conducted to face the failure of optimization.

2.4 Traffic Simulation

Due to the complexity of field implementation, most researchers used traffic simulation to validate their developed strategies for CAV control. Some researchers developed software for simulations that had their own interfaces (Dresner and Stone, 2005a, 2005b; Jin et al., 2012a). However, simulation tools developed by the authors of those studies were used in evaluation process, making the results hard to compare to each other. Some simulation platforms were conducted under the environment of Java (Gregoire et al., 2014), while several other platforms were developed in Matlab (Ilgin Guler et al., 2014; Lee and Park, 2012; Li et al., 2014;

Mundewadikar et al., 2008). Only limited existing studies used standard commercial traffic simulation software, such as VISSIM or CORSIM, to evaluate the performance of their proposed strategies (Le Vine et al., 2015; Lee and Park, 2012; Li et al., 2013b). Furthermore, some researchers applied their control algorithm through robots (Au et al., 2012b; Fok et al., 2012; Perronnet et al., 2013) and real vehicles (Alonso et al., 2011; Quinlan et al., 2010).

Standard simulation packages like VISSIM and CORSIM can provide standard parameter settings and outputs. In addition, using a standard simulation package can guarantee reliable vehicle generation, car-following, lane-changing, and many other driving behavior-related modeling in the simulation. Flexible settings of speed distribution, heavy vehicle percentage, and distributions of acceleration and deceleration rates can also be simply achieved, along with strong evaluation outputs like travel time, delay and queue length.

CHAPTER 3. CAV-ENABLED INTERSECTION MANAGEMENT MECHANISM

3.1 Introduction

A Connected and Autonomous Vehicle (CAV)-enabled traffic system has a great potential to mitigate congestion, reduce traffic delay, and improve traffic mobility and safety performance. Based on seamless V2V and V2I communication as well as autonomous driving technologies, CAVs approaching intersections from all directions can be globally coordinated by managing them all together in a predictive control framework. The safety issue can be illustrated by assigning the intersection limited time and space resource to each approaching CAV without conflicts. The efficiency issue can be solved by determining the passing sequence of all conflicting CAVs. Both safety and efficiency issues are addressed by a centralized Intersection Control Center (ICC) that is designed for CAV coordination at intersections based on an advanced intersection control system, a CAV-enabled Intersection Management Mechanism (CAVIMM).

In the CAVIMM system, no other traffic control methods, including priority rules, signals, and stop or yield signs, are used for intersection operation. The whole intersection operation is controlled by the ICC. In order to outline the procedures of the ICC control mechanism, the logic of the CAVIMM system is introduced in this section. The intersection is also precisely represented in this section as a basic structure for developments of the safety model and efficiency model, which are presented in the following Chapters.

3.2 Mechanism Development Assumptions

The CAVIMM system is developed based on the following assumptions:

1) All vehicles on the road are CAVs, so that the ICC can be established at intersections to coordinate the movements of all approaching CAVs.
2) Real-time communications between CAVs and ICC are assumed to never fail. The approaching vehicle should send all movement information (such as current speed, acceleration/deceleration rate, position and its destination) to the ICC. All CAVs are assumed to follow the guidance of the ICC immediately after receiving it, and the time delay is ignored.
3) The rates of acceleration and deceleration are constant.
4) The speed of CAVs within intersections is constant and is equal to intersection the Design Speed (DS).

A CAV whose request of passing through intersections has not been accepted by the ICC will be guided by the ICC to decelerate and send a request in the next cycle until its request is approved. The speeds of decelerated CAVs are lower than DS if their requests keep being rejected. Dresner and Stone (2005a) concluded that slow-speed reservation would occupy many intersection resources so that the intersection efficiency is reduced. With higher speeds within the intersection, the total traverse time for CAVs are also reduced. In order to address the slow-speed issue and consider the fact that acceleration in vehicle turning movements may result in discomfort of people inside the vehicles, all CAVs are required to adjust their speeds to the DS before entering the intersection and pass through the intersection at a constant DS.

5) Lane changing is not allowed upstream and within the intersection.

Improper lane changing behavior was identified as one of the major contributing factors for intersection-related crashes in the previous studies (Lord and Mannering, 2010; National

Highway Traffic Safety Administration, 2010). Restriction of lane changing on upstream and within intersections can help to improve safety performance around intersections.

6) All CAVs travel on a level terrain; Acceleration of gravity has no impacts on acceleration and deceleration processes.
7) Pedestrians, bicyclists and other street crossings are absent at the subject intersections in this study.

The technologies of detecting and predicting pedestrian and bicyclist behaviors have not been competitive to that of vehicle control. This research aims to investigate the capability of CAV in improving the intersection efficiency; nonautomotive modes are not considered due to the characteristic of non-determinacy in the system.

3.3 CAVIMM System Development Logic

In the CAVIMM system, all approaching CAVs send reservation requests with all information, such as location, speed, acceleration rate, etc., to the ICC when they are approaching an intersection. For every analysis cycle period (0.1s in this study), the ICC will check if there is a collision between the new approaching CAV and the CAVs with approved requests. If any potential collision is found, the request will be rejected by the ICC and the new CAV will decelerate guided by the ICC. Otherwise, the ICC will approve this CAV's request and make a reservation at the same time. Then the CAV follows the guidance of the ICC to adjust their speed to intersection DS and then cross the intersection. All CAVs with unapproved requests and new approaching CAVs send another request with current updated information to the ICC in the next cycle until the reservation is made. If the requests from CAVs have not been approved until their speed are decelerated to zero (stopped), the ICC will assign the top priority to them and lead them to traverse the intersection safely, which helps avoid blocking the whole lane.

The entire logic of CAVIMM can be interpreted and presented in Figure 3.1. When a new CAV is approaching the intersection and sending a request, the ICC checks if it has the top priority, such as emergency vehicles or the speed of this vehicle is zero. If it has, this CAV is assigned at the top priority in the passing sequence, indicating any conflicting CAVs should decelerate due to lower priority. If no, the ICC detects the possibility of the new CAV having a collision with the CAVs whose requests have been approved previously. If there is no conflict between the new CAV and existing CAVs with approval request, all waiting CAVs in this cycle, including new CAVs and existing CAVs which have decelerated during last cycle, will be checked if they have any conflicts with each other. If yes, an optimization algorithm, which determines passing sequence based on achieving the specified goal (for example, minimum total delay or number of vehicle stops), will be employed to assign the right-of-way to conflicting CAVs with different priority order.

Previous research has found that the optimization algorithm may not always have a solution (Li et al., 2013a). If no solution is found in a cycle, the conflicting CAVs will be required to decelerate and send their request in the next cycle.

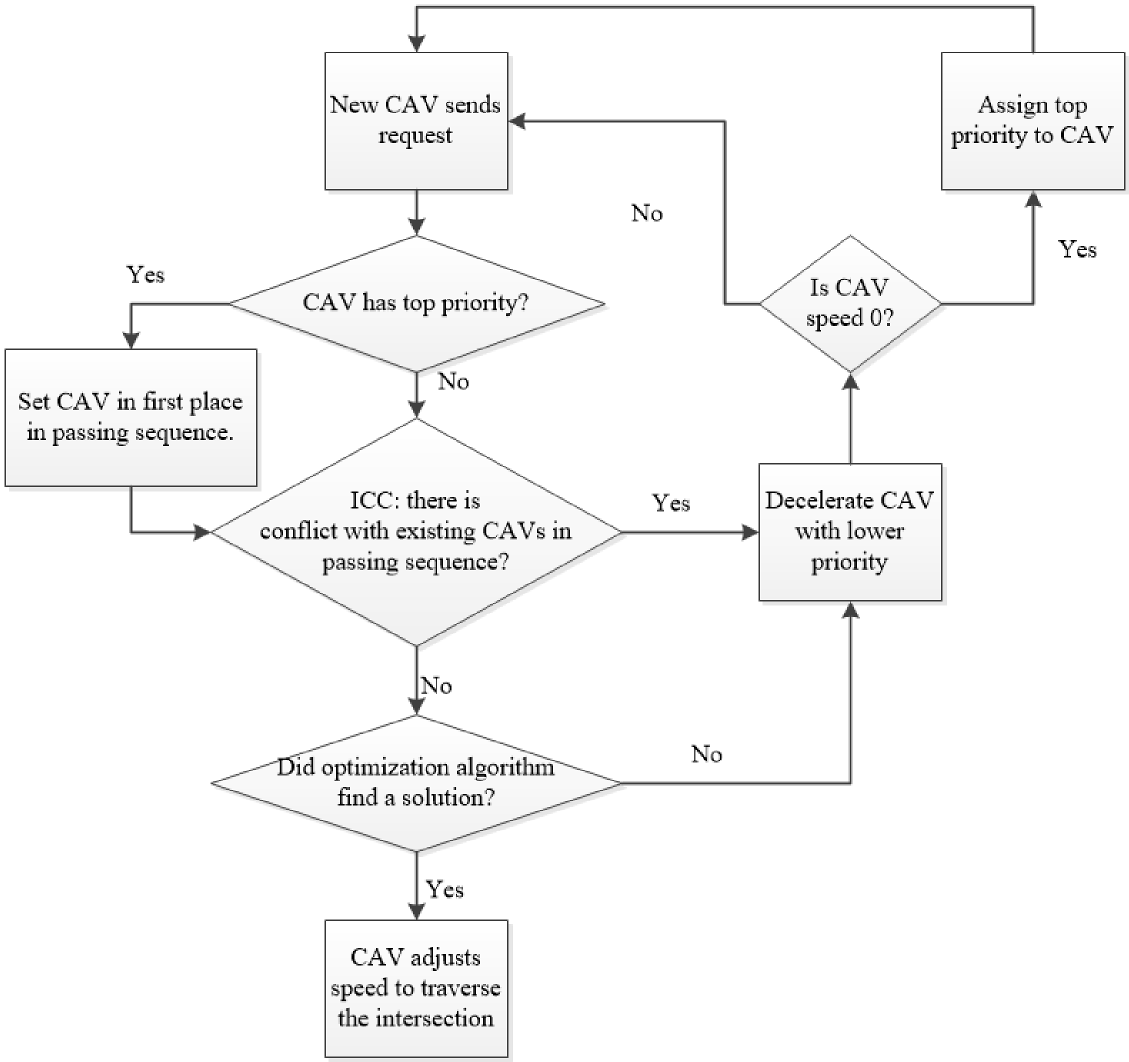

Figure 3.1 Process of a CAV Movement at Intersections

3.4 Intersection Model Development

For traditional signalized intersections with dedicated turning lanes, vehicles should change lanes according to their directions of destination before entering intersections. Improper lane changing is one of the top contributing factors for crashes around intersections and traffic delay. Therefore, in this study, CAVs are not allowed to change lanes after sending a request to the ICC until exiting the intersection. Instead of setting dedicated turning lanes at traditional intersections, CAVs can make turns from any lane in the CAVIMM system. The trajectories for all possible CAV's movements in three-lane 4-leg intersections are illustrated in Figure 3.2.

3.4.1 Control area definition

According to the basic procedures discussed previously, the CAVIMM control space consists of the following parts:

1) Detection Zone (DZ): the DZ defines a zone in which vehicles send their movement information to the ICC and request for a reservation of time-space resource to cross the intersection. The ICC records the CAVs request times. After sending the movement information, the vehicles cannot change lane until they departure the intersection. The length of DZ is set at 10 feet.
2) Decision Waiting Zone (DWZ): The DWZ indicates a zone where CAVs wait for decisions made by the ICC. If the vehicle does not get permission from the ICC, it will decelerate in this zone until a reservation is made successfully. The length of DWZ will be calculated and determined in the Section of Performance Evaluation. CAVs will stop at the Potential Stop Line (PSL) if their requests from CAVs have not been approved until their speeds are decelerating to zero (fully stop). In order to avoid intersection blockage, the ICC will assign the first priority to them and lead them to traverse the intersection safely. By setting PSL at an upstream distance away from intersection entrance rather than traditional stop line at the entrance of the intersection, the slow-speed related intersection resource over-occupied issue can be addressed by allowing acceleration of CAVs within sufficient distance before entering the intersection.

3) Intersection Zone (IZ): the vehicle is required to maintain a constant speed (Designed Speed) when crossing the intersection. The level of utilization of the IZ time and space resources determines the magnitude of intersection efficiency improvement. Lane changing is not allowed within the IZ. CAVs can make any movements, including turning left, going through and turning right, at any lane within intersections. Centerlines of all the possible CAV trajectories are illustrated by dash lines in Figure 3.2. By allowing three movements (left turn, straight, right turn) at any lanes, the conflict areas increase dramatically compared to traditional intersection with dedicated turning lanes. However, all CAVs are controlled by the ICC that helps to detect potential collisions instead of human beings.

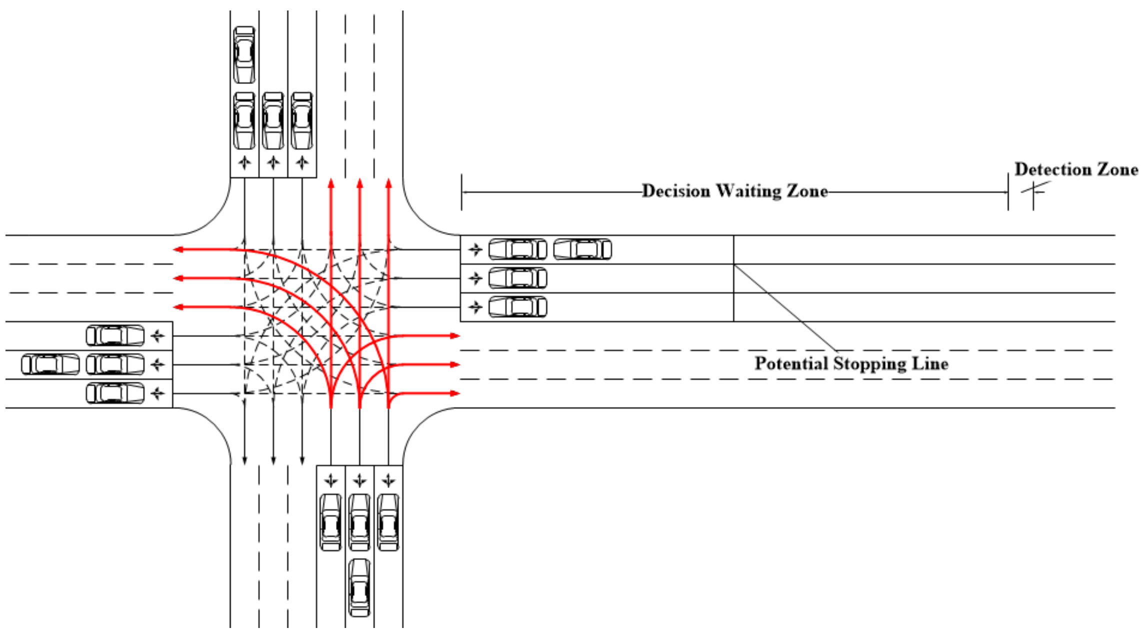

Figure 3.2 Intersection Configuration

3.4.2 Intersection model formulation

It is important to determine the geometrical representation of an intersection to fulfill the requirement of vehicle trajectory formulation. In light of previous studies conducted by Kiwi-W Consortium (2000) and Zhang et al. (2016), the physical intersection is composed of a movement matrix and intersection attributes, which is defined as:

$$\boldsymbol{C} = (\boldsymbol{T}, \boldsymbol{Q_C}) \tag{3.1}$$

where $\boldsymbol{T}$ is a traffic matrix with element $\boldsymbol{t_{ij}}$, indicating the features for a CAV traveling trajectory from entering road, i, to exiting road, j, at the intersection. $\boldsymbol{Q_C}$ represents the attributes and characteristics of the intersection, such as type, traffic control method and name.

The road $\boldsymbol{r}$ is the mathematical abstraction of a physical road (centerline of a real road) which may contain one or more lanes, and it is defined as:

$$\boldsymbol{r} = (\boldsymbol{L}, \boldsymbol{Q_R}) \tag{3.2}$$

where $\boldsymbol{L}$ is the set of lanes $\{\lambda_n\}_{n=1}^{N}$ and $\boldsymbol{Q_R}$ is the attributes of the road, including road name, i, number of lanes, N. Then the traffic lane λ can be defined as:

$$\lambda_{in} = (i, n, \boldsymbol{Q_\lambda}) \tag{3.3}$$

where n is the lane lateral sequence number. If the sequence number of the lane most to the left is assigned as 1, the lateral sequence number of the rest lanes in the same road r_i can be labeled as 2, 3,…, N, respectively, from left to right. $\boldsymbol{Q_\lambda}$ includes the common attributes for traffic lanes, such as lane width, W, and speed limit, V.

Then the traffic matrix element $\boldsymbol{t_{imjn}}$ is defined as follows:

$$t_{imjn} = (S_t, \lambda_{im}, \lambda_{jn}, Q_t) \tag{3.4}$$

where $\boldsymbol{S}_t$ is the shape of the traveling trajectory from lane λ_{im} to lane λ_{jn}. $\boldsymbol{Q_t}$ indicates the attributes of possible trajectories (same with lane attributes).

3.4.3 Intersection sketch

Based on the definition shown above, the physical intersection in Figure 3.2 can be represented by the model sketch figure as shown in Figure 3.3. The two directional roads in the south leg are assigned as 1 and 2, and the rest of the other directional roads are assigned from 3 to 8 in counter-clockwise order, respectively. The intersection helps to connect different roads $\boldsymbol{r}$, and the traffic matrix $\boldsymbol{T}$ includes all possible trajectories at intersections. According to the setting discussed in the section of CAVIMM System Logic, lane changing is prohibited after entering the detection zone, indicating that the lateral sequence numbers of the CAV entering lane, *m*, is equal to that of exiting lane, *n*, all the time. Therefore, a trajectory term, t_{ijk}, is defined to represent all possible trajectories in the CAVIMM controlled intersection, where $m = n = k$. Different from traditional intersections with dedicated left-turn or right-turn lanes, CAVs can make turning movements from any lane. For example, the CAVs from lane λ_{21} can turn left at the intersection and therefore connect to lane λ_{71}, go straight to lane λ_{51} and turn right to the lane λ_{31}. Similarly, CAVs from lane λ_{22} can also turn left/right or go straight by connecting to the lanes λ_{72}, λ_{32} or λ_{52}, respectively. All possible CAVs trajectories within the intersection are illustrated as dashed lines in Figure 3.3 that is also defined by the traffic matrix $\boldsymbol{T}$ as shown in Table 3.1.

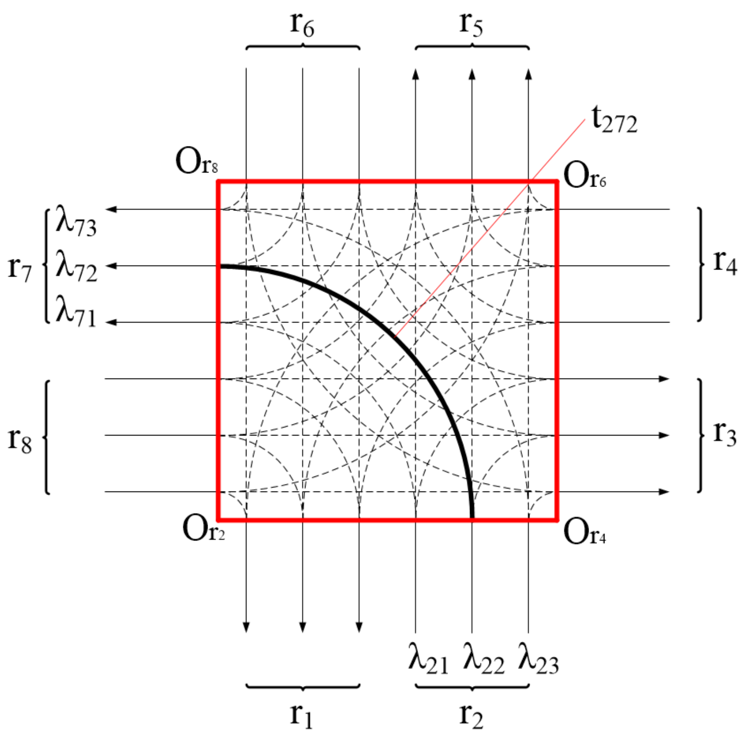

Figure 3.3 Representation of 4-leg Intersection

Table 3.1 Traffic Matrix of the CAVIMM Intersection

			Enter Lane (λ_{im})											
			i=2			*i*=4			*i*=6			*i*=8		
			λ_{21}	λ_{22}	λ_{23}	λ_{41}	λ_{42}	λ_{43}	λ_{61}	λ_{62}	λ_{63}	λ_{81}	λ_{82}	λ_{83}
Exit Lane (λ_{jn})	*j*=1	λ_{11}	×	×	×	t_{411}	×	×	t_{611}	×	×	t_{811}	×	×
		λ_{12}	×	×	×	×	t_{412}	×	×	t_{612}	×	×	t_{812}	×
		λ_{13}	×	×	×	×	×	t_{413}	×	×	t_{613}	×	×	t_{813}
	j=3	λ_{31}	t_{231}	×	×	×	×	×	t_{631}	×	×	t_{831}	×	×
		λ_{32}	×	t_{232}	×	×	×	×	×	t_{632}	×	×	t_{832}	×
		λ_{33}	×	×	t_{233}	×	×	×	×	×	t_{633}	×	×	t_{833}
	j=5	λ_{51}	t_{251}	×	×	t_{451}	×	×	×	×	×	t_{851}	×	×
		λ_{52}	×	t_{252}	×	×	t_{452}	×	×	×	×	×	t_{852}	×
		λ_{53}	×	×	t_{253}	×	×	t_{453}	×	×	×	×	×	t_{853}
	j=7	λ_{71}	t_{271}	×	×	t_{471}	×	×	t_{671}	×	×	×	×	×
		λ_{72}	×	t_{272}	×	×	t_{472}	×	×	t_{672}	×	×	×	×
		λ_{73}	×	×	t_{273}	×	×	t_{473}	×	×	t_{673}	×	×	×

3.5 Summary

In this chapter, the intersection temporal and spatial resources are formulated. The framework of an advanced intersection management mechanism, CAVIMM, is developed and presented, which is the basic structure for the following research work. By formulating the intersection, all possible trajectories of CAVs passing through intersections are identified.

CHAPTER 4. TRAJECTORY COORDINATION MODEL DEVELOPMENT

4.1 Introduction

Safety issue can be addressed by identifying potential conflict areas for any two approaching vehicles and preventing conflicting vehicles arriving at these areas at the same time. Many previous researchers utilized trajectory-based approaches, where certain time-space of the intersection is occupied for vehicles to cross the intersection based on predicted vehicle trajectory. Although vehicle trajectories can be simplified as lines (represented by centerlines of trajectories), the real trajectories should be presented as planes (quarter-circles for turning movements and rectangles for straight movements) with borders considering vehicle size factors (widths and lengths) in the horizontal plane. Intersection capacities are not fully utilized, making the magnitude of intersection efficiency increase not significant. Considering vehicle widths and lengtsh and time continuity, a Temporal-Spatial Dimension Extension-based Trajectory Coordination Model (TSDTCM) was developed in this study by adding time as the third axis. Then the real trajectories will be 3D circular solids for turning movements and cuboids for straight movement, which helps to take advantage of limited intersection time-space resources.

This section presents the method of precise CAV trajectory formulation based on the intersection model developed in Chapter 3.

4.2 Temporal-Spatial Trajectory Formulation

When a CAV with no top priority passing order approaches an intersection, the ICC must check if its possible future trajectory has any conflicts with the trajectories of existing CAVs that have permission to pass through the intersection. Potential conflicting trajectories are firstly identified and then the ICC calculates the time to arrive at the conflict areas for both the new

CAV and existing CAVs. Therefore, all potential trajectories of CAVs should be formulated in the 3D space so that collisions can be detected spatially and temporally at the same time. If 3D trajectories between two CAVs are found to intersect within the intersection, indicating a collision will happen if those two CAVs keep their statuses. Considering trajectory formulations of those two CAVs, intersection of trajectories means there must be at least one solution for the formulation set of two trajectories. After identifying the coordinate information (x and y coordinates) of conflict area projections on the horizontal plane, the projection of trajectory formulations on the time axis (e coordinate) represents the time for each CAV arriving at conflict areas. The entire trajectory is divided into two processes by intersection entrance, including process before intersections and that within intersections.

In this study, a 4-leg intersection with N lanes per approach is used to develop the trajectory formulation. Different from the representation of vehicle trajectories as centerlines in previous studies, the 3D trajectory representations are developed to account for vehicle widths and lengths. By adding time as the third axis, the vertical height of trajectory projection on the time axis is equal to the result that the length of vehicle (L) divided by the vehicle speed (v). The speed of the vehicle within the intersection is equal to the DS. Then the trajectory projection on the time axis is equal to $\frac{L}{DS}$. Since the widths of vehicles vary across types and brands, the trajectory widths are set to be equal to the lane width (W).

If the corner at the leftmost in each approach is defined as the ordinate origin (as shown in Figure 3.3), the trajectories of three possible vehicle movements for CAVs traveling through traffic matrix element, t_{ijk} , can be predicted and formulated as $f_{ijk}^{s}(x,y,e)$ for going straight, $f_{ijk}^{l}(x,y,e)$ for turning left and $f_{ijk}^{r}(x,y,e)$ for turning right. The subject intersection is symmetrical with four legs. The turning trajectories are assumed to follow circular movements around the four intersection corners. The trajectory widths are set to be equal to the lane widths to allow variation of CAV paths within the lanes.

Based on the intersection model developed in Chapter 3, all possible trajectories are formulated and summarized in Table 4.1.

Table 4.1 CAVs Possible Trajectory Function Matrix

		Enter Road (*i*)			
		i=2	i=4	i=6	i=8
Exit Road (*j*)	j=1		$f_{41k}^{l}(x,y,e)$ (Eq.4.4)	$f_{61k}^{s}(x,y,e)$ (Eq.4.8)	$f_{81k}^{r}(x,y,e)$ (Eq.4.12)
	j=3	$f_{23k}^{r}(x,y,e)$ (Eq.4.3)		$f_{63k}^{l}(x,y,e)$ (Eq.4.7)	$f_{83k}^{s}(x,y,e)$ (Eq.4.11)
	j=5	$f_{25k}^{s}(x,y,e)$ (Eq.4.2)	$f_{45k}^{r}(x,y,e)$ (Eq.4.6)		$f_{85k}^{l}(x,y,e)$ (Eq.4.10)
	j=7	$f_{27k}^{l}(x,y,e)$ (Eq.4.1)	$f_{47k}^{s}(x,y,e)$ (Eq.4.5)	$f_{67k}^{r}(x,y,e)$ (Eq.4.9)	

The trajectories illustrated by $f_{ijk}^{s}(x,y,e)$ are cuboids, and those of $f_{ijk}^{l}(x,y,e)$ and $f_{ijk}^{r}(x,y,e)$ are circular solids in 3D space. In this study, the number of lanes, N, and lane width, W, are set to be constant. The vehicle length is represented by L.

If the left side corner is set as circle center, the trajectory formulations for movements of left-turn, straight and right-turn are:

$$f_{ijk}^{l}(x,y,e)=\begin{cases} x_{ijk}=R_{ijk}\cdot cos\theta_{ijk} \\ y_{ijk}=R_{ijk}\cdot sin\theta_{ijk} \\ \frac{(N+k-0.5)\cdot W\cdot arctan\frac{y_{ijk}}{x_{ijk}}-0.5\cdot L_{ijk}}{v_{ijk}}+e_{ijk}^{0}\le e_{ijk}\le\frac{(N+k-0.5)\cdot W\cdot arctan\frac{y_{ijk}}{x_{ijk}}+0.5\cdot L_{ijk}}{v_{ijk}}+e_{ijk}^{0} \\ (N+k-1)\cdot W\le R_{ijk}\le(N+k)\cdot W \\ 0\le\theta_{ijk}\le\pi/2 \end{cases} \tag{4.1}$$

$$f_{ijk}^{s}(x,y,e)=\begin{cases} (N+k-1)\cdot W\le x_{ijk}\le(N+k)\cdot W \\ 0\le y_{ijk}\le 2N\cdot W \\ \frac{y_{ijk}-0.5\cdot L_{ijk}}{v_{ijk}}+\ e_{ijk}^{0}\le e_{ijk}\le\frac{y_{ijk}+0.5\cdot L_{ijk}}{v_{ijk}}+\ e_{ijk}^{0} \end{cases} \tag{4.2}$$

$$f_{ijk}^{r}(x,y,e)=\begin{cases} x_{ijk}=2N\cdot W-R_{ijk}\cdot cos\theta_{ijk} \\ y_{ijk}=R_{ijk}\cdot sin\theta_{ijk} \\ \frac{(N-k+0.5)\cdot W\cdot arctan\frac{y_{ijk}}{2N\cdot W-x_{ijk}}-0.5\cdot L_{ijk}}{v_{ijk}}+e_{ijk}^{0}\le e_{ijk}\le\frac{(N-k+0.5)\cdot W\cdot arctan\frac{y_{ijk}}{2N\cdot W-x_{ijk}}+0.5\cdot L_{ijk}}{v_{ijk}}+e_{ijk}^{0} \\ (N-k)\cdot W\le R_{ijk}\le(N-k+1)\cdot W \\ 0\le\theta_{ijk}\le\pi/2 \end{cases} \tag{4.3}$$

where x and y are coordinates of projection of the trajectories on horizontal plane, and e is coordinate of trajectory projections on time axis. The value of e_{ijk} indicates the time a CAV travels from DZ to the predicted position (x, y) in the intersection, and e_{ijk}^{0} means the total time a vehicle takes to travel from the DZ to the entrance of the intersection. The CAV length is considered through variable, L_{ijk}. R and θ in the Eq.4.1 and Eq.4.3 are the radius and angle, respectively, used to define the 3D circular solid projection areas on the horizontal plane. The possibility of a collision between any two CAVs from the same approach can be checked by solving the function set of those two CAVs trajectory formulations.

The coordinate system transformation is conducted to formulated trajectories of CAVs from different approaches in a function set. If the lower left corner of the intersection is set as ordinate origin (which is the ordinate origin for CAVs from r_2), the trajectory functions of CAVs from the other directions (r_4, r_6, and r_8) can be obtained by substituting x_{ijk} and y_{ijk} as follows: $\begin{cases} x_{ijk} = y'_{ijk} \\ y_{ijk} = 2N \cdot W - x'_{ijk} \end{cases}$ when CAVs are approaching from r_4, $\begin{cases} x_{ijk} = 2N \cdot W - x'_{ijk} \\ y_{ijk} = 2N \cdot W - y'_{ijk} \end{cases}$ for CAVs from r_6, and $\begin{cases} x_{ijk} = 2N \cdot W - y'_{ijk} \\ y_{ijk} = x'_{ijk} \end{cases}$ for CAVs from r_8, where $x_{i'j'k'}$ and $y_{i'j'k'}$ are coordinates of CAV trajectories on the horizontal plane in the new coordinate system. Then the trajectory functions of CAVs from r_2 are the same with Eq. 4.1, Eq. 4.2 and Eq. 4.3. Those of CAVs from r_4 can be obtained as follows:

$$f_{41k}^{l}(x, y, e) = \begin{cases} x_{41k} = 2N \cdot W - R_{41k} \cdot sin\theta_{41k} \\ y_{41k} = R_{41k} \cdot cos\theta_{41k} \\ \frac{(N+k-0.5) \cdot W \cdot arctan\frac{2N \cdot W - x_{41k}}{y_{41k}} - 0.5 \cdot L_{ijk}}{v_{41k}} + e_{41k}^{0} \le e_{ijk} \le \frac{(N+k-0.5) \cdot W \cdot arctan\frac{2N \cdot W - x_{41k}}{y_{41k}} + 0.5 \cdot L_{41k}}{v_{41k}} + e_{41k}^{0} \\ (N + k - 1) \cdot W \le R_{41k} \le (N + k) \cdot W \\ 0 \le \theta_{41k} \le \pi/2 \end{cases} \tag{4.4}$$

$$f_{47k}^{s}(x, y, e) = \begin{cases} 0 \le x_{47k} \le 2N \cdot W \\ (N + k - 1) \cdot W \le y_{47k} \le (N + k) \cdot W \\ \frac{2N \cdot W - y_{47k} - 0.5 \cdot L_{ijk}}{v_{47k}} + e_{47k}^{0} \le e_{47k} \le \frac{2N \cdot W - y_{47k} + 0.5 \cdot L_{47k}}{v_{47k}} + e_{47k}^{0} \end{cases} \tag{4.5}$$

$$f_{45k}^{r}(x,y,e) =$$

$$\begin{cases} x_{45k} = 2N \cdot W - R_{45k} \cdot sin\theta_{45k} \\ y_{45k} = 2N \cdot W - R_{45k} \cdot cos\theta_{45k} \\ \frac{(N-k+0.5)\cdot W\cdot arctan\frac{2N\cdot W - x_{45k}}{2N\cdot W - y_{45k}} - 0.5\cdot L_{ijk}}{v_{45k}} + e_{45k}^{0} \le e_{45k} \le \frac{(N-k+0.5)\cdot W\cdot arctan\frac{2N\cdot W - x_{45k}}{2N\cdot W - y_{45k}} + 0.5\cdot L_{45k}}{v_{45k}} + e_{45k}^{0} \\ (N-k)\cdot W \le R_{45k} \le (N-k+1)\cdot W \\ 0 \le \theta_{45k} \le \pi/2 \end{cases} \tag{4.6}$$

The trajectory functions of CAVs from r_6 are:

$$f_{63k}^{l}(x,y,e) =$$

$$\begin{cases} x_{63k} = 2N \cdot W - R_{63k} \cdot cos\theta_{63k} \\ y_{63k} = 2N \cdot W - R_{63k} \cdot sin\theta_{63k} \\ \frac{(N+k-0.5)\cdot W\cdot arctan\frac{2N\cdot W - y_{63k}}{2N\cdot W - x_{63k}} - 0.5\cdot L_{ijk}}{v_{63k}} + e_{63k}^{0} \le e_{ijk} \le \frac{(N+k-0.5)\cdot W\cdot arctan\frac{2N\cdot W - y_{63k}}{2N\cdot W - x_{63k}} + 0.5\cdot L_{63k}}{v_{63k}} + e_{63k}^{0} \\ (N+k-1)\cdot W \le R_{63k} \le (N+k)\cdot W \\ 0 \le \theta_{63k} \le \pi/2 \end{cases} \tag{4.7}$$

$$f_{61k}^{s}(x,y,e) = \begin{cases} (N-k)\cdot W \le x_{61k} \le (N-k+1)\cdot W \\ 0 \le y_{61k} \le 2N\cdot W \\ \frac{2N\cdot W - y_{61k} - 0.5\cdot L_{ijk}}{v_{61k}} + e_{61k}^{0} \le e_{61k} \le \frac{2N\cdot W - y_{61k} + 0.5\cdot L_{61k}}{v_{61k}} + e_{61k}^{0} \end{cases} \tag{4.8}$$

$$f_{67k}^{r}(x,y,e) =$$

$$\begin{cases} x_{67k} = R_{67k} \cdot cos\theta_{67k} \\ y_{67k} = 2N \cdot W - R_{67k} \cdot sin\theta_{67k} \\ \frac{(N-k+0.5)\cdot W\cdot arctan\frac{2N\cdot W - y_{67k}}{x_{67k}} - 0.5\cdot L_{ijk}}{v_{67k}} + e_{67k}^{0} \le e_{67k} \le \frac{(N-k+0.5)\cdot W\cdot arctan\frac{2N\cdot W - y_{67k}}{x_{67k}} + 0.5\cdot L_{67k}}{v_{67k}} + e_{67k}^{0} \\ (N-k)\cdot W \le R_{67k} \le (N-k+1)\cdot W \\ 0 \le \theta_{67k} \le \pi/2 \end{cases} \tag{4.9}$$

The trajectory functions of CAVs from r_8 are:

$$f_{85k}^{l}(x,y,e) = \begin{cases} x_{85k} = R_{85k} \cdot sin\theta_{85k} \\ y_{85k} = 2N \cdot W - R_{85k} \cdot cos\theta_{85k} \\ \frac{(N+k-0.5)\cdot W \cdot arctan\frac{x_{85k}}{2N\cdot W - y_{85k}} - 0.5\cdot L_{ijk}}{v_{85k}} + e_{85k}^{0} \le e_{85k} \le \frac{(N+k-0.5)\cdot W \cdot arctan\frac{x_{85k}}{2N\cdot W - y_{85k}} + 0.5\cdot L_{85k}}{v_{85k}} + e_{85k}^{0} \\ (N+k-1)\cdot W \le R_{85k} \le (N+k)\cdot W \\ 0 \le \theta_{85k} \le \pi/2 \end{cases} \tag{4.10}$$

$$f_{83k}^{s}(x,y,e) = \begin{cases} 0 \le x_{83k} \le 2N \cdot W \\ (N-k)\cdot W \le y_{83k} \le (N-k+1)\cdot W \\ \frac{x_{83k} - 0.5\cdot L_{ijk}}{v_{83k}} + \ e_{83k}^{0} \le e_{83k} \le \frac{x_{83k} + 0.5\cdot L_{ijk}}{v_{83k}} + \ e_{83k}^{0} \end{cases} \tag{4.11}$$

$$f_{81k}^{r}(x,y,e) = \begin{cases} x_{81k} = R_{81k} \cdot sin\theta_{81k} \\ y_{81k} = R_{81k} \cdot cos\theta_{81k} \\ \frac{(N-k+0.5)\cdot W \cdot arctan\frac{x_{81k}}{y_{81k}} - 0.5\cdot L_{ijk}}{v_{81k}} + e_{81k}^{0} \le e_{81k} \le \frac{(N-k+0.5)\cdot W \cdot arctan\frac{x_{81k}}{y_{81k}} + 0.5\cdot L_{81k}}{v_{81k}} + e_{81k}^{0} \\ (N-k)\cdot W \le R_{81k} \le (N-k+1)\cdot W \\ 0 \le \theta_{81k} \le \pi/2 \end{cases} \tag{4.12}$$

4.3 Conflict Area Detection

The possibility of a collision between any two CAVs can be checked by solving the trajectory functions of those two CAVs. The paired trajectories, which may cross at the intersection in the temporal-spatial domain, are analyzed through traffic matrices as shown in Tables 4.2 to 4.10. The total number of potential conflicting trajectories of CAVs from r_2, r_4, r_6 and r_8, respectively, is summarized in Table 4.11. If any solution of the function set of two CAV trajectories is found, there will be a collision between them if they keep their current kinetic status. Then the ICC will reject the request of CAV with lower priority. The level of priority is determined by the ICC in terms of obtaining specified objectives.

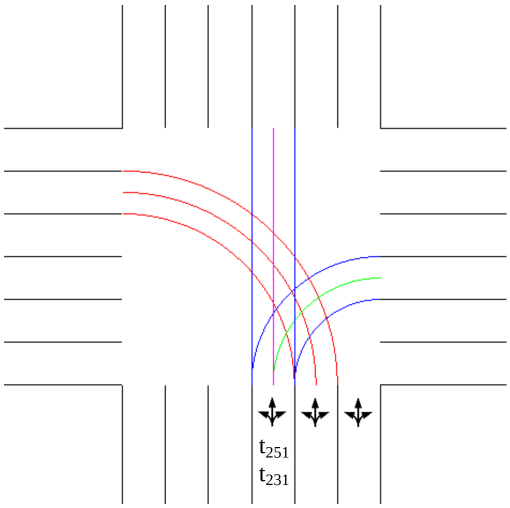

a) Conflicting Trajectories from r_2

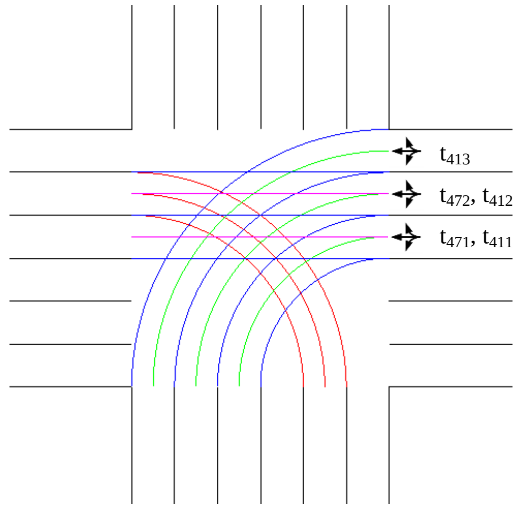

b) Conflicting Trajectories from r_4

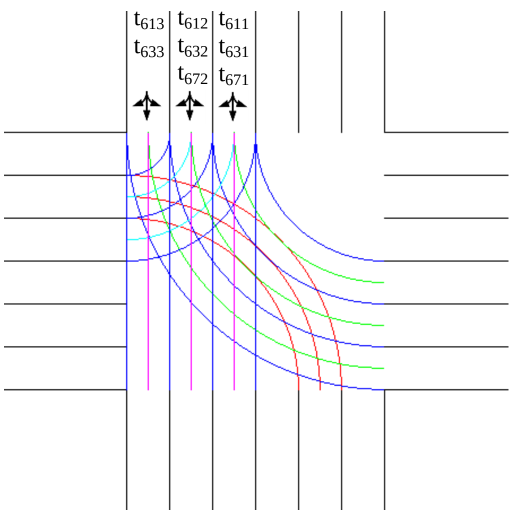

c) Conflicting Trajectories from r_6

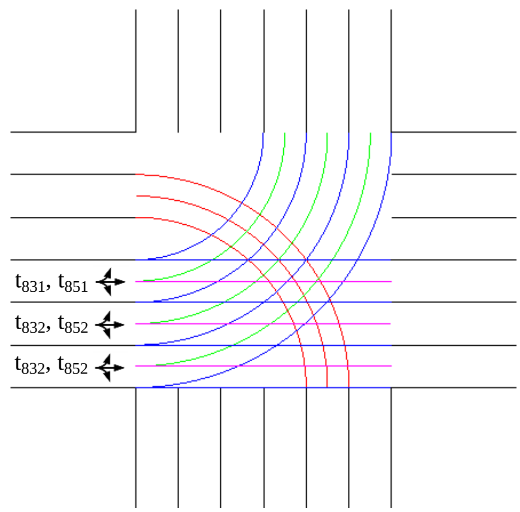

d) Conflicting Trajectories from r_8

Figure 4.1 Conflicting Trajectories for CAVs Trajectory t_{272}

Table 4.2 Conflicting Trajectory Matrix for t_{231}

			Enter Lane (λ_{im})											
			i=2			*i*=2			*i*=2			*i*=2		
			λ_{21}	λ_{22}	λ_{23}	λ_{41}	λ_{42}	λ_{43}	λ_{61}	λ_{62}	λ_{63}	λ_{81}	λ_{82}	λ_{83}
Exit Lane (λ_{jn})	*j*=1	λ_{11}	×	×	×	t_{411}	×	×	t_{611}	×	×	t_{811}	×	×
		λ_{12}	×	×	×	×	t_{412}	×	×	t_{612}	×	×	t_{812}	×
		λ_{13}	×	×	×	×	×	t_{413}	×	×	t_{613}	×	×	t_{813}
	j=3	λ_{31}	t_{231}	×	×	×	×	×	t_{631}	×	×	t_{831}	×	×
		λ_{32}	×	t_{232}	×	×	×	×	×	t_{632}	×	×	t_{832}	×
		λ_{33}	×	×	t_{233}	×	×	×	×	×	t_{633}	×	×	t_{833}
	j=5	λ_{51}	t_{251}	×	×	t_{451}	×	×	×	×	×	t_{851}	×	×
		λ_{52}	×	t_{252}	×	×	t_{452}	×	×	×	×	×	t_{852}	×
		λ_{53}	×	×	t_{253}	×	×	t_{453}	×	×	×	×	×	t_{853}
	j=7	λ_{71}	t_{271}	×	×	t_{471}	×	×	t_{671}	×	×	×	×	×
		λ_{72}	×	t_{272}	×	×	t_{472}	×	×	t_{672}	×	×	×	×
		λ_{73}	×	×	t_{273}	×	×	t_{473}	×	×	t_{673}	×	×	×

Table 4.3 Conflicting Trajectory Matrix for t_{232}

			Enter Lane (λ_{im})											
			i=2			*i*=4			*i*=6			*i*=8		
			λ_{21}	λ_{22}	λ_{23}	λ_{41}	λ_{42}	λ_{43}	λ_{61}	λ_{62}	λ_{63}	λ_{81}	λ_{82}	λ_{83}
Exit Lane (λ_{jn})	*j*=1	λ_{11}	×	×	×	t_{411}	×	×	t_{611}	×	×	t_{811}	×	×
		λ_{12}	×	×	×	×	t_{412}	×	×	t_{612}	×	×	t_{812}	×
		λ_{13}	×	×	×	×	×	t_{413}	×	×	t_{613}	×	×	t_{813}
	j=3	λ_{31}	t_{231}	×	×	×	×	×	t_{631}	×	×	t_{831}	×	×
		λ_{32}	×	t_{232}	×	×	×	×	×	t_{632}	×	×	t_{832}	×
		λ_{33}	×	×	t_{233}	×	×	×	×	×	t_{633}	×	×	t_{833}
	j=5	λ_{51}	t_{251}	×	×	t_{451}	×	×	×	×	×	t_{851}	×	×
		λ_{52}	×	t_{252}	×	×	t_{452}	×	×	×	×	×	t_{852}	×
		λ_{53}	×	×	t_{253}	×	×	t_{453}	×	×	×	×	×	t_{853}
	j=7	λ_{71}	t_{271}	×	×	t_{471}	×	×	t_{671}	×	×	×	×	×
		λ_{72}	×	t_{272}	×	×	t_{472}	×	×	t_{672}	×	×	×	×
		λ_{73}	×	×	t_{273}	×	×	t_{473}	×	×	t_{673}	×	×	×

Table 4.4 Conflicting Trajectory Matrix for t_{233}

			Enter Lane (λ_{im})											
			i=2			i=2			i=2			i=2		
			λ_{21}	λ_{22}	λ_{23}	λ_{41}	λ_{42}	λ_{43}	λ_{61}	λ_{62}	λ_{63}	λ_{81}	λ_{82}	λ_{83}
Exit Lane (λ_{jn})	j=1	λ_{11}	×	×	×	t_{411}	×	×	t_{611}	×	×	t_{811}	×	×
		λ_{12}	×	×	×	×	t_{412}	×	×	t_{612}	×	×	t_{812}	×
		λ_{13}	×	×	×	×	×	t_{413}	×	×	t_{613}	×	×	t_{813}
	j=3	λ_{31}	t_{231}	×	×	×	×	×	t_{631}	×	×	t_{831}	×	×
		λ_{32}	×	t_{232}	×	×	×	×	×	t_{632}	×	×	t_{832}	×
		λ_{33}	×	×	t_{233}	×	×	×	×	×	t_{633}	×	×	t_{833}
	j=5	λ_{51}	t_{251}	×	×	t_{451}	×	×	×	×	×	t_{851}	×	×
		λ_{52}	×	t_{252}	×	×	t_{452}	×	×	×	×	×	t_{852}	×
		λ_{53}	×	×	t_{253}	×	×	t_{453}	×	×	×	×	×	t_{853}
	j=7	λ_{71}	t_{271}	×	×	t_{471}	×	×	t_{671}	×	×	×	×	×
		λ_{72}	×	t_{272}	×	×	t_{472}	×	×	t_{672}	×	×	×	×
		λ_{73}	×	×	t_{273}	×	×	t_{473}	×	×	t_{673}	×	×	×

Table 4.5 Conflicting Trajectory Matrix for t_{251}

			Enter Lane (λ_{im})											
			i=2			i=2			i=2			i=2		
			λ_{21}	λ_{22}	λ_{23}	λ_{41}	λ_{42}	λ_{43}	λ_{61}	λ_{62}	λ_{63}	λ_{81}	λ_{82}	λ_{83}
Exit Lane (λ_{jn})	j=1	λ_{11}	×	×	×	t_{411}	×	×	t_{611}	×	×	t_{811}	×	×
		λ_{12}	×	×	×	×	t_{412}	×	×	t_{612}	×	×	t_{812}	×
		λ_{13}	×	×	×	×	×	t_{413}	×	×	t_{613}	×	×	t_{813}
	j=3	λ_{31}	t_{231}	×	×	×	×	×	t_{631}	×	×	t_{831}	×	×
		λ_{32}	×	t_{232}	×	×	×	×	×	t_{632}	×	×	t_{832}	×
		λ_{33}	×	×	t_{233}	×	×	×	×	×	t_{633}	×	×	t_{833}
	j=5	λ_{51}	t_{251}	×	×	t_{451}	×	×	×	×	×	t_{851}	×	×
		λ_{52}	×	t_{252}	×	×	t_{452}	×	×	×	×	×	t_{852}	×
		λ_{53}	×	×	t_{253}	×	×	t_{453}	×	×	×	×	×	t_{853}
	j=7	λ_{71}	t_{271}	×	×	t_{471}	×	×	t_{671}	×	×	×	×	×
		λ_{72}	×	t_{272}	×	×	t_{472}	×	×	t_{672}	×	×	×	×
		λ_{73}	×	×	t_{273}	×	×	t_{473}	×	×	t_{673}	×	×	×

Table 4.6 Conflicting Trajectory Matrix for t_{252}

			Enter Lane (λ_{im})											
			i=2			i=2			i=2			i=2		
			λ_{21}	λ_{22}	λ_{23}	λ_{41}	λ_{42}	λ_{43}	λ_{61}	λ_{62}	λ_{63}	λ_{81}	λ_{82}	λ_{83}
Exit Lane (λ_{jn})	j=1	λ_{11}	×	×	×	t_{411}	×	×	t_{611}	×	×	t_{811}	×	×
		λ_{12}	×	×	×	×	t_{412}	×	×	t_{612}	×	×	t_{812}	×
		λ_{13}	×	×	×	×	×	t_{413}	×	×	t_{613}	×	×	t_{813}
	j=3	λ_{31}	t_{231}	×	×	×	×	×	t_{631}	×	×	t_{831}	×	×
		λ_{32}	×	t_{232}	×	×	×	×	×	t_{632}	×	×	t_{832}	×
		λ_{33}	×	×	t_{233}	×	×	×	×	×	t_{633}	×	×	t_{833}
	j=5	λ_{51}	t_{251}	×	×	t_{451}	×	×	×	×	×	t_{851}	×	×
		λ_{52}	×	t_{252}	×	×	t_{452}	×	×	×	×	×	t_{852}	×
		λ_{53}	×	×	t_{253}	×	×	t_{453}	×	×	×	×	×	t_{853}
	j=7	λ_{71}	t_{271}	×	×	t_{471}	×	×	t_{671}	×	×	×	×	×
		λ_{72}	×	t_{272}	×	×	t_{472}	×	×	t_{672}	×	×	×	×
		λ_{73}	×	×	t_{273}	×	×	t_{473}	×	×	t_{673}	×	×	×

Table 4.7 Conflicting Trajectory Matrix for t_{253}

			Enter Lane (λ_{im})											
			i=2			i=2			i=2			i=2		
			λ_{21}	λ_{22}	λ_{23}	λ_{41}	λ_{42}	λ_{43}	λ_{61}	λ_{62}	λ_{63}	λ_{81}	λ_{82}	λ_{83}
Exit Lane (λ_{jn})	j=1	λ_{11}	×	×	×	t_{411}	×	×	t_{611}	×	×	t_{811}	×	×
		λ_{12}	×	×	×	×	t_{412}	×	×	t_{612}	×	×	t_{812}	×
		λ_{13}	×	×	×	×	×	t_{413}	×	×	t_{613}	×	×	t_{813}
	j=3	λ_{31}	t_{231}	×	×	×	×	×	t_{631}	×	×	t_{831}	×	×
		λ_{32}	×	t_{232}	×	×	×	×	×	t_{632}	×	×	t_{832}	×
		λ_{33}	×	×	t_{233}	×	×	×	×	×	t_{633}	×	×	t_{833}
	j=5	λ_{51}	t_{251}	×	×	t_{451}	×	×	×	×	×	t_{851}	×	×
		λ_{52}	×	t_{252}	×	×	t_{452}	×	×	×	×	×	t_{852}	×
		λ_{53}	×	×	t_{253}	×	×	t_{453}	×	×	×	×	×	t_{853}
	j=7	λ_{71}	t_{271}	×	×	t_{471}	×	×	t_{671}	×	×	×	×	×
		λ_{72}	×	t_{272}	×	×	t_{472}	×	×	t_{672}	×	×	×	×
		λ_{73}	×	×	t_{273}	×	×	t_{473}	×	×	t_{673}	×	×	×

Table 4.8 Conflicting Trajectory Matrix for t_{271}

			Enter Lane (λ_{im})											
			i=2			*i*=2			*i*=2			*i*=2		
			λ_{21}	λ_{22}	λ_{23}	λ_{41}	λ_{42}	λ_{43}	λ_{61}	λ_{62}	λ_{63}	λ_{81}	λ_{82}	λ_{83}
Exit Lane (λ_{jn})	*j*=1	λ_{11}	×	×	×	t_{411}	×	×	t_{611}	×	×	t_{811}	×	×
		λ_{12}	×	×	×	×	t_{412}	×	×	t_{612}	×	×	t_{812}	×
		λ_{13}	×	×	×	×	×	t_{413}	×	×	t_{613}	×	×	t_{813}
	j=3	λ_{31}	t_{231}	×	×	×	×	×	t_{631}	×	×	t_{831}	×	×
		λ_{32}	×	t_{232}	×	×	×	×	×	t_{632}	×	×	t_{832}	×
		λ_{33}	×	×	t_{233}	×	×	×	×	×	t_{633}	×	×	t_{833}
	j=5	λ_{51}	t_{251}	×	×	t_{451}	×	×	×	×	×	t_{851}	×	×
		λ_{52}	×	t_{252}	×	×	t_{452}	×	×	×	×	×	t_{852}	×
		λ_{53}	×	×	t_{253}	×	×	t_{453}	×	×	×	×	×	t_{853}
	j=7	λ_{71}	t_{271}	×	×	t_{471}	×	×	t_{671}	×	×	×	×	×
		λ_{72}	×	t_{272}	×	×	t_{472}	×	×	t_{672}	×	×	×	×
		λ_{73}	×	×	t_{273}	×	×	t_{473}	×	×	t_{673}	×	×	×

Table 4.9 Conflicting Trajectory Matrix for t_{272}

			Enter Lane (λ_{im})											
			i=2			*i*=2			*i*=2			*i*=2		
			λ_{21}	λ_{22}	λ_{23}	λ_{41}	λ_{42}	λ_{43}	λ_{61}	λ_{62}	λ_{63}	λ_{81}	λ_{82}	λ_{83}
Exit Lane (λ_{jn})	*j*=1	λ_{11}	×	×	×	t_{411}	×	×	t_{611}	×	×	t_{811}	×	×
		λ_{12}	×	×	×	×	t_{412}	×	×	t_{612}	×	×	t_{812}	×
		λ_{13}	×	×	×	×	×	t_{413}	×	×	t_{613}	×	×	t_{813}
	j=3	λ_{31}	t_{231}	×	×	×	×	×	t_{631}	×	×	t_{831}	×	×
		λ_{32}	×	t_{232}	×	×	×	×	×	t_{632}	×	×	t_{832}	×
		λ_{33}	×	×	t_{233}	×	×	×	×	×	t_{633}	×	×	t_{833}
	j=5	λ_{51}	t_{251}	×	×	t_{451}	×	×	×	×	×	t_{851}	×	×
		λ_{52}	×	t_{252}	×	×	t_{452}	×	×	×	×	×	t_{852}	×
		λ_{53}	×	×	t_{253}	×	×	t_{453}	×	×	×	×	×	t_{853}
	j=7	λ_{71}	t_{271}	×	×	t_{471}	×	×	t_{671}	×	×	×	×	×
		λ_{72}	×	t_{272}	×	×	t_{472}	×	×	t_{672}	×	×	×	×
		λ_{73}	×	×	t_{273}	×	×	t_{473}	×	×	t_{673}	×	×	×

Table 4.10 Conflicting Trajectory Matrix for t_{273}

			Enter Lane (λ_{im})											
			i=2			i=2			i=2			i=2		
			λ_{21}	λ_{22}	λ_{23}	λ_{41}	λ_{42}	λ_{43}	λ_{61}	λ_{62}	λ_{63}	λ_{81}	λ_{82}	λ_{83}
Exit Lane (λ_{jn})	j=1	λ_{11}	×	×	×	t_{411}	×	×	t_{611}	×	×	t_{811}	×	×
		λ_{12}	×	×	×	×	t_{412}	×	×	t_{612}	×	×	t_{812}	×
		λ_{13}	×	×	×	×	×	t_{413}	×	×	t_{613}	×	×	t_{813}
	j=3	λ_{31}	t_{231}	×	×	×	×	×	t_{631}	×	×	t_{831}	×	×
		λ_{32}	×	t_{232}	×	×	×	×	×	t_{632}	×	×	t_{832}	×
		λ_{33}	×	×	t_{233}	×	×	×	×	×	t_{633}	×	×	t_{833}
	j=5	λ_{51}	t_{251}	×	×	t_{451}	×	×	×	×	×	t_{851}	×	×
		λ_{52}	×	t_{252}	×	×	t_{452}	×	×	×	×	×	t_{852}	×
		λ_{53}	×	×	t_{253}	×	×	t_{453}	×	×	×	×	×	t_{853}
	j=7	λ_{71}	t_{271}	×	×	t_{471}	×	×	t_{671}	×	×	×	×	×
		λ_{72}	×	t_{272}	×	×	t_{472}	×	×	t_{672}	×	×	×	×
		λ_{73}	×	×	t_{273}	×	×	t_{473}	×	×	t_{673}	×	×	×

Table 4.11 Number of Conflicting Trajectories for Each Trajectory

			Enter Lane (λ_{im})															
			i=2				i=2				i=2				i=2			
			λ_{21}	λ_{22}	λ_{23}	T[a]	λ_{41}	λ_{42}	λ_{43}	T	λ_{61}	λ_{62}	λ_{63}	T	λ_{81}	λ_{82}	λ_{83}	T
Exit Lane (λ_{jn})	j=1	λ_{11}	×	×	×		16	×	×		18	×	×		11	×	×	
		λ_{12}	×	×	×	0	×	21	×	63	×	18	×	54	×	6	×	19
		λ_{13}	×	×	×		×	×	26		×	×	18		×	×	2	
	j=3	λ_{31}	11	×	×		×	×	×		16	×	×		18	×	×	
		λ_{32}	×	6	×	19	×	×	×	0	×	21	×	63	×	18	×	54
		λ_{33}	×	×	2		×	×	×		×	×	26		×	×	18	
	j=5	λ_{51}	18	×	×		11	×	×		×	×	×		16	×	×	
		λ_{52}	×	18	×	54	×	6	×	19	×	×	×	0	×	21	×	63
		λ_{53}	×	×	18		×	×	2		×	×	×		×	×	26	
	j=7	λ_{71}	16	×	×		18	×	×		11	×	×		×	×	×	
		λ_{72}	×	21	×	63	×	18	×	54	×	6	×	19	×	×	×	0
		λ_{73}	×	×	26		×	×	18		×	×	2		×	×	×	
	T		45	45	46	136	45	45	46	136	45	45	46	136	45	45	46	136

Note: [a]Total number of Conflicting trajectories

4.4 Conflicting Trajectory Case Study

Consider a 4-leg intersection with 12 ft wide lanes. The first approaching CAV (V1) comes from lane λ_{22} of road r_2, and wants to turn left at the intersection through trajectory t_{272}. Another CAV (V2) comes from lane λ_{61} of road r_6, and wants to travel straight through trajectory t_{611}. The trajectory of V1 is a 3D circular arc and that of V2 is a cuboid.

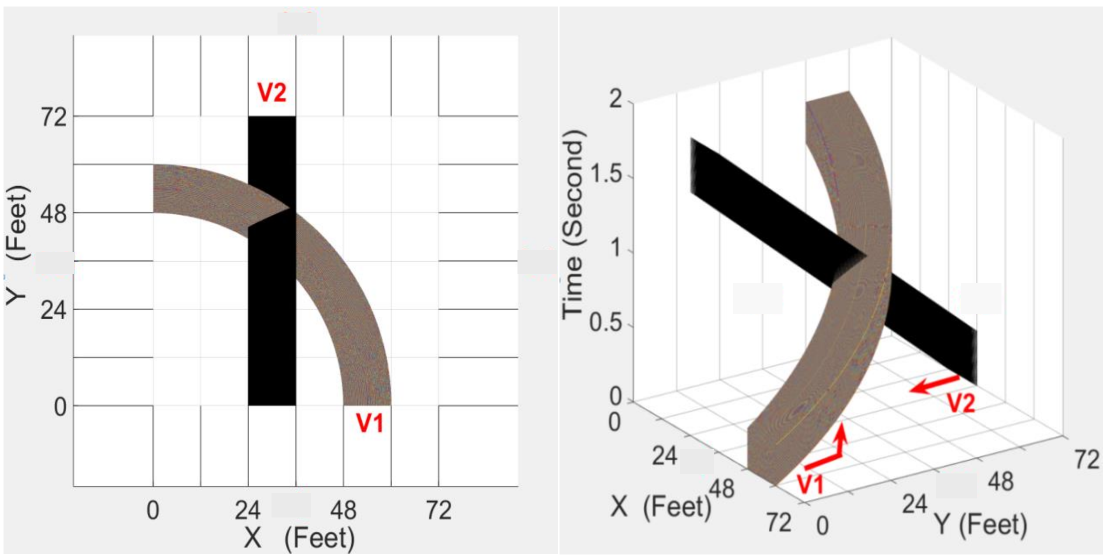

(a) 2D View **(b) 3D View**

Figure 4.2 Predicted Trajectories of Two Vehicles with Collision

If these two CAVs arrive at the overlap areas at the same time, those two 3D geometries will intersect as shown in Figure 4.2 (b). The trajectory formulation for V1 is:

$$f_{272}^{l}(x,y,e) = \begin{cases} x_{272} = r_{272} \cdot cos\theta_{272} \\ y_{272} = r_{272} \cdot sin\theta_{272} \\ \frac{4.5W \cdot arctan\frac{y_{272}}{x_{272}} - 0.5 \cdot L_{272}}{v_{272}} + e_{272}^{0} \leq e_{272} \leq \frac{4.5W \cdot arctan\frac{y_{272}}{x_{272}} + 0.5 \cdot L_{272}}{v_{272}} + e_{272}^{0} \\ 4W \leq R_{272} \leq 5W \\ 0 \leq \theta_{272} \leq \pi/2 \end{cases} \tag{4.13}$$

Since the V2 comes from the road r_6 and goes straight in this intersection, input $\begin{cases} x_{ijk} = 2N \cdot W - x'_{ijk} \\ y_{ijk} = 2N \cdot W - y'_{ijk} \end{cases}$ into Eq.(4.2) to get the functions about x'_{ijk} and y'_{ijk}:

$$f_{611}^{s}(x, y, e) = \begin{cases} 2W \le x'_{611} \le 3W \\ 0 \le y'_{611} \le 6W \\ \frac{6W - y'_{611} - 0.5 \cdot L_{611}}{v_{611}} + e_{611}^{0} \le e_{611} \le \frac{6W - y'_{611} + 0.5 \cdot L_{611}}{v_{611}} + e_{611}^{0} \end{cases} \tag{4.14}$$

In order to check if there will be a collision between V1 and V2, it is necessary to combine $f_{272}^{l}(x, y, t)$ and $f_{611}^{s}(s, y, t)$ as a set. The problem becomes to check if there is a solution for Eq. (4.15). Any solution for this function set indicates that it is possible to have a collision between V1 and V2 if they keep their statuses to pass through intersections, as presented in Figure 4.2 (b).

$$\begin{cases} x = R \cdot cos\theta \\ y = R \cdot sin\theta \\ \frac{4.5W \cdot arctan\frac{y}{x} - 0.5 \cdot L_{272}}{v_{272}} + e_{272}^{0} \le e_{272} \le \frac{4.5W \cdot arctan\frac{y}{x} + 0.5 \cdot L_{272}}{v_{272}} + e_{272}^{0} \\ 4W \le R \le 5W \\ 0 \le \theta \le \frac{\pi}{2} \\ 2W \le x \le 3W \\ 0 \le y \le 6W \\ \frac{6W - y - 0.5 \cdot L_{611}}{v_{611}} + e_{611}^{0} \le e_{611} \le \frac{6W - y + 0.5 \cdot L_{611}}{v_{611}} + e_{611}^{0} \end{cases} \tag{4.15}$$

4.5 Summary

By adding time as the third axis, the whole intersection is represented by a cube in the temporal-spatial domain. Then a trajectory coordination model, TSDRCM, is developed with precise formulation of CAV trajectories considering CAV widths and lengths. All potential collision areas are identified through the intersection formation model developed in Chapter 3. With a TSDTCM model, the intersection area is efficiently utilized by preventing conflicting

CAVs from arriving at a potential collision area at the same time. The results from the TSDRCM model are the safety constraints in the development of passing sequence optimization for ensuring CAVs to pass through intersections without collisions.

CHAPTER 5. PASSING SEQUENCE ALGORITHM DEVELOPMENT

5.1 Introduction

The passing sequence of conflicting CAVs is another major problem that needs to be addressed in the CAVIMM. Based on the vehicle trajectory formulation, various CAV intersection control strategies have been developed. The First-Come-First-Serve (FCFS) is the most widely used strategy in CAV-enabled intersection management due to its advantage in logic simplicity. If two conflicting CAVs are identified, the passing sequence is assigned by the Intersection Control Center (ICC) according to the sequence of approaching vehicles. However, the FCFS may not be the optimal strategy in terms of minimizing intersection total delay, maximizing overall throughput and accommodating emergency vehicles. A new CAV-based control algorithm entitled Discrete Forward-Rolling Optimal Control (DFROC) algorithm, is developed in this study, aiming to reduce intersection total traffic delay. Considering the complexity of control problems, dynamic programming techniques have been applied to break the problem into multiple sub-problems with optimal sub-structures. This section presents the development of two control algorithms for coordinating approaching CAVs with potential conflicts, including the FCFS algorithm and the DFROC algorithm, in the CAVIMM, and the following Chapter shows performance evaluation of those two algorithms in terms of efficiency performance at the intersection.

5.2 FCFS Algorithm

5.2.1 FCFS implementation logic

In the CAVIMM system developed in Chapter 3, the ICC is deployed for data collection and decision-making. The FSFC algorithm requires the ICC to assign the right-of-way to approaching CAVs according to their arrival time. When the ICC receives information and reservation request from an approaching CAV, it will check if its required resource (time and space) has been reserved by a previous vehicle or not. If the time-space resource has not been reserved, the vehicle will receive the permission to cross the intersection and its required resources will be reserved. On the other hand, if the required time-space resource has been reserved, the ICC will deny the request and the CAV will decelerate and prepare to send a second request in the next cycle until its request is approved. If two decelerating CAVs are found to have a potential collision, the ICC will assign the right-of-way to the CAV that arrives at the DZ earlier. Once the reservation is successfully made, the vehicle must adjust its speed to the DS to pass through the intersection.

5.2.2 Evaluation

The benefits of an advanced CAV-enabled intersection control mechanism using the FCFS control algorithm are: 1) It will never fail in terms of determining passing sequences of all CAVs. No matter how many stops there are before entering intersections in the end, all CAVs successfully pass through the intersection. 2) The FCFS logic is easy to be understood and implemented in practice. This control algorithm is a fair policy for all intersection users. The intersection travelers want to pass through intersections as soon as possible. They do not consider the operation situation of the whole intersection. Therefore, any optimal control algorithm aiming to achieve the best overall intersection operation performance may have some negative impacts on some users.

5.3 DFROC Algorithm

The ICC checks the CAVs' statuses and the intersection operation performance every analysis cycle. Within each analysis cycle, all CAVs are required to move with a fixed speed. Therefore, the whole process of CAVs under the control of the ICC is discrete. For each cycle, the ICC determines the right-of-way according to an optimal algorithm aiming at achieving a certain goal, such as minimizing total delay or maximizing overall throughput. In this study, a Discrete Forward-Rolling Optimal Control (DFROC) model is developed by formulating the optimization problem with constraints to avoid collisions in each cycle.

5.3.1 Objective function

In this study, the main goal of the DFROC algorithm is minimizing total traffic delay at the intersection. As stated in previous Chapters, CAVs traverse intersection with the DS without any stops. Therefore, the optimal solution can only be achieved during the process from the DZ to the intersection entrance. Assuming CAVs pass the DZ with a speed of DS, they will be required to decelerate at a fixed rate, a, if a potential collision is detected. The ICC determines the sequence of assigning the right-of-way to conflicting CAVs. Once the CAV request is accepted by the ICC, the CAV will accelerate with the same fixed rate (a) until the speed is equal to the DS before entering the intersection. Then, the movement of each CAV is formulated by fixed the acceleration/deceleration rates, a, and the total deceleration time, q.

The total delay for each CAV can be formulated as follows:

$$Delay_{ijk} = \frac{a \cdot (q_{ijk})^2}{v_{ijk}} \tag{5.1}$$

where v_{ijk} is the speed of CAV entering the DZ, and it is equal to the DS in current CAVIMM system setting. The speed-time graph for each CAV is presented in Figure 5.1.

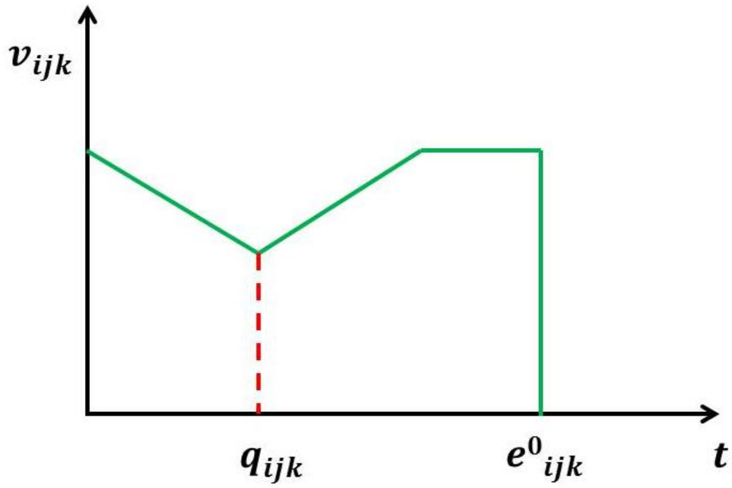

Figure 5.1 Speed-Time Graph for Each CAV Before Entering Intersection

5.3.2 DFROC implementation logic

All approaching CAVs will send requests to pass through the intersection to the ICC upon entering the DZ. The whole process is illustrated in Figure 5.2. The ICC puts together all information (including coming from direction, i, destination direction, j, and lateral lane number, k, time of entering DZ, p) from new CAVs with the CAVs that have not entered the intersection in a dynamic matrix named as Waiting Zone Matrix (WZM). It is a dynamic matrix since it is updated every cycle by adding new CAVs (e.g. CAV6 and CAV7 in Figure 5.2) and removing CAVs which have departed from the intersection (e.g. CAV2 and CAV3 in Figure 5.2). The possibility of a collision both between any new CAV and previous CAVs, and between any pair of new CAVs in the WZM is checked by the ICC through its TSDTCM. The results are saved as constraints in a Dynamic Conflicting Trajectory Matrix (DCTM) for further optimization analysis, which is also updated every cycle.

The total number of constrains is determined by the total number of existing CAVs and that of new CAVs. Then an optimization is conducted for each cycle by figuring out the shortest deceleration time for each CAV to achieve the objective with safety constraints. Then the departure time for each vehicle, T'^{d}_{ijk}, can be obtained from its trajectory prediction. If the departure time of existing CAVs, T'^{d}_{ijk}, is earlier than current system global time, T, they will be removed from the WZM by the ICC to avoid checking of redundant potential conflicts with new CAVs.

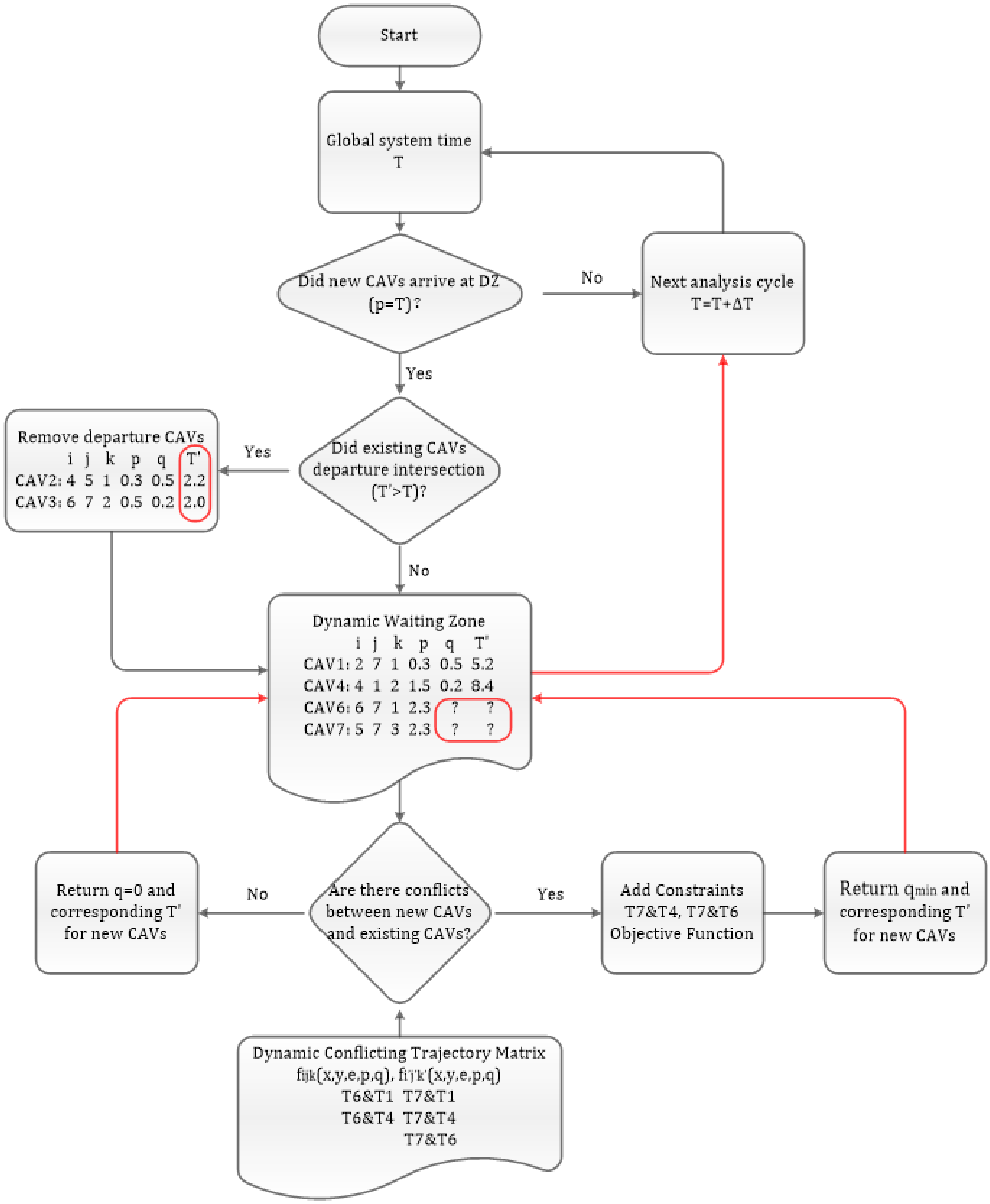

Figure 5.2 Flowchart for DFROC

5.3.3 DFROC pseudo-codes

Based on the development logic of the DFROC, the pseudo-codes are established as follows:

Algorithm 1: Dynamic waiting zone

Data: current system time T, new CAV set R_t, Dynamic Waiting Zone P_t , rth CAV in the new CAV set is $C_r^R(t)$ $(r \in R)$, R is the total number of elements in R_t, , pth CAV in the existing CAV set is $C_p^P(t)$ $(p \in P)$, P is the total number of elements in P_t, trajectories of the two vehicles are $\boldsymbol{f}[C_r^R(t)]$ and $\boldsymbol{f}[C_p^P(t)]$

Result: Dynamic Waiting Zone P_t

while $r \le R$ **do**

 if $\boldsymbol{f}[C_r^R(t)]$ and $\boldsymbol{f}\left[C_p^P(t)\right]$ $(\forall p \in P)$ have no potential conflicts **then**

  $v_{min}[C_r^R(t)] \leftarrow v$; #indicating $C_r^R(t)$ does not need to decelerate

 else then

  $v_{min}[{C^R}_r(t)] \leftarrow v_{op}[{C^R}_r(t)]$; #indicating ${C^R}_r(t)$ needs to decelerate (using Algorithm 2)

 end

 $r \leftarrow r + 1$;

 $P \leftarrow P + 1$;

 ${C^P}_P(t) \leftarrow {C^R}_r(t)$; #put the request vehicle into current existing passing sequence

end

Algorithm 2: Minimize total delay

Data: given a CAV, $C_{ijk}^{n_1}(q)$, and its trajectory $\boldsymbol{f}[C_{ijk}^{n_1}(q)\,]$, and deceleration time q_{n_1}, a new coming CAV $C_{ijk}^{n_2}(q)$, and its possible trajectory $\boldsymbol{f}[C_{ijk}^{n_2}(q)\,]$, design speed v

Result: deceleration time q_{n_2}, minimum total delay $OPT_{min}(q_{n_1}, q_{n_2})$ and departure time T'_{n_2}

```
#Taking two CAVs as an example
v_{n_2} ← v; #Set initial speed as maximum speed
q_{n_2} ← 0; #Set initial delay as 0
#Checking if there are any potential conflicts
while x* ∈ 𝕏 do
   while y* ∈ 𝕐 do
      while e* ∈ E do
         if f[C_{ijk}^{n_1}(q)]|_(x*,y*,e*) equals to f[C_{ijk}^{n_2}(q)]|_(x*,y*,e*) , then
            v_{n_2} ← v_{n_2}|_(x*,y*,e*); #Let the new coming vehicle decelerate
            q_{n_2} ← q_{n_2}|_(x*,y*,e*); #The delay of the new coming vehicle
            OPT(q_{n_1}, q_{n_2}) ← OPT(q_{n_1}, q_{n_2})|_(x*,y*,e*); #The value of optimization goal
            if OPT(q_{n_1}, q_{n_2}) < OPT_min(q_{n_1}, q_{n_2}) , then
               OPT_min(q_{n_1}, q_{n_2}) ← OPT(q_{n_1}, q_{n_2}); #Update the minimum total delay
            end
         end
      end
   end
```

```
end
```

5.4 Summary

Both the FCFS intersection management strategy and the DFROC optimization algorithm are employed for determining the passing sequence of CAVs in the CAVIMM. Considering the status of all CAVs, an optimization problem with nonlinear constraints (trajectories are nonlinear) is proposed and solved in this study to minimize the total traffic delay at intersections by constraining any pair of conflicting CAVs not passing through the potential collision areas at the same time. The trajectory coordinate model created in Chapter 4 helps to formulate and predict all CAV movement status within the intersection. The constraints in the optimization process to ensure that there are no global solutions to the trajectory sets of any two potentially conflicting vehicles (any solution for the trajectory formulation set indicates a collision between conflicting CAVs). Minimization of total traffic delay by identifying the passing order of all approaching CAVs through the intersection helps reduce unused intersection resources (space and time) and improve traffic mobility.

CHAPTER 6. PERFORMANCE EVALUATION

6.1 Introduction

Due to the complexity of field implementation, most researchers use traffic simulation to validate their proposed strategies for CAV control (Li et al., 2013a). The commercial microscopic traffic simulation software, PTV VISSIM, which has been used worldwide, is deployed for evaluating the performance of the CAVIMM. In this Chapter, a VISSIM-based simulation platform is developed and the performance of CAVIMM is compared with traditional signal control at a 4-leg intersection. Traffic volume during peak hours was collected and used as the input in the simulation. This section presents the experimental simulation platform development and discusses the experimental results.

6.2 Data Description

Previous studies (Au et al., 2011; Shahidi et al., 2011) have found that there would be a starvation issue when the traffic demands are unbalanced. Due to the difficulty of making a reservation, the approaching vehicles formulate a waiting queue at the entrance of the intersection in the approach of the side street. Therefore, this study is conducted on a 4-leg intersection with balanced traffic demands.

6.2.1 Signalized intersection geometric configuration

The evaluation of the CAVIMM system's performance is conducted for a real signalized 4-leg intersection with three lanes per direction, which is located at Lomas Boulevard at Eubank Boulevard, Albuquerque, New Mexico, USA. Lomas Boulevard at this intersection is a six-lane, two-way, divided roadway with the functional classification of urban major collector and a posted speed limit of 35 mph. Eubank Blvd is a six-lane, two-way, divided roadway. It has the functional classification of urban major collector and a posted speed limit of 35 mph as well. The intersection of Lomas Boulevard and Eubank Boulevard is controlled by an actuated signal. There are no dedicated turning lanes along any approach. The three lanes in each approach include one shared left-turn/through lane, one through lane and one shared through/right-turn lane with width of 12 ft for each lane. This intersection is shown in Figure 6.1.

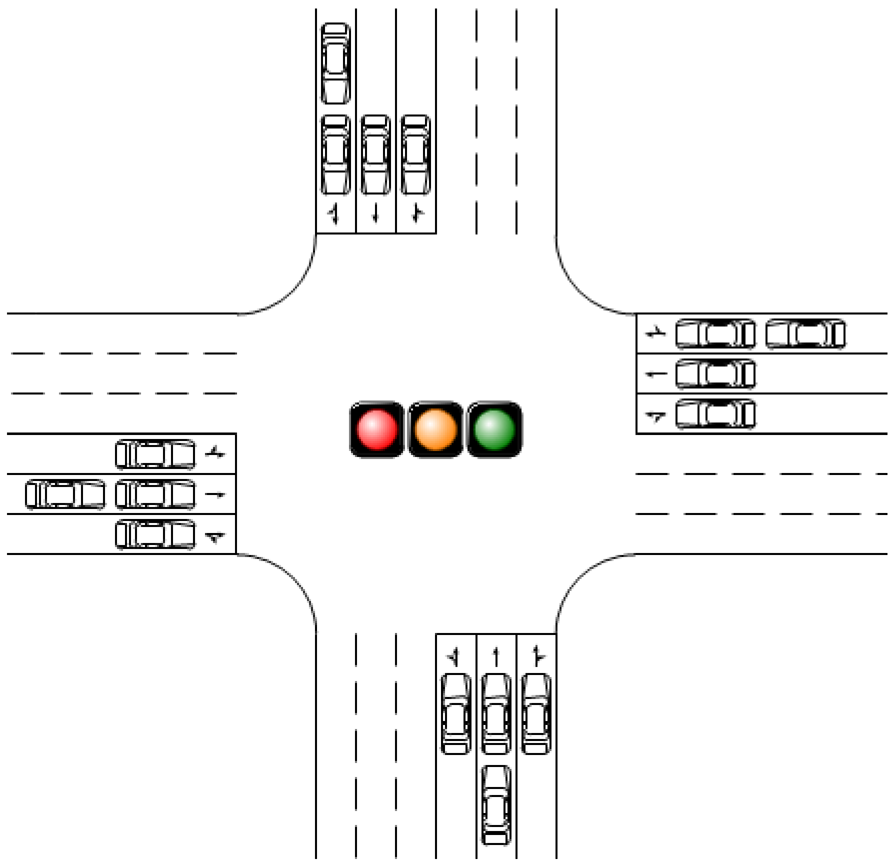

Figure 6.1 Signalized Intersection Configuration for Simulation

6.2.2 Traffic volume data

Manual intersection traffic counts were taken at the subject intersection during 3:30 PM-5:30 PM, and the average peak hour volume is shown in Table 6.1. The volume of through traffic is much higher than that of turning movement traffic. The northbound and southbound traffic are the highest during PM peak hours.

Table 6.1 Traffic Volume (Peak Hour)

	Left Turn	Through	Right Turn	Total
Northbound (r_2)	113	895	146	1154
Westbound (r_4)	155	679	88	922
Southbound (r_6)	162	1046	146	1354
Eastbound (r_8)	108	806	243	1157

6.3 Experiment Design

6.3.1 Simulation scenario design

There are three systems designed for simulation in this study in order to compare the performance of the CAVIMM with traditional signal control. The first simulation system is an isolated intersection with actuated signal control. The subject intersection has pedestrian and bicycle facilities. However, the CAVIMM system is developed based on the assumption that pedestrians and bicyclists are not considered. In order to avoid impacts of pedestrians and bicyclists on performance comparison, the signal control system is also developed without considering non-motorized mode signal plan and volumes. The CAVs in the CAVIMM system can make any movements at any lane, which is different from the signalized configuration with turning movement restriction. Therefore, the second simulation system, CAVIMM with Existing intersection Configuration (CAVIMM-EC), is designed and shown in Figure 6.2 (a). The third system is designed for CAVIMM system as shown in Figure 6.2 (b).

Manual traffic counts were collected in the field during PM peak hours at the studied intersection. In order to test the performance of the proposed intersection management mechanism under different volumes, different traffic volume inputs, which vary from 50% to 150% of collected peak hour counts, are tested. Scenarios using volume input under actual collected volume data represent the conditions of non-peak hour, and these of volume above the collected volume data show situations with volume growth in the future. Therefore, 11 scenarios with different volume inputs are tested for each of the three control systems, including signal control, CAVIMM-EC and CAVIMM.

A buffer zone is set in the trajectory coordination model, TSDTCM, by adding a time interval, ΔE, when identifying potential collisions between any two CAVs. The critical condition to check if any two CAVs have the possibility to collide is set when any edges of a CAV can intersect, assuming perfect condition. However, in the simulation process, a buffer zone is added around the CAVs. If the buffer zones of any two CAVs intersect, a collision is assumed. This setting can help to account for some unpredictable situations such as the variation of speed and acceleration (or deceleration) rate, or emergency stops. In this study, two values of the buffer time intervals ΔE, including 1.5s and 2.0s, are tested.

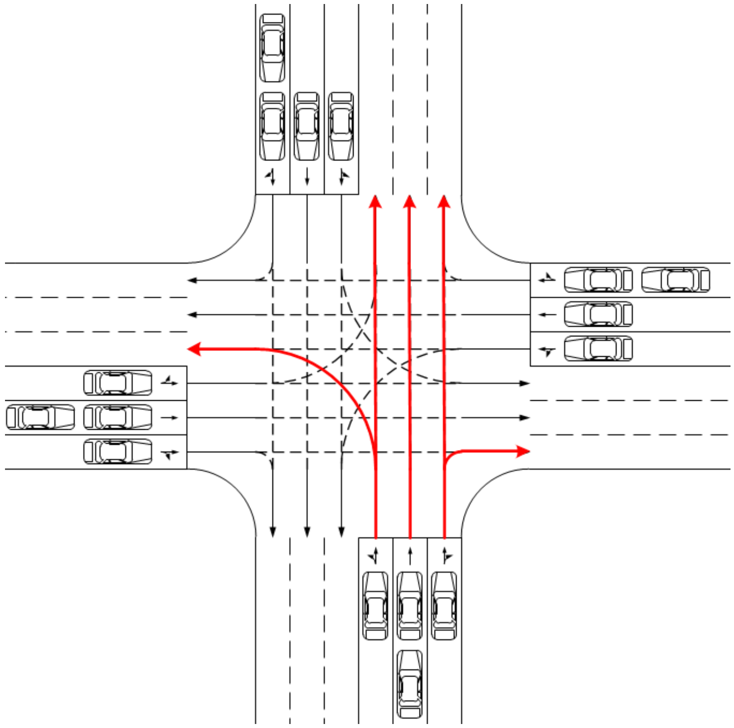

(a) Signalized/CAVIMM-EC Intersection

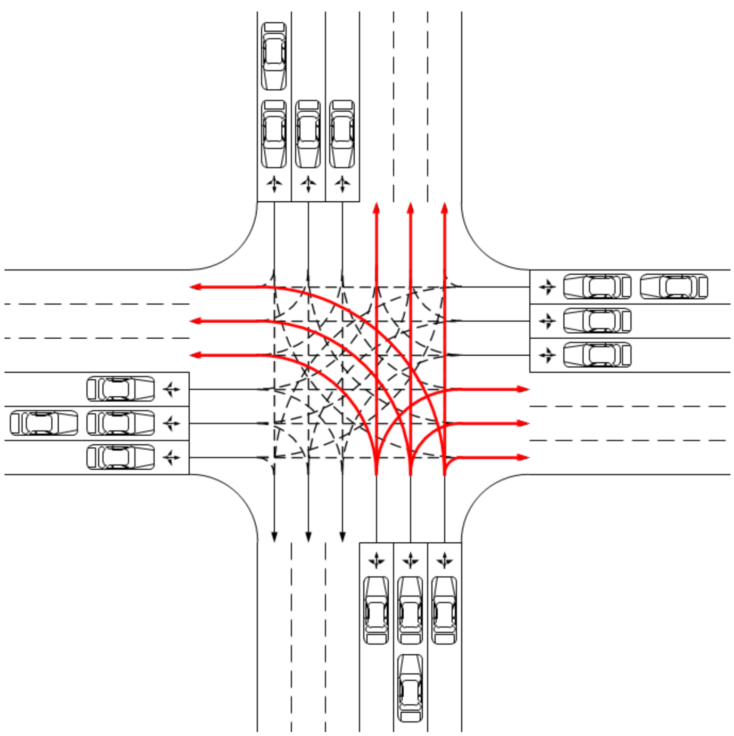

(b) CAVIMM Intersection

Figure 6.2 Intersection Configuration for Simulation

6.3.2 *Conflict area analysis for CAVIMM-EC*

Based on the TSDTCM system developed in Chapter 4, the possible trajectories in the CAVIMM-EC system have changed significantly. The traffic matrix of possible trajectories for CAVIMM-EC system is analyzed and summarized in Table 6.2. The cells colored as gray represent vehicle movement restrictions due to the intersection configuration. The leftmost lane for each approach is a shared left-turn/through lane; the right-turn movement is prohibited. The center lane of each approach is designed for through traffic; all turning movements are not allowed. The rightmost lane is a shared lane designed for right-turn and through traffic; the left-turn movement is prohibited.

Table 6.2 Traffic Matrix of the CAVIMM-EC Intersection

			Enter Lane (λ_{im})											
			i=2			*i*=4			*i*=6			*i*=8		
			λ_{21}	λ_{22}	λ_{23}	λ_{41}	λ_{42}	λ_{43}	λ_{61}	λ_{62}	λ_{63}	λ_{81}	λ_{82}	λ_{83}
Exit Lane (λ_{jn})	*j*=1	λ_{11}	×	×	×	t_{411}	×	×	t_{611}	×	×	×	×	×
		λ_{12}	×	×	×	×	×	×	×	t_{612}	×	×	×	×
		λ_{13}	×	×	×	×	×	×	×	×	t_{613}	×	×	t_{813}
	j=3	λ_{31}	×	×	×	×	×	×	t_{631}	×	×	t_{831}	×	×
		λ_{32}	×	×	×	×	×	×	×	×	×	×	t_{832}	×
		λ_{33}	×	×	t_{233}	×	×	×	×	×	×	×	×	t_{833}
	j=5	λ_{51}	t_{251}	×	×	×	×	×	×	×	×	t_{851}	×	×
		λ_{52}	×	t_{252}	×	×	×	×	×	×	×	×	×	×
		λ_{53}	×	×	t_{253}	×	×	t_{453}	×	×	×	×	×	×
	j=7	λ_{71}	t_{271}	×	×	t_{471}	×	×	×	×	×	×	×	×
		λ_{72}	×	×	×	×	t_{472}	×	×	×	×	×	×	×
		λ_{73}	×	×	×	×	×	t_{473}	×	×	t_{673}	×	×	×

According to the trajectory matrix of CAVIMM-EC, the potential conflicting trajectory tables should also be updated using the existing intersection configuration. The updated matrices for the northbound approach (r_2) are shown in Tables 6.3 to 6.7 as examples.

Table 6.3 Conflicting Trajectory Matrix for t_{233}

			Enter Lane (λ_{im})											
			i=2			i=2			i=2			i=2		
			λ_{21}	λ_{22}	λ_{23}	λ_{41}	λ_{42}	λ_{43}	λ_{61}	λ_{62}	λ_{63}	λ_{81}	λ_{82}	λ_{83}
Exit Lane (λ_{jn})	j=1	λ_{11}	×	×	×	t_{411}	×	×	t_{611}	×	×	×	×	×
		λ_{12}	×	×	×	×	×	×	×	t_{612}	×	×	×	×
		λ_{13}	×	×	×	×	×	×	×	×	t_{613}	×	×	t_{813}
	j=3	λ_{31}	×	×	×	×	×	×	t_{631}	×	×	t_{831}	×	×
		λ_{32}	×	×	×	×	×	×	×	×	×	×	t_{832}	×
		λ_{33}	×	×	t_{233}	×	×	×	×	×	×	×	×	t_{833}
	j=5	λ_{51}	t_{251}	×	×	×	×	×	×	×	×	t_{851}	×	×
		λ_{52}	×	t_{252}	×	×	×	×	×	×	×	×	×	×
		λ_{53}	×	×	t_{253}	×	×	t_{453}	×	×	×	×	×	×
	j=7	λ_{71}	t_{271}	×	×	t_{471}	×	×	×	×	×	×	×	×
		λ_{72}	×	×	×	×	t_{472}	×	×	×	×	×	×	×
		λ_{73}	×	×	×	×	×	t_{473}	×	×	t_{673}	×	×	×

Table 6.4 Conflicting Trajectory Matrix for t_{251}

			Enter Lane (λ_{im})											
			i=2			i=2			i=2			i=2		
			λ_{21}	λ_{22}	λ_{23}	λ_{41}	λ_{42}	λ_{43}	λ_{61}	λ_{62}	λ_{63}	λ_{81}	λ_{82}	λ_{83}
Exit Lane (λ_{jn})	j=1	λ_{11}	×	×	×	t_{411}	×	×	t_{611}	×	×	×	×	×
		λ_{12}	×	×	×	×	×	×	×	t_{612}	×	×	×	×
		λ_{13}	×	×	×	×	×	×	×	×	t_{613}	×	×	t_{813}
	j=3	λ_{31}	×	×	×	×	×	×	t_{631}	×	×	t_{831}	×	×
		λ_{32}	×	×	×	×	×	×	×	×	×	×	t_{832}	×
		λ_{33}	×	×	t_{233}	×	×	×	×	×	×	×	×	t_{833}
	j=5	λ_{51}	t_{251}	×	×	×	×	×	×	×	×	t_{851}	×	×
		λ_{52}	×	t_{252}	×	×	×	×	×	×	×	×	×	×
		λ_{53}	×	×	t_{253}	×	×	t_{453}	×	×	×	×	×	×
	j=7	λ_{71}	t_{271}	×	×	t_{471}	×	×	×	×	×	×	×	×
		λ_{72}	×	×	×	×	t_{472}	×	×	×	×	×	×	×
		λ_{73}	×	×	×	×	×	t_{473}	×	×	t_{673}	×	×	×

Table 6.5 Conflicting Trajectory Matrix for t_{252}

			Enter Lane (λ_{im})											
			i=2			i=2			i=2			i=2		
			λ_{21}	λ_{22}	λ_{23}	λ_{41}	λ_{42}	λ_{43}	λ_{61}	λ_{62}	λ_{63}	λ_{81}	λ_{82}	λ_{83}
Exit Lane (λ_{jn})	j=1	λ_{11}	×	×	×	t_{411}	×	×	t_{611}	×	×	×	×	×
		λ_{12}	×	×	×	×	×	×	×	t_{612}	×	×	×	×
		λ_{13}	×	×	×	×	×	×	×	×	t_{613}	×	×	t_{813}
	j=3	λ_{31}	×	×	×	×	×	×	t_{631}	×	×	t_{831}	×	×
		λ_{32}	×	×	×	×	×	×	×	×	×	×	t_{832}	×
		λ_{33}	×	×	t_{233}	×	×	×	×	×	×	×	×	t_{833}
	j=5	λ_{51}	t_{251}	×	×	×	×	×	×	×	×	t_{851}	×	×
		λ_{52}	×	t_{252}	×	×	×	×	×	×	×	×	×	×
		λ_{53}	×	×	t_{253}	×	×	t_{453}	×	×	×	×	×	×
	j=7	λ_{71}	t_{271}	×	×	t_{471}	×	×	×	×	×	×	×	×
		λ_{72}	×	×	×	×	t_{472}	×	×	×	×	×	×	×
		λ_{73}	×	×	×	×	×	t_{473}	×	×	t_{673}	×	×	×

Table 6.6 Conflicting Trajectory Matrix for t_{253}

			Enter Lane (λ_{im})											
			i=2			i=2			i=2			i=2		
			λ_{21}	λ_{22}	λ_{23}	λ_{41}	λ_{42}	λ_{43}	λ_{61}	λ_{62}	λ_{63}	λ_{81}	λ_{82}	λ_{83}
Exit Lane (λ_{jn})	j=1	λ_{11}	×	×	×	t_{411}	×	×	t_{611}	×	×	×	×	×
		λ_{12}	×	×	×	×	×	×	×	t_{612}	×	×	×	×
		λ_{13}	×	×	×	×	×	×	×	×	t_{613}	×	×	t_{813}
	j=3	λ_{31}	×	×	×	×	×	×	t_{631}	×	×	t_{831}	×	×
		λ_{32}	×	×	×	×	×	×	×	×	×	×	t_{832}	×
		λ_{33}	×	×	t_{233}	×	×	×	×	×	×	×	×	t_{833}
	j=5	λ_{51}	t_{251}	×	×	×	×	×	×	×	×	t_{851}	×	×
		λ_{52}	×	t_{252}	×	×	×	×	×	×	×	×	×	×
		λ_{53}	×	×	t_{253}	×	×	t_{453}	×	×	×	×	×	×
	j=7	λ_{71}	t_{271}	×	×	t_{471}	×	×	×	×	×	×	×	×
		λ_{72}	×	×	×	×	t_{472}	×	×	×	×	×	×	×
		λ_{73}	×	×	×	×	×	t_{473}	×	×	t_{673}	×	×	×

Table 6.7 Conflicting Trajectory Matrix for t_{271}

			Enter Lane (λ_{im})											
			i=2			*i*=2			*i*=2			*i*=2		
			λ_{21}	λ_{22}	λ_{23}	λ_{41}	λ_{42}	λ_{43}	λ_{61}	λ_{62}	λ_{63}	λ_{81}	λ_{82}	λ_{83}
Exit Lane (λ_{jn})	*j*=1	λ_{11}	×	×	×	t_{411}	×	×	t_{611}	×	×	×	×	×
		λ_{12}	×	×	×	×	×	×	×	t_{612}	×	×	×	×
		λ_{13}	×	×	×	×	×	×	×	×	t_{613}	×	×	t_{813}
	j=3	λ_{31}	×	×	×	×	×	×	t_{631}	×	×	t_{831}	×	×
		λ_{32}	×	×	×	×	×	×	×	×	×	×	t_{832}	×
		λ_{33}	×	×	t_{233}	×	×	×	×	×	×	×	×	t_{833}
	j=5	λ_{51}	t_{251}	×	×	×	×	×	×	×	×	t_{851}	×	×
		λ_{52}	×	t_{252}	×	×	×	×	×	×	×	×	×	×
		λ_{53}	×	×	t_{253}	×	×	t_{453}	×	×	×	×	×	×
	j=7	λ_{71}	t_{271}	×	×	t_{471}	×	×	×	×	×	×	×	×
		λ_{72}	×	×	×	×	t_{472}	×	×	×	×	×	×	×
		λ_{73}	×	×	×	×	×	t_{473}	×	×	t_{673}	×	×	×

Since some movements are restricted at specified lanes in CAVIMM-EC, the total number of conflicting trajectories for each approach (Appendix A) decreases significantly compared to that of CAVIMM; this is summarized in Table 6.8. The total number of conflicting trajectories for each approach decreases from 136 to 36. The number of conflicting trajectories for right turning movements reduces from 19 to 1 after restricting right-turn movements on the two left lanes. The prohibition of left-turns from the right two lanes reduces the total number of potential conflicting trajectories from 63 to 9. The number of conflicting trajectory for straight movement reduces from 54 to 26; it is not as significant as the other two movements.

Table 6.8 Number of Conflicting Trajectories for Each Trajectory in CAVIMM-EC

			Enter Lane (λ_{im})															
			i=2				i=4				i=6				i=8			
			λ_{21}	λ_{22}	λ_{23}	T[a]	λ_{41}	λ_{42}	λ_{43}	T	λ_{61}	λ_{62}	λ_{63}	T	λ_{81}	λ_{82}	λ_{83}	T
		λ_{11}	×	×	×		9	×	×		9	×	×		×	×	×	
	j=1	λ_{12}	×	×	×	0	×	×	×	9	×	8	×	26	×	×	×	1
		λ_{13}	×	×	×		×	×	×		×	×	9		×	×	1	
		λ_{31}	×	×	×		×	×	×		9	×	×		9	×	×	
	j=3	λ_{32}	×	×	×	1	×	×	×	0	×	×	×	9	×	8	×	26
Exit Lane (λ_{jn})		λ_{33}	×	×	1		×	×	×		×	×	×		×	×	9	
		λ_{51}	9	×	×		×	×	×		×	×	×		9	×	×	
	j=5	λ_{52}	×	8	×	26	×	×	×	1	×	×	×	0	×	×	×	9
		λ_{53}	×	×	9		×	×	1		×	×	×		×	×	×	
		λ_{71}	9	×	×		9	×	×		×	×	×		×	×	×	
	j=7	λ_{72}	×	×	×	9	×	8	×	26	×	×	×	1	×	×	×	0
		λ_{73}	×	×	×		×	×	9		×	×	1		×	×	×	
	T		18	8	10	36	18	8	10	36	18	8	10	36	18	8	10	36

Note: [a]Total number of conflicting trajectories

6.3.3 Evaluation criteria

In this study, the total traffic delay is used for evaluating the performance of intersection management mechanism. Level of Service (LOS), which is a function of total vehicle delay, is proposed in the Highway Capacity Manual 6th Edition (Transportation Reserach Board of The National Academies, 2010) to evaluate intersection operation conditions. It can be estimated for the entire intersection, for each intersection approach, and for each lane group. There are six levels in the LOS rating system ranging from A (best) to F (worst). The LOS for the entire signalized intersection is defined and shown in Table 6.9. If the total delay at an intersection is below 10 sec, the operation LOS of the intersection will be LOS A, indicating the least interrupted flow conditions with little or no delay. The operations with delay between 10 to 20 sec per vehicle (sec/veh) are defined as LOS B. Its cycle length is short and the progression is highly favorable. As the total traffic delay increases from 20 sec to 35 sec, the operation LOS will also fall into more inferior category, LOS C. Individual cycle failures may happen at this level and some vehicles may stop before passing through the intersection. LOS D describes operations with control delay between 35 and 55 sec/veh. Individual cycle failures become noticeable and many vehicles may stop before entering the intersection. When the total control delay increases up to between 55 and 80 sec/veh, the operation LOS is at LOS E, showing unfavorable progression and individual cycle failure is frequent. If the total delay is more than 80 sec/veh, the operational LOS will be the worst at LOS F. LOS F describes operations where most cycles fail to clear the queue.

Table 6.9 LOS Criteria for Signalized Intersection (HCM 2010)

Average Control Delay (sec/veh)	LOS by Volume-to-Capacity Ratio	
	<=1.0	>1.0
≤ 10.0	A	F
>10 and ≤20	B	F
>20 and ≤35	C	F
>35 and ≤55	D	F
>55 and ≤80	E	F
>80	F	F

The green book, A Policy on Geometric Design of Highways and Streets (AASHTO, 2011), provides appropriate LOS standards according to different combinations of area and terrain type as shown in Table 6.11. The urban major collector, which the study roadways are classified as, should be designed to be operated at an appropriate LOS D or better.

Table 6.10 Guidelines for Selection of Design Levels of Service (AASHTO, 2011)

Functional Class	Appropriate Level of Service for Specified Combinations of Area and Terrain Type			
	Rural Level	Rural Rolling	Rural Mountainous	Urban and Suburban
Freeway	B	B	C	C or D
Arterial	B	B	C	C or D
Collector	C	C	D	D
Local	D	D	D	D

6.4 Evaluation Platform Development

6.4.1 Basic settings

1) Intersection configuration

There are three simulation systems conducted to evaluate the individual performance of the intersection management mechanisms, including traditional signal control system, CAVIMM-EC system and CAVIMM system, under the same intersection geometric layout. Traffic movement restriction is applied on specified lanes in the systems for signal control and CAVIMM-EC: for each approach, the leftmost lane is designed for left-turn and through traffic only, the central lane is for through traffic only and the right lane is for through and right-turn traffic only. Note that no exclusive turning lane exists in all simulation scenarios. Therefore, two intersection configurations with different lane settings are developed in VISSIM using the same intersection layout. The width of each lane is 12 ft (W=12 ft).

2) Control area design

The Design Speed (DS) for this intersection is 35 mph (DS=51.33 ft/s), which is the posted speed limit of the two roadways crossing the studied intersection. The acceleration or deceleration rate is equal to 11.26 ft/s^2 (0.35g). After sending a request to the ICC within DZ, CAVs are waiting for the decision made by the ICC in the DWZ. All CAVs without request approval have to decelerate with a rate of 11.26 ft/s^2. The extreme scenario for the CAVs whose requests are rejected all the time is that their speeds reduce to zero. If the speeds of CAVs are equal to zero, the ICC will assign the right-of-way to these stopped CAVs to avoid blocking the whole traffic lanes. Then the stopped CAVs will accelerate with a rate of 11.26 ft/s^2 until the speed reaches the DS before entering the intersection. Based on the settings of DS and acceleration/deceleration rate, the length of DWZ is set at 240 feet to ensure the CAVs in the worst scenario can accelerate to the DS before entering the intersection. The whole process for CAVs which are fully stopped within the DWZ are presented in Table 6.11, and the corresponding settings are shown in Figure 6.3.

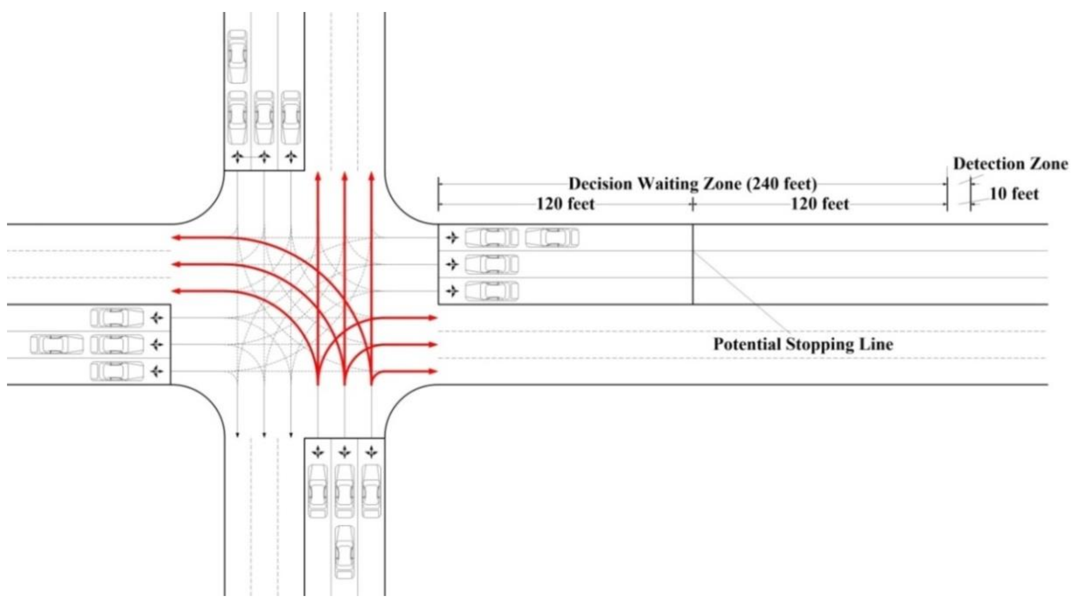

Figure 6.3 CAVIMM Intersection Configuration

Table 6.11 Full Process of Deceleration and Acceleration of a CAV

Deceleration Zone				Acceleration Zone			
Time (s)	Speed (ft/s)	Deceleration Rate (ft/s^2)	Distance to Intersection (ft)	Time (s)	Speed (ft/s)	Acceleration Rate (ft/s^2)	Distance to Intersection (ft)
0	51.33	11.26	240	0	0	11.26	120
0.1	50.2	11.26	234.87	0.1	1.13	11.26	119.89
0.2	49.08	11.26	229.85	0.2	2.25	11.26	119.66
0.3	47.95	11.26	224.94	0.3	3.38	11.26	119.32
0.4	46.83	11.26	220.14	0.4	4.5	11.26	118.87
0.5	45.7	11.26	215.46	0.5	5.63	11.26	118.31
0.6	44.57	11.26	210.89	0.6	6.76	11.26	117.64
0.7	43.45	11.26	206.43	0.7	7.88	11.26	116.85
0.8	42.32	11.26	202.09	0.8	9.01	11.26	115.95
0.9	41.2	11.26	197.86	0.9	10.13	11.26	114.93
1	40.07	11.26	193.74	1	11.26	11.26	113.81
1.1	38.94	11.26	189.73	1.1	12.39	11.26	112.57
1.2	37.82	11.26	185.84	1.2	13.51	11.26	111.22
1.3	36.69	11.26	182.05	1.3	14.64	11.26	109.75
1.4	35.57	11.26	178.38	1.4	15.76	11.26	108.18
1.5	34.44	11.26	174.83	1.5	16.89	11.26	106.49
1.6	33.31	11.26	171.38	1.6	18.02	11.26	104.69
1.7	32.19	11.26	168.05	1.7	19.14	11.26	102.77
1.8	31.06	11.26	164.83	1.8	20.27	11.26	100.75
1.9	29.94	11.26	161.73	1.9	21.39	11.26	98.61

Table 6.11 (Continued) Full Process of Deceleration and Acceleration of a CAV

2	28.81	11.26	158.73	2	22.52	11.26	96.35
2.1	27.68	11.26	155.85	2.1	23.65	11.26	93.99
2.2	26.56	11.26	153.08	2.2	24.77	11.26	91.51
2.3	25.43	11.26	150.43	2.3	25.9	11.26	88.92
2.4	24.31	11.26	147.89	2.4	27.02	11.26	86.22
2.5	23.18	11.26	145.46	2.5	28.15	11.26	83.41
2.6	22.05	11.26	143.14	2.6	29.28	11.26	80.48
2.7	20.93	11.26	140.93	2.7	30.4	11.26	77.44
2.8	19.8	11.26	138.84	2.8	31.53	11.26	74.28
2.9	18.68	11.26	136.86	2.9	32.65	11.26	71.02
3	17.55	11.26	134.99	3	33.78	11.26	67.64
3.1	16.42	11.26	133.24	3.1	34.91	11.26	64.15
3.2	15.3	11.26	131.59	3.2	36.03	11.26	60.55
3.3	14.17	11.26	130.06	3.3	37.16	11.26	56.83
3.4	13.05	11.26	128.65	3.4	38.28	11.26	53
3.5	11.92	11.26	127.34	3.5	39.41	11.26	49.06
3.6	10.79	11.26	126.15	3.6	40.54	11.26	45.01
3.7	9.67	11.26	125.07	3.7	41.66	11.26	40.84
3.8	8.54	11.26	124.1	3.8	42.79	11.26	36.56
3.9	7.42	11.26	123.25	3.9	43.91	11.26	32.17
4	6.29	11.26	122.51	4	45.04	11.26	27.67
4.1	5.16	11.26	121.88	4.1	46.17	11.26	23.05
4.2	4.04	11.26	121.36	4.2	47.29	11.26	18.32

Table 6.11 (Continued) Full Process of Deceleration and Acceleration of a CAV

4.3	2.91	11.26	120.96	4.3	48.42	11.26	13.48
4.4	1.79	11.26	120.67	4.4	49.54	11.26	8.53
4.5	0.66	11.26	120.49	4.5	50.67	11.26	3.46
4.6	0	6.6	120	4.6	51.33	0.66	0

3) Traffic volume input

According to the conflict point distribution of through movements (shown in Table 6.8), the volume input for through traffic in the system of CAVIMM-EC is assumed to be evenly distributed on three lanes, whereas the volume input of all movements in the CAVIMM system is evenly distributed of three movements on three lanes. Therefore, the volume for each approach is slightly adjusted based on the data shown in Table 6.1, so that the even distribution of traffic counts for three movements on three lanes can be met in the CAVIMM system.

Table 6.12 Traffic Volume Input for Simulation

		Left Turn	Through	Right Turn	Total
50% Collected Traffic Counts	r_2	57	447	75	579
	r_4	78	339	45	462
	r_6	81	525	75	681
	r_8	54	405	123	582
60% Collected Traffic Counts	r_2	69	537	87	693
	r_4	93	408	51	552
	r_6	96	627	87	810
	r_8	66	483	147	696

Table 6.12 (Continued) Traffic Volume Input for Simulation

70% Collected Traffic Counts	r_2	81	627	102	810
	r_4	108	474	60	642
	r_6	114	732	102	948
	r_8	75	564	171	810
80% Collected Traffic Counts	r_2	90	714	117	921
	r_4	126	543	69	738
	r_6	129	837	117	1083
	r_8	87	645	195	927
90% Collected Traffic Counts	r_2	102	804	132	1038
	r_4	141	609	78	828
	r_6	147	942	132	1221
	r_8	96	726	219	1041
100% Collected Traffic Counts	r_2	114	894	147	1155
	r_4	156	678	87	921
	r_6	162	1047	147	1356
	r_8	108	807	243	1158
110% Collected Traffic Counts	r_2	126	984	162	1272
	r_4	171	747	96	1014
	r_6	177	1152	162	1491
	r_8	120	888	267	1275

Table 6.12 (Continued) Traffic Volume Input for Simulation

120% Collected Traffic Counts	r_2	138	1074	177	1389
	r_4	186	813	105	1104
	r_6	195	1257	177	1629
	r_8	129	969	291	1389
130% Collected Traffic Counts	r_2	147	1161	192	1500
	r_4	204	882	114	1200
	r_6	210	1362	192	1764
	r_8	141	1050	315	1506
140% Collected Traffic Counts	r_2	159	1251	207	1617
	r_4	219	948	123	1290
	r_6	228	1467	207	1902
	r_8	150	1131	339	1620
150% Collected Traffic Counts	r_2	171	1341	222	1734
	r_4	234	1017	132	1383
	r_6	243	1572	222	2037
	r_8	162	1212	366	1740

6.4.2 Simulation model setup in VISSIM

The traffic simulation software, VISSIM, is used to evaluate the performance of the proposed intersection control mechanisms. The intersection with three lanes for each direction in VISSIM is shown in Figure 6.4.

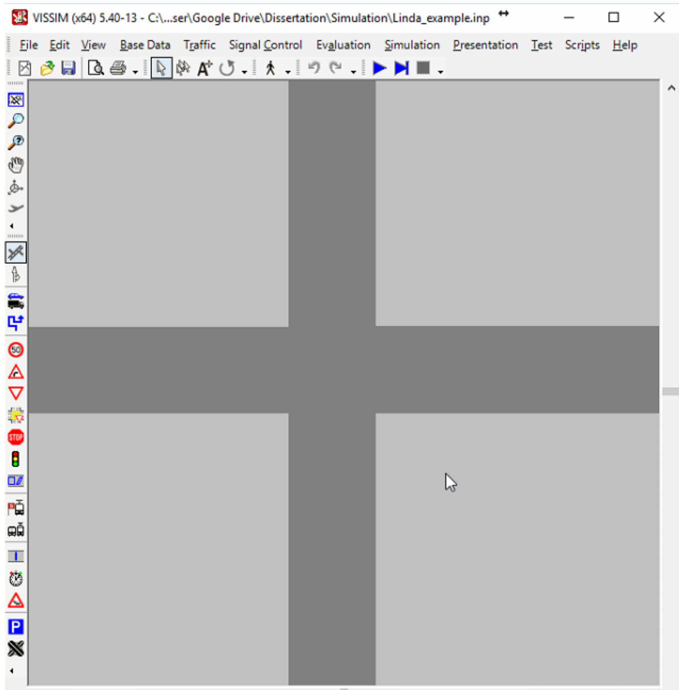

Figure 6.4 Intersection Layout in VISSIM

Based on the settings discussed above, three intersection models are conducted in VISSIM, including signal control intersection, the CAVIMM-EC intersection and the CAVIMM intersection, as shown in Figure 6.5. CAVs can turn from any lane in the CAVIMM intersection. Therefore, no en-route lane change is required for turning vehicles, which theoretically minimizes the delay resulting from the conflicts caused by vehicle lane change maneuvers. Roadways are assumed to have zero grades.

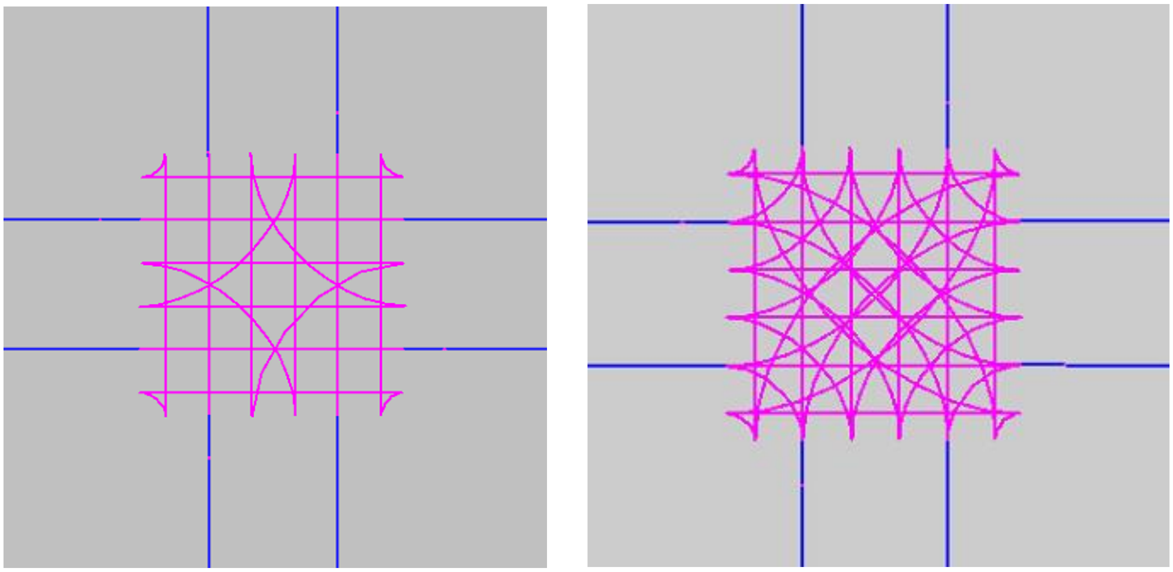

(a) Signal Control/CAVIMM-EC Intersection **(b) CAVIMM Intersection**

Figure 6.5 Intersection Design for Simulation in VISSIM

6.4.3 VISSIM COM server

VISSIM can be applied from within other applications serving as a toolbox for any traffic simulation purposes (PTV, 2012). A novel external module is developed via the VISSIM Component Object Model (COM) interface. The COM interface provides access to data and simulation parameters, allowing VISSIM to simulate them as an Automation Server and to export simulation results requested by users. The COM interface is quite flexible and user-friendly in collecting vehicle information and modifying vehicle parameters during the simulation process. It supports Microsoft Automation so that any of the Rapid Application Development (RAD) tools using various scripting languages, including Visual Basic Script and Java Script, and programming environments such as Visual C++ or Visual J++, can be deployed.

The proposed CAVIMM-EC and CAVIMM are developed and implemented through the VISSIM COM server. This external module can provide sufficient flexibility to satisfy any specific demands from particular researchers and practitioners for CAV control operations.

6.4.4 Simulation process

During a simulation run, VISSIM calls the COM at every simulation step (0.1s), and communication between CAVs and the ICC is conducted at each simulation step. The ICC processes all reservation requests at the beginning of each simulation step, and passes its decision (position in passing sequence) to the CAVs in the same simulation step, and thus the real-time control of each CAV in the intersection is realized. Simulation time is set as one hour (3600 seconds).

CAVs in three stages are labeled with three colors. The original color of CAVs is blue. After entering the DZ, CAVs with rejected requests start to decelerate with the color of red. Once they make a reservation successfully, CAVs will accelerate at a rate of 11.26 ft/s^2, and they are marked with the green color. The color of CAVs turns to blue when they exit the intersection. Figures 6.6 and 6.7 show the screen shots of a simulation run in the CAVIMM-EC or CAVIMM intersection.

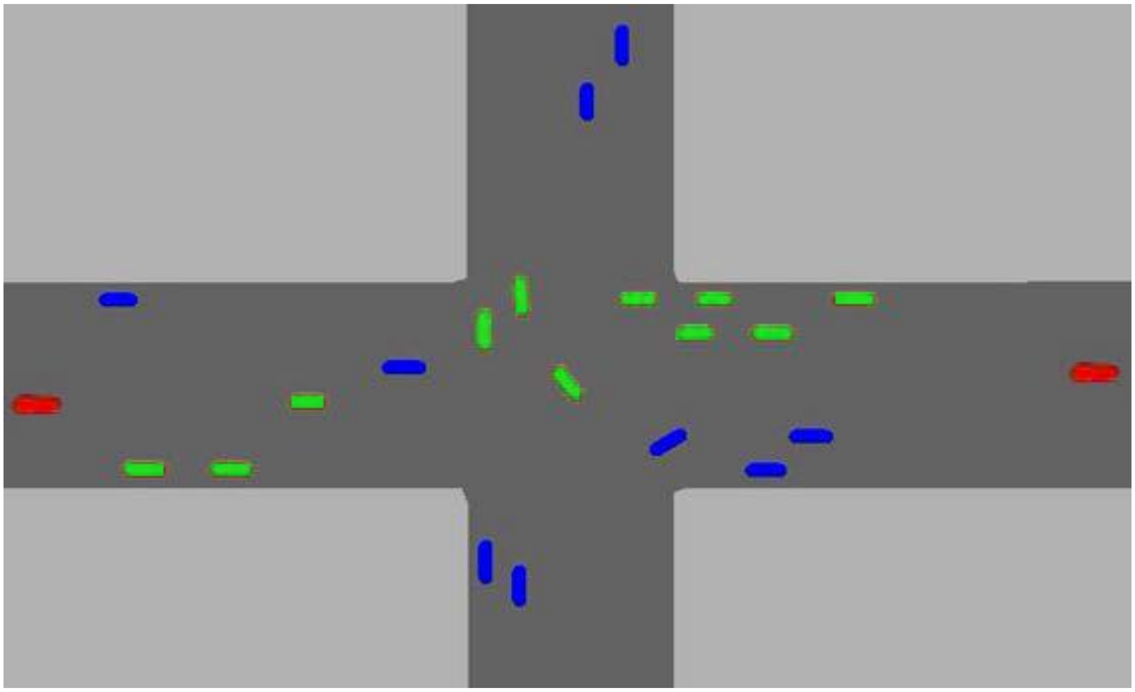

Figure 6.6 Example of Simulation Animation of DFROC Model in VISSIM

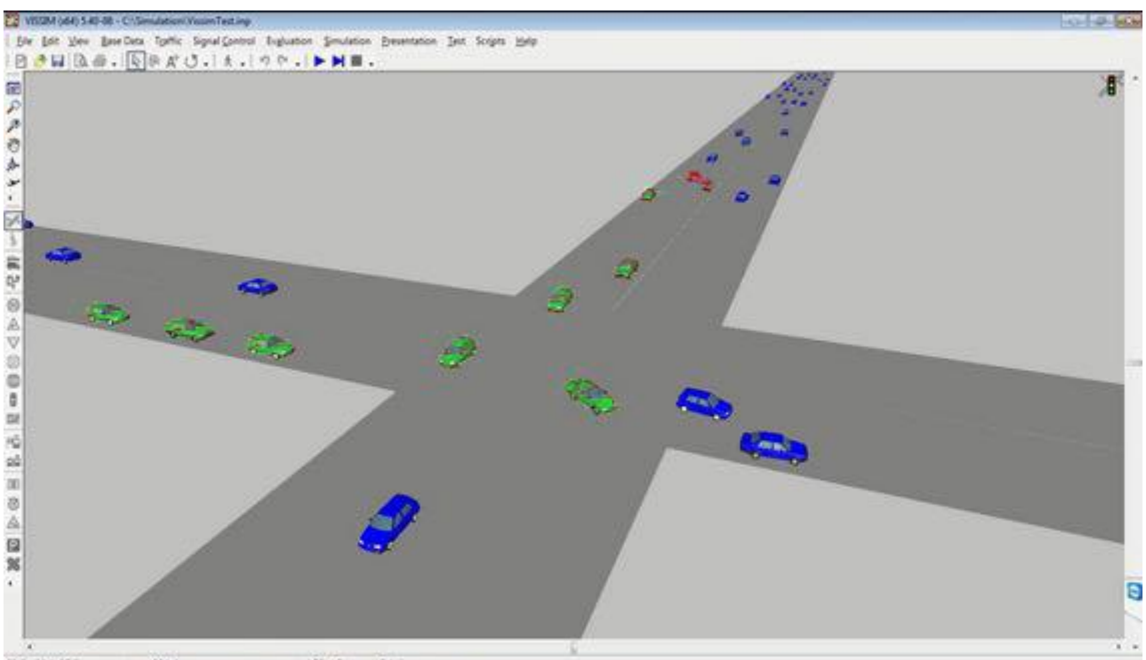

Figure 6.7 3D View of Simulation in VISSIM

6.5 Experimental Results and Discussion

Evaluation results for all the scenarios are summarized and compared in Table 6.13, including total traffic delay and total number of vehicle throughout the intersection. The LOS for the intersection is also shown in Table 6.13. The comparison among those control strategies in terms of total traffic delay and total number of vehicle throughput is shown in Figure 6.7.

6.5.1 Comparison between CAVIMM and traditional signal control

As shown in Figure 6.8, both CAVIMM-EC and CAVIMM significantly outperform signal control by resulting in much lower traffic delay under all simulation scenarios. The influence of volume increase on total traffic delay at the signalized intersection varies as the volume changes. The total delay increases slowly from 43.5s (LOS D) to 62.0s (LOS E) as the traffic volume increases from 50% to 110% of collected peak hour volume. The total delay for signal control reaches 105.0s with operation LOS F when the traffic volume is equal to 110% of peak hour volume, indicating extreme delay and oversaturated traffic flow. After reaching the intersection capacity, traffic delay goes up dramatically as traffic volume increases. However, the impact of traffic volume on traffic delay in CAVIMM-EC and CAVIMM is not as significant as that under signal control. With the same intersection geometric configuration with signal control, the total delay in CAVIMM-EC and CAVIMM range from 1.3s to 14.7s as the traffic volumes increase from 50% to 150% of peak hour volume, which is dramatically lower than that of signal control. The operation LOS for each scenario in both CAVIMM-EC and CAVIMM is LOS B or better. The experimental results show that the proposed CAVIMM system far outperforms traditional signal control in terms of significant improvement of intersection total traffic delay.

Furthermore, as shown in Figure 6.7(b), after reaching the capacity of intersection under signal control, the intersection cannot handle the increasing volume due to oversaturation, making the total number of throughput vehicles lower than that in CAVIMM-EC and CAVIMM. The capacity of the intersection was improved by switching control strategy to CAVIMM.

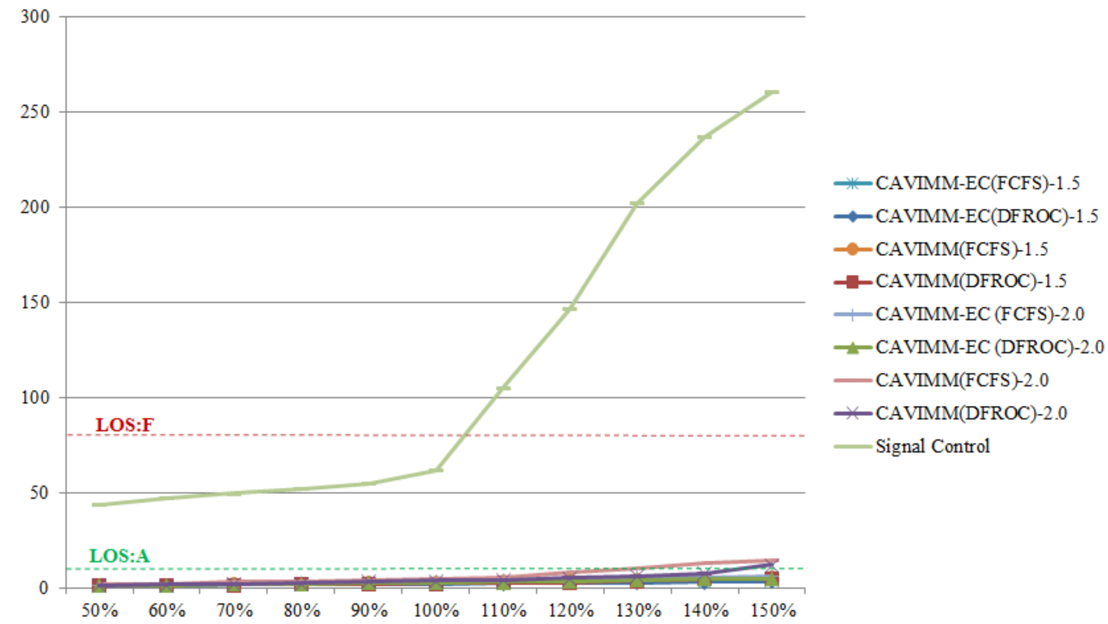

(a) Total Traffic Delay

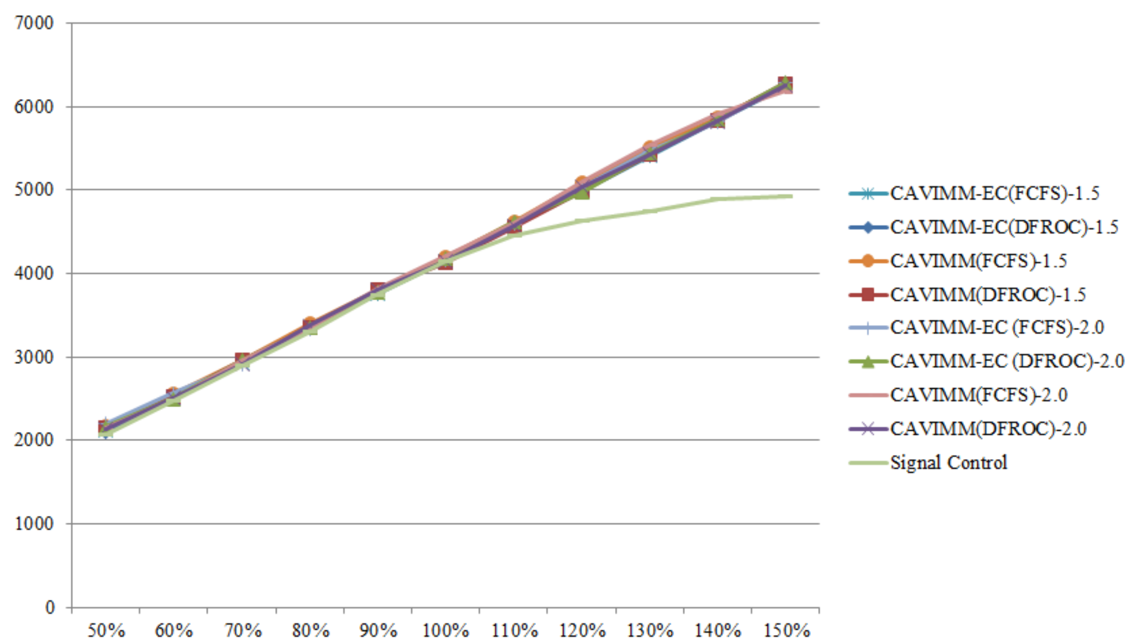

(b) Total Number of Vehicle Throughput

Figure 6.8 Simulation Result Comparison

6.5.2 Comparison between CAVIMM-EC and CAVIMM

The movement restrictions in signalized intersection and CAVIMM-EC are released in CAVIMM which is expected to outperform CAVIMM-EC through increasing intersection capacity especially for turning movements by enabling CAVs make any movement from any lane. However, as shown in Figure 6.9, if the total traffic volume is lower than 110% of collected peak hour volume, the total delay in CAVIMM is slightly higher than that in the CAVIMM-EC for both scenarios with buffer zone ΔE of 1.5s and 2.0s and the scenarios with different passing sequence algorithms FCFS and DFROC, respectively. The operation levels are LOS A, which are also much lower than those of signal control. For each scenario with traffic volumes larger than 120% of collected peak hour volume, the difference between the CAVIMM-EC and the CAVIMM regarding the total traffic delay becomes significant.

This may be explained by the reduction of potential conflicting trajectories due to restricting turn movements on specific lanes. The traffic conflict matrices for CAVIMM-EC are presented in Tables 6.15 to 6.29 at the end of this chapter and summarized in Table 6.8. The total number of conflict points decreases from 136 to 36 using signalized intersection geometric configuration. Simultaneously, as the total traffic volume increases, the possibility of potential collisions also decreases in the CAVIMM-EC compared with the CAVIMM. Then the possibility for conflicting CAVs speed reduction to avoid collision will also reduce, which helps reduce the total traffic delay.

The delay in CAVIMM-EC and CAVIMM are both below 16s with operation LOS B or better across all volume inputs, showing the least interrupted flow conditions with little or no delay.

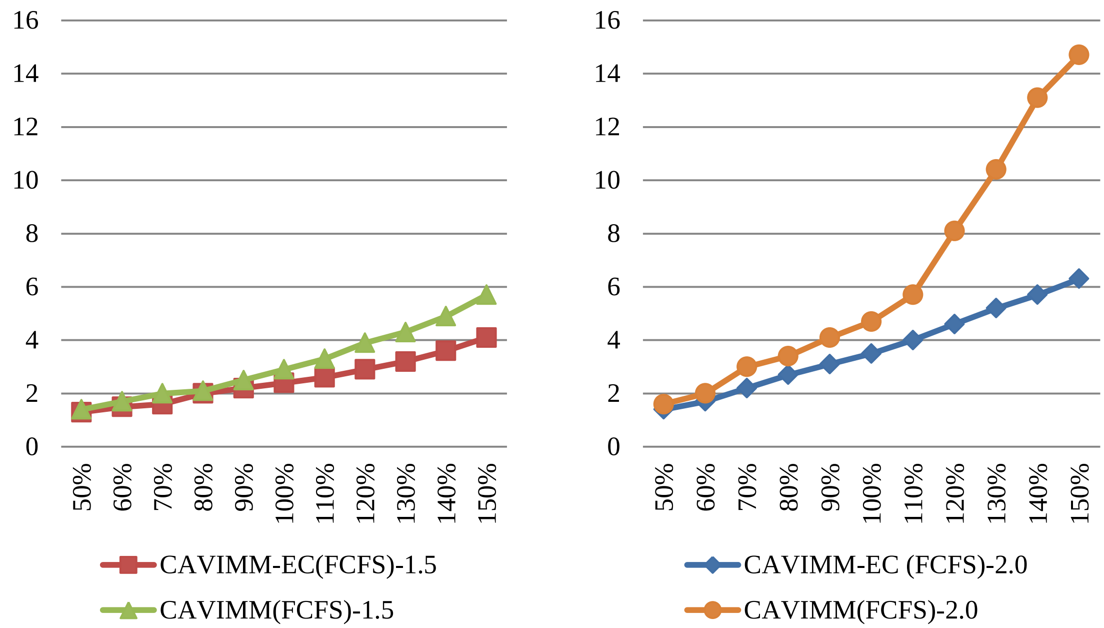

(a) Total traffic delay for CAVIMM-EC and CAVIMM with FCFS algorithm

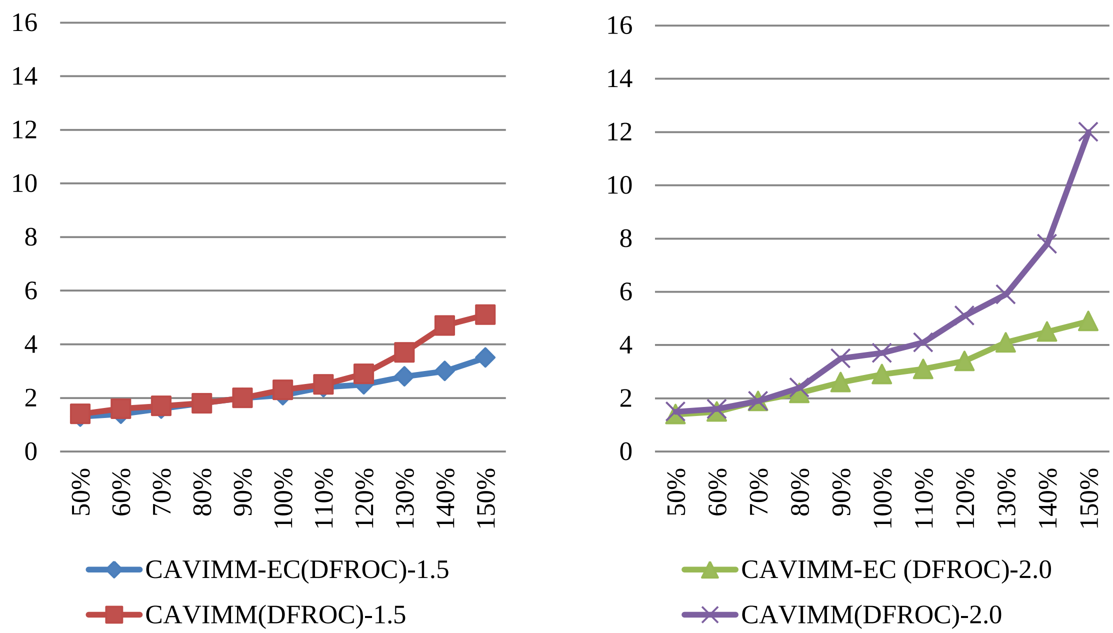

(b) Total traffic delay for CAVIMM-EC and CAVIMM with DFROC algorithm

Figure 6.9 Comparison between CAVIMM-EC and CAVIMM

6.5.3 Comparison between FCFS and DFROC

The total traffic delay for both the CAVIMM-EC and the CAVIMM is reduced if the DFROC is employed compared to the FCFS control. By implementing the DFROC, the objective function is optimized through assigning right-of-way to conflicting CAVs in an optimal order instead of doing that based on their arrival times. When the traffic volume is low, the difference between control system with FCFS and that with DFROC is not significant regardless of the size of buffer zone. This may be explained by the fact that the vehicle headway is larger when traffic volume is low, making the optimal passing sequence become roughly equal to the passing sequence determined by the arrival time. As the traffic volume increases, vehicle headway becomes shorter, which increases the number of conflicting CAVs. Then the passing sequence of an increasing number of CAVs with potential conflicts matters. As the buffer zone size increases from 1.5s to 2.0s, the improvement of reducing total traffic delay by the DFROC becomes significant compared to the FCFS. This may be attributed to the fact that larger size of buffer zones increases the possibility of potential conflicting CAVs. Then the impacts of passing sequence algorithm on reducing traffic delay increase.

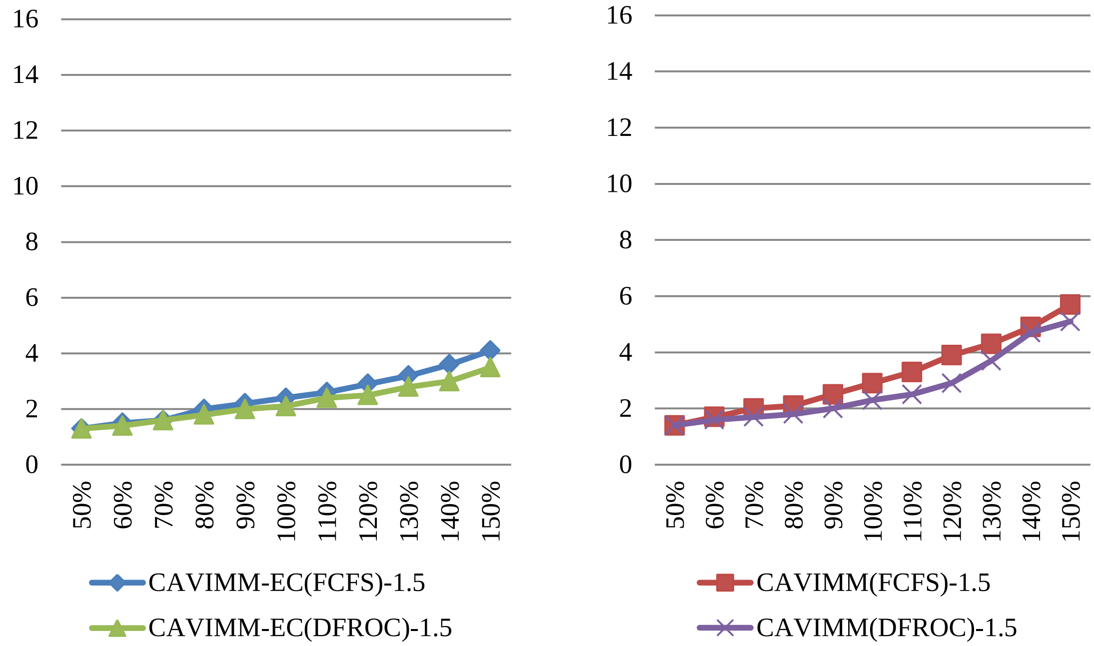

(a) Total traffic delay for different passing sequence algorithms

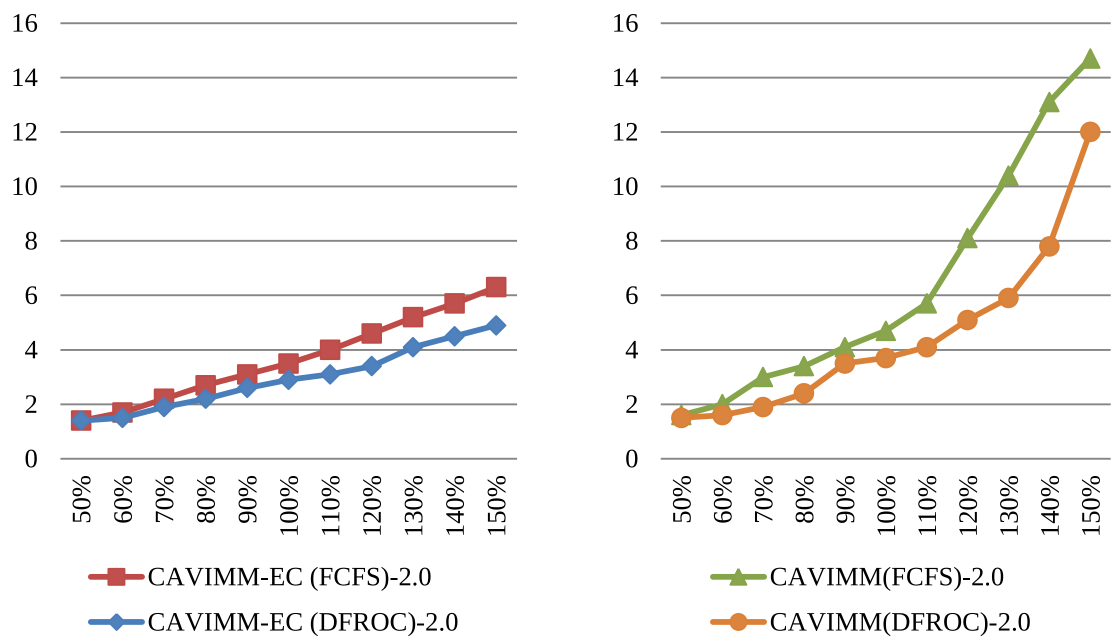

(a) Total traffic delay for different passing sequence algorithms

Figure 6.10 Comparison between FCFS and DFROC

6.5.4 *Comparison between different sizes of buffer zone*

Two sizes of buffer zone are tested in this study, including 1.5s and 2.0s. As expected, the total traffic delay increases as the size of buffer zone grows. Larger buffer zone means the size of potential collision areas is enlarged, and therefore, larger buffer zone generates a higher collision potential of two CAVs. A larger number of conflicting CAVs identified by ICC will result in additional delay at intersections, which can account for the simulation result that total delay in the CAVIMM is larger than that of the corresponding CAVIMM-EC. The rate of total delay increase for the CAVIMM becomes significant when the traffic volume increases from 130% to 150% of peak hour volume. The total delay for the CAVIMM using the FCFS with 130% of peak hour volume arrives at operation LOS B when the buffer zone is 2.0s. The delay for the CAVIMM using the FCFS, under all scenarios of various traffic volumes, is below 10s, resulting in LOS A.

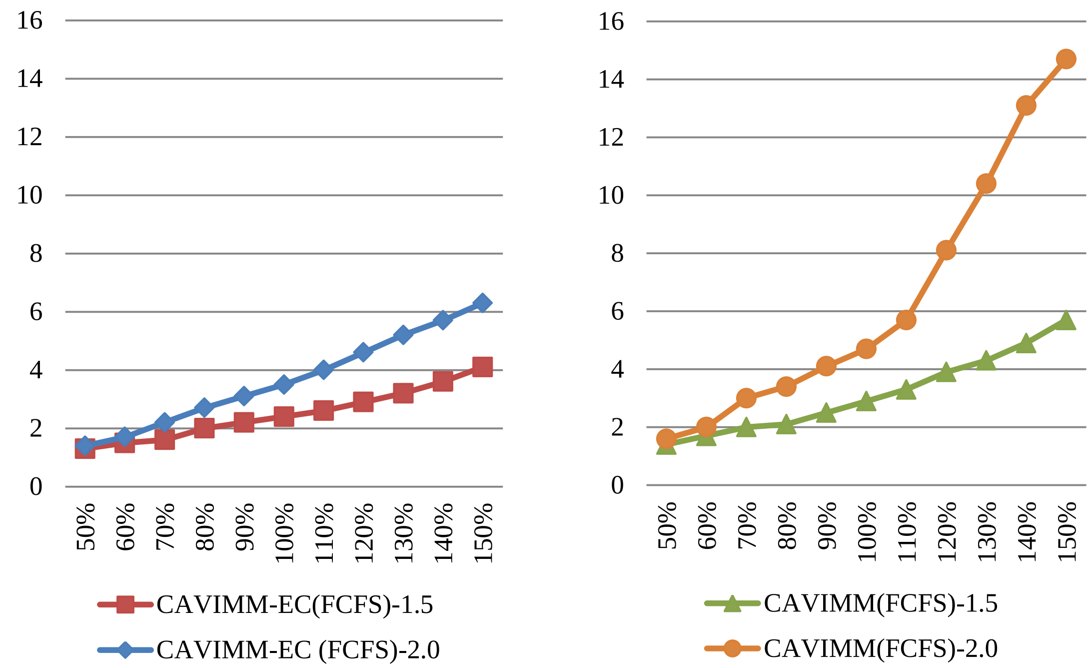

(a) Total traffic delay in CAVIMM-EC and CAVIMM with different buffer zone

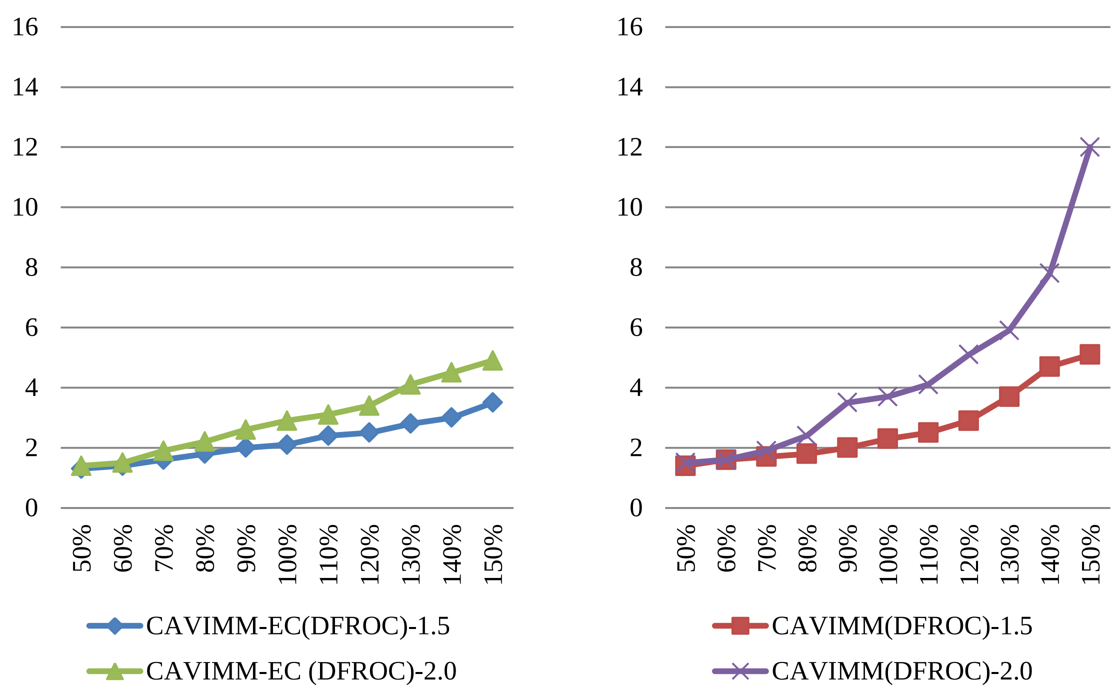

(b) Total traffic delay in CAVIMM-EC and CAVIMM with different buffer zone

Figure 6.11 Comparison between Different Buffer Zones

Table 6.13 Comparison for Signal Control, CAVIMM-EC and CAVIMM with FCFS

	Signal Control			CAVIMM-EC(FCFS)			CAVIMM-EC(FCFS)			CAVIMM (FCFS)			CAVIMM(FCFS)		
				Δt = 1.5s						Δt = 2.0s					
	TD[a]	VN[d]	LOS	TD[a]	VN[d]	LOS	TD[a]	VN[d]	LOS	TD[a]	VN[d]	LOS	TD[a]	VN[d]	LOS
50%	43.5	2070	D	1.3	2121	A	1.4	2166	A	1.4	2201	A	1.6	2154	A
60%	47.3	2481	D	1.5	2507	A	1.7	2555	A	1.7	2566	A	2	2498	A
70%	49.6	2898	D	1.6	2941	A	2	2963	A	2.2	2916	A	3	2961	A
80%	51.8	3307	D	2	3356	A	2.1	3405	A	2.7	3342	A	3.4	3359	A
90%	54.7	3750	D	2.2	3764	A	2.5	3801	A	3.1	3779	A	4.1	3822	A
100%	62.0	4145	E	2.4	4154	A	2.9	4194	A	3.5	4163	A	4.7	4207	A
110%	105.0	4453	F	2.6	4566	A	3.3	4617	A	4	4604	A	5.7	4596	A
120%	146.4	4630	F	2.9	4993	A	3.9	5090	A	4.6	5032	A	8.1	5104	A
130%	202.0	4752	F	3.2	5406	A	4.3	5503	A	5.2	5467	A	10.4	5542	B
140%	236.5	4890	F	3.6	5831	A	4.9	5870	A	5.7	5822	A	13.1	5910	B
150%	260.4	4923	F	4.1	6244	A	5.7	6271	A	6.3	6291	A	14.7	6182	B

Note: [a]Total delay of all approaches and [d]Total number of vehicles traveling through the intersection

Table 6.14 Comparison for Signal Control, CAVIMM-EC and CAVIMM with DFROC

	Signal Control			CAVIMM-EC (DFROC)			CAVIMM-EC (DFROC)			CAVIMM (DFROC)			CAVIMM (DFROC)		
				Δt = 1.5s						Δt = 2.0s					
	TD[a]	VN[d]	LOS	TD[a]	VN[d]	LOS	TD[a]	VN[d]	LOS	TD[a]	VN[d]	LOS	TD[a]	VN[d]	LOS
50%	43.5	2070	D	1.3	2104	A	1.4	2158	A	1.4	2162	A	1.5	2140	A
60%	47.3	2481	D	1.4	2496	A	1.6	2521	A	1.5	2501	A	1.6	2514	A
70%	49.6	2898	D	1.6	2945	A	1.7	2958	A	1.9	2959	A	1.9	2921	A
80%	51.8	3307	D	1.8	3360	A	1.8	3359	A	2.2	3353	A	2.4	3378	A
90%	54.7	3750	D	2	3774	A	2	3801	A	2.6	3769	A	3.5	3813	A
100%	62.0	4145	E	2.1	4142	A	2.3	4134	A	2.9	4181	A	3.7	4142	A
110%	105.0	4453	F	2.4	4584	A	2.5	4556	A	3.1	4615	A	4.1	4564	A
120%	146.4	4630	F	2.5	5005	A	2.9	4989	A	3.4	4977	A	5.1	5042	A
130%	202.0	4752	F	2.8	5453	A	3.7	5427	A	4.1	5442	A	5.9	5428	A
140%	236.5	4890	F	3	5837	A	4.7	5840	A	4.5	5849	A	7.8	5825	A
150%	260.4	4923	F	3.5	6257	A	5.1	6278	A	4.9	6293	A	12	6255	B

Note: [a]Total delay of all approaches and [d]Total number of vehicles traveling through the intersection

6.6 Summary

This chapter concentrates on the evaluation of the proposed CAV handling methods through a VISSIM-based simulation platform. A total of nine intersection control systems are developed with different intersection configurations (if there is movement restriction for specified lanes), different buffer zones (1.5s and 2.0s), and different passing sequence algorithms (FCFS and DFROC). Their performance with respect to total traffic delay is evaluated under different traffic volume levels (from 50% to 150% of peak hour volume). The evaluation under different traffic flow conditions and control mechanisms reveals that the proposed CAVIMM system significantly improves intersection operation efficiency compared to the traditional signal control. There are several factors affecting the CAVIMM performance with respect to total traffic delay reduction. As the traffic volume increases, the total traffic delay slowly grows. Due to the reduction of potential conflicting trajectories in the CAVIMM-EC intersection configurations, the total delay in the CAVIMM is slightly higher than those in the CAVIMM-EC. The total traffic delays for both CAVIMM-EC and CAVIMM are reduced if the algorithm DFROC is employed. As expected, the total traffic delay increases as the size of buffer zone grows from 1.5s to 2.0s.

CHAPTER 7. CONCLUSIONS AND FUTURE RESEARCH

7.1 Conclusions of This Study

Traffic congestion has become a serious issue all over the world due to the rapid increase of population and traffic demands. Improvement in intersection control can significantly benefit the overall transportation network especially for urban areas. The major sources of delay at signalized intersections are driver perception and reaction-related delay and the efficiency losses due to lane changing. With the help of V2V and V2I communications, AVs are capable of self-driving in real-world highway systems and performing complex tasks, which benefits the entire transportation system. A CAV-enabled traffic system has demonstrated great potential to mitigate congestion, reduce traffic delay, and improve traffic mobility and safety performance. Previous studies on intersection control mechanisms for CAVs have developed various systems, which can be classified into centralized control systems and decentralized control systems. The basic logic of those systems is to optimize the passing sequence of CAVs by achieving specified objectives (e.g. minimizing traffic delay, reducing the total number of stops, maximizing traffic throughput, etc.) and ensure traffic safety through coordinating predicted trajectories of conflicting CAVs. However, the lack of precise trajectory formulations by considering the widths and lengths of CAV makes the intersection temporal and spatial resources less fully utilized. In addition, a comprehensive and standardized performance evaluation platform, which can provide standard parameter settings and outputs to guarantee reliable vehicle generation, car-following, lane-changing, and many other driving behavior-related modeling, is needed for performance evaluation on the proposed control systems and for meaningful comparisons with those in other studies.

This study proposed an advanced CAV-based intersection control mechanism, CAVIMM, to reduce both congestion and crash rates at intersections. It is a centralized control system, where all approaching CAVs are coordinated and controlled by the ICC. Based on the assumptions made for the CAVIMM development, the intersection temporal and spatial resources of a 4-leg intersection with three lanes in each approach were formulated. The CAVIMM released vehicle movement restriction from dedicated turning lanes in traditional intersection configuration by enabling both through and turning movements from any lane on all the four approaches. All possible trajectories within an intersection for all approaching CAVs were identified based on the intersection formulation model. A trajectory coordination model, TSDTCM, was developed to formulate all possible temporal-spatial dimension trajectories of CAVs within the intersection. It provided a better means to increase intersection operation efficiency. Different from the previous studies where vehicle trajectories were predicted as lanes or chains of cubes, all CAV trajectories were formulated in a 3-dimention domain in this study through adding time as the third axis. Then the conflicting trajectories within the intersection were identified for any two approaching CAVs. In order to maximize intersection operation efficiency, both the FCFS and a newly proposed algorithm, DFROC, were employed in CAVIMM for determining CAVs passing sequence. Different from the FCFS that assigned right-of-way to approaching CAVs according to their arrival time at the intersection, the DFROC determined the passing sequence of them by aiming to minimize total traffic delay. The DWZ, which was updated every cycle by deleting departing CAVs and adding newly arriving CAVs, was designed. By applying the TSDTCM to develop optimization constraints to ensure traffic safety, the optimization for minimizing total traffic delay at the intersection was conducted every cycle by lowering the minimum of deceleration time for each approaching CAV. The passing sequence was determined through the optimized deceleration time.

Using the collected peak hour traffic counts data of a real intersection, the performance of the proposed CAVIMM with the FCFS and the DFROC was evaluated and compared with traditional signal control. The impacts of different factors, including traffic volumes, buffer zone sizes, and intersection configurations, on the CAVIMM performance regarding total traffic delay were evaluated through VISSIM-based simulation. Ninety-nine simulation scenarios were developed with different intersection configurations (if there is movement restriction for specified lanes), traffic volumes (50% to 150% of peak hour volume), buffer zones (1.5s and 2.0s), and passing sequence algorithms (FCFS and DFROC). The experimental results indicated that the proposed CAVIMM system improved intersection operation efficiency compared to the traditional signal control by significantly reducing total traffic delay at the subject intersection and increasing intersection capacity and efficiency. At the 100% level of volume, the total traffic delay was reduced by more than 90% for all scenarios of the CAVIMM system.

7.2 Limitations and Suggestions for Future Work

Although the proposed CAVIMM illustrated satisfactory performance in improving traffic safety and operation efficiency at the subject intersection, further research is still needed regarding releasing system development assumptions and achieving different optimization objectives.

For the CAVIMM development assumptions, firstly, all approaching vehicles were assumed to be CAVs. This study aimed to investigate the maximum capability of the CAVIMM in improving intersection operational efficiency and congestion release. Therefore, the CAVIMM was developed under an ideal scenario that all vehicles were CAVs. However, the most common situation in the near future is that only a small percentage of vehicles will be AVs, CVs or CAVs. In order to coordinate all kinds of 'smart vehicle' and human-driven vehicles passing through intersections safely and smoothly, a decentralized intersection control system may be widely deployed. Instead of centralized communication, the communications among vehicles and right-of-way negotiations with other vehicles are enabled in a decentralized control system. Although the decentralized control system was not found to outperform the centralized control system, it was still effective in reducing traffic delay and improving traffic mobility at intersections than traditional signal control.

Secondly, real-time communications between CAVs and ICC were never assumed to fail. All CAVs were assumed to follow the guidance by the ICC immediately after receiving it, where communication delay is assumed minimal and could be neglected. This ideal situation might not be fully met even with advanced corresponding technology development. Therefore, special designs in the CAVIMM have been added, including longer distance of the DWZ and sufficient buffer zone in the TSDTCM. Given the basic settings of parameters in the simulation, the speed and location of an approaching CAV under an extreme case (it is required to stop at the potential stop line) can be calculated as shown in Table 6.11. The last step of acceleration (or deceleration) is not a full step. This is a kind of buffer zone to account for any short communication failure. In the development of the TSDTCM, the critical condition is set as any two edges of different CAVs cannot intersect under the pre-assumed perfect control of CAVs. However, in the simulation process, a buffer zone is added around each CAV. If the buffer zones of any two CAVs intersect, a collision is assumed. This buffer zone setting can also help to release the impacts of communication failure to some extent. A long-time communication failure is not considered in this study. Therefore, it is desirable to propose an alternative control mechanism to deal with this extreme situation in further studies.

Thirdly, all CAVs were assumed to accelerate or decelerate with a constant rate, and the speed of CAVs within the subject intersection was kept constant (equal to DS). This assumption simplified the objective functions in the development of passing sequence optimization algorithm. However, it might reduce the capability of CAVIMM in maximizing the utilization of intersection temporal and spatial resources. Therefore, additional effort could be made to explore the maximum capability of CAVIMM by enabling changes of acceleration/deceleration rate.

Similar assumption of constant DS within the intersection was developed to reduce the total traverse time of CAVs. Although the slow-speed issue was addressed by making this assumption, turning movements of CAVs with small radius (e.g. right-turn from the rightmost lane) at a relatively high speed (the design speed) may result in discomfort of people inside the vehicle. A better intersection control mechanism is desirable not only to improve intersection safety and operational efficiency but also to provide a comfortable driving environment for all intersection users. Therefore, further study could also focus on establishing a comprehensive intersection control system by enabling varying speeds for different movements in the intersection.

Fifthly, lane changing was not allowed upstream and within the intersection in the CAVIMM. It was assumed to reduce delay and crash rates due to improperly changing lanes. The CAVIMM enabled three movements from any lane to address the restriction of lane changing. However, this setting was found to significantly increase the number of possible conflicting trajectories, as shown in Table 4.11. As evaluated through the VISSIM-based simulation, the intersection configurations affected the performance of CAVIMM in minimizing total traffic delay. A comprehensive analysis is desirable to evaluate the impacts of lane changing on traffic delay.

Sixthly, this study was conducted under the perfect situation that the subjective intersection was located on a level terrain, where the gravity effect on acceleration/deceleration was not considered. While for intersections in mountainous areas (e.g. Denver, CO), vehicle gravity has significant impact on CAV's movements and the control accuracy of CAVs by the ICC. Considering the gravity effect, appropriate settings of CAVIMM system should be specified. For example, the length of DWZ would be extended or shorten based on the impact of gravity on CAV deceleration or acceleration. Hence, additional effort can be made to adjust the CAVIMM system settings considering the potential influence of gravity on CAV operation and control.

In addition, pedestrians, bicyclists and street crossing facilities were absent in this study. This study aimed to investigate the capability of CAV in improving the intersection operational efficiency and reducing congestion. Therefore, non-motorized travel modes such as pedestrians and bicyclists were not considered due to the non-determinacy characteristics. To enhance the simulation capability of CAVIMM, non-motorized road users and crossing facilities, including overpasses, underpasses, and mid-block crossings, etc., can be added.

In terms of passing sequence optimization algorithm, considerable improvements could be conducted through setting various objectives. In this study, minimum traffic delay at intersections was set as the major objective to reduce the waiting time for a CAV to pass through the subject intersection. If the maximum throughput was set as the objective, the passing sequence of approaching CAVs may change and the performance of CAVIMM may also change significantly. Further investigation could be made to develop advanced optimization algorithms for various objectives. Furthermore, even for the objective of minimizing total traffic delay, the DFROC algorithm could be improved by releasing certain assumptions made in this study. For example, the speed of vehicle traveling through the intersection can vary in order to reduce the total travel delay. In current study, approaching CAVs are only allowed to decelerate once before entering the subject intersection. However, if several times of deceleration are enabled, which enlarges the capability of optimization choices, the intersection resources could be better utilized and so as the intersection efficiency.

Appendix A. CONFLICTING TRAJECTORY MATRIX

Table A.1 Conflicting Trajectory Matrix for t_{453}

			Enter Lane (λ_{im})											
			i=2			i=4			i=6			i=8		
			λ_{21}	λ_{22}	λ_{23}	λ_{41}	λ_{42}	λ_{43}	λ_{61}	λ_{62}	λ_{63}	λ_{81}	λ_{82}	λ_{83}
Exit Lane (λ_{jn})	j=1	λ_{11}	×	×	×	t_{411}	×	×	t_{611}	×	×	×	×	×
		λ_{12}	×	×	×	×	×	×	×	t_{612}	×	×	×	×
		λ_{13}	×	×	×	×	×	×	×	×	t_{613}	×	×	t_{813}
	j=3	λ_{31}	×	×	×	×	×	×	t_{631}	×	×	t_{831}	×	×
		λ_{32}	×	×	×	×	×	×	×	×	×	×	t_{832}	×
		λ_{33}	×	×	t_{233}	×	×	×	×	×	×	×	×	t_{833}
	j=5	λ_{51}	t_{251}	×	×	×	×	×	×	×	×	t_{851}	×	×
		λ_{52}	×	t_{252}	×	×	×	×	×	×	×	×	×	×
		λ_{53}	×	×	t_{253}	×	×	t_{453}	×	×	×	×	×	×
	j=7	λ_{71}	t_{271}	×	×	t_{471}	×	×	×	×	×	×	×	×
		λ_{72}	×	×	×	×	t_{472}	×	×	×	×	×	×	×
		λ_{73}	×	×	×	×	×	t_{473}	×	×	t_{673}	×	×	×

Table A.2 Conflicting Trajectory Matrix for t_{471}

			Enter Lane (λ_{im})											
			i=2			i=2			i=2			i=2		
			λ_{21}	λ_{22}	λ_{23}	λ_{41}	λ_{42}	λ_{43}	λ_{61}	λ_{62}	λ_{63}	λ_{81}	λ_{82}	λ_{83}
Exit Lane (λ_{jn})	j=1	λ_{11}	×	×	×	t_{411}	×	×	t_{611}	×	×	×	×	×
		λ_{12}	×	×	×	×	×	×	×	t_{612}	×	×	×	×
		λ_{13}	×	×	×	×	×	×	×	×	t_{613}	×	×	t_{813}
	j=3	λ_{31}	×	×	×	×	×	×	t_{631}	×	×	t_{831}	×	×
		λ_{32}	×	×	×	×	×	×	×	×	×	×	t_{832}	×
		λ_{33}	×	×	t_{233}	×	×	×	×	×	×	×	×	t_{833}
	j=5	λ_{51}	t_{251}	×	×	×	×	×	×	×	×	t_{851}	×	×
		λ_{52}	×	t_{252}	×	×	×	×	×	×	×	×	×	×
		λ_{53}	×	×	t_{253}	×	×	t_{453}	×	×	×	×	×	×
	j=7	λ_{71}	t_{271}	×	×	t_{471}	×	×	×	×	×	×	×	×
		λ_{72}	×	×	×	×	t_{472}	×	×	×	×	×	×	×
		λ_{73}	×	×	×	×	×	t_{473}	×	×	t_{673}	×	×	×

Table A.3 Conflicting Trajectory Matrix for t_{472}

			Enter Lane (λ_{im})											
			i=2			*i*=2			*i*=2			*i*=2		
			λ_{21}	λ_{22}	λ_{23}	λ_{41}	λ_{42}	λ_{43}	λ_{61}	λ_{62}	λ_{63}	λ_{81}	λ_{82}	λ_{83}
Exit Lane (λ_{jn})	*j*=1	λ_{11}	×	×	×	t_{411}	×	×	t_{611}	×	×	×	×	×
		λ_{12}	×	×	×	×	×	×	×	t_{612}	×	×	×	×
		λ_{13}	×	×	×	×	×	×	×	×	t_{613}	×	×	t_{813}
	j=3	λ_{31}	×	×	×	×	×	×	t_{631}	×	×	t_{831}	×	×
		λ_{32}	×	×	×	×	×	×	×	×	×	×	t_{832}	×
		λ_{33}	×	×	t_{233}	×	×	×	×	×	×	×	×	t_{833}
	j=5	λ_{51}	t_{251}	×	×	×	×	×	×	×	×	t_{851}	×	×
		λ_{52}	×	t_{252}	×	×	×	×	×	×	×	×	×	×
		λ_{53}	×	×	t_{253}	×	×	t_{453}	×	×	×	×	×	×
	j=7	λ_{71}	t_{271}	×	×	t_{471}	×	×	×	×	×	×	×	×
		λ_{72}	×	×	×	×	t_{472}	×	×	×	×	×	×	×
		λ_{73}	×	×	×	×	×	t_{473}	×	×	t_{673}	×	×	×

Table A.4 Conflicting Trajectory Matrix for t_{473}

			Enter Lane (λ_{im})											
			i=2			*i*=2			*i*=2			*i*=2		
			λ_{21}	λ_{22}	λ_{23}	λ_{41}	λ_{42}	λ_{43}	λ_{61}	λ_{62}	λ_{63}	λ_{81}	λ_{82}	λ_{83}
Exit Lane (λ_{jn})	*j*=1	λ_{11}	×	×	×	t_{411}	×	×	t_{611}	×	×	×	×	×
		λ_{12}	×	×	×	×	×	×	×	t_{612}	×	×	×	×
		λ_{13}	×	×	×	×	×	×	×	×	t_{613}	×	×	t_{813}
	j=3	λ_{31}	×	×	×	×	×	×	t_{631}	×	×	t_{831}	×	×
		λ_{32}	×	×	×	×	×	×	×	×	×	×	t_{832}	×
		λ_{33}	×	×	t_{233}	×	×	×	×	×	×	×	×	t_{833}
	j=5	λ_{51}	t_{251}	×	×	×	×	×	×	×	×	t_{851}	×	×
		λ_{52}	×	t_{252}	×	×	×	×	×	×	×	×	×	×
		λ_{53}	×	×	t_{253}	×	×	t_{453}	×	×	×	×	×	×
	j=7	λ_{71}	t_{271}	×	×	t_{471}	×	×	×	×	×	×	×	×
		λ_{72}	×	×	×	×	t_{472}	×	×	×	×	×	×	×
		λ_{73}	×	×	×	×	×	t_{473}	×	×	t_{673}	×	×	×

Table A.5 Conflicting Trajectory Matrix for t_{411}

			Enter Lane (λ_{im})											
			i=2			*i*=2			*i*=2			*i*=2		
			λ_{21}	λ_{22}	λ_{23}	λ_{41}	λ_{42}	λ_{43}	λ_{61}	λ_{62}	λ_{63}	λ_{81}	λ_{82}	λ_{83}
Exit Lane (λ_{jn})	*j*=1	λ_{11}	×	×	×	t_{411}	×	×	t_{611}	×	×	×	×	×
		λ_{12}	×	×	×	×	×	×	×	t_{612}	×	×	×	×
		λ_{13}	×	×	×	×	×	×	×	×	t_{613}	×	×	t_{813}
	j=3	λ_{31}	×	×	×	×	×	×	t_{631}	×	×	t_{831}	×	×
		λ_{32}	×	×	×	×	×	×	×	×	×	×	t_{832}	×
		λ_{33}	×	×	t_{233}	×	×	×	×	×	×	×	×	t_{833}
	j=5	λ_{51}	t_{251}	×	×	×	×	×	×	×	×	t_{851}	×	×
		λ_{52}	×	t_{252}	×	×	×	×	×	×	×	×	×	×
		λ_{53}	×	×	t_{253}	×	×	t_{453}	×	×	×	×	×	×
	j=7	λ_{71}	t_{271}	×	×	t_{471}	×	×	×	×	×	×	×	×
		λ_{72}	×	×	×	×	t_{472}	×	×	×	×	×	×	×
		λ_{73}	×	×	×	×	×	t_{473}	×	×	t_{673}	×	×	×

Table A.6 Conflicting Trajectory Matrix for t_{673}

			Enter Lane (λ_{im})											
			i=2			*i*=2			*i*=2			*i*=2		
			λ_{21}	λ_{22}	λ_{23}	λ_{41}	λ_{42}	λ_{43}	λ_{61}	λ_{62}	λ_{63}	λ_{81}	λ_{82}	λ_{83}
Exit Lane (λ_{jn})	*j*=1	λ_{11}	×	×	×	t_{411}	×	×	t_{611}	×	×	×	×	×
		λ_{12}	×	×	×	×	×	×	×	t_{612}	×	×	×	×
		λ_{13}	×	×	×	×	×	×	×	×	t_{613}	×	×	t_{813}
	j=3	λ_{31}	×	×	×	×	×	×	t_{631}	×	×	t_{831}	×	×
		λ_{32}	×	×	×	×	×	×	×	×	×	×	t_{832}	×
		λ_{33}	×	×	t_{233}	×	×	×	×	×	×	×	×	t_{833}
	j=5	λ_{51}	t_{251}	×	×	×	×	×	×	×	×	t_{851}	×	×
		λ_{52}	×	t_{252}	×	×	×	×	×	×	×	×	×	×
		λ_{53}	×	×	t_{253}	×	×	t_{453}	×	×	×	×	×	×
	j=7	λ_{71}	t_{271}	×	×	t_{471}	×	×	×	×	×	×	×	×
		λ_{72}	×	×	×	×	t_{472}	×	×	×	×	×	×	×
		λ_{73}	×	×	×	×	×	t_{473}	×	×	t_{673}	×	×	×

Table A.7 Conflicting Trajectory Matrix for t_{671}

			Enter Lane (λ_{im})											
			i=2			i=2			i=2			i=2		
			λ_{21}	λ_{22}	λ_{23}	λ_{41}	λ_{42}	λ_{43}	λ_{61}	λ_{62}	λ_{63}	λ_{81}	λ_{82}	λ_{83}
Exit Lane (λ_{jn})	j=1	λ_{11}	×	×	×	t_{411}	×	×	t_{611}	×	×	×	×	×
		λ_{12}	×	×	×	×	×	×	×	t_{612}	×	×	×	×
		λ_{13}	×	×	×	×	×	×	×	×	t_{613}	×	×	t_{813}
	j=3	λ_{31}	×	×	×	×	×	×	t_{631}	×	×	t_{831}	×	×
		λ_{32}	×	×	×	×	×	×	×	×	×	×	t_{832}	×
		λ_{33}	×	×	t_{233}	×	×	×	×	×	×	×	×	t_{833}
	j=5	λ_{51}	t_{251}	×	×	×	×	×	×	×	×	t_{851}	×	×
		λ_{52}	×	t_{252}	×	×	×	×	×	×	×	×	×	×
		λ_{53}	×	×	t_{253}	×	×	t_{453}	×	×	×	×	×	×
	j=7	λ_{71}	t_{271}	×	×	t_{471}	×	×	×	×	×	×	×	×
		λ_{72}	×	×	×	×	t_{472}	×	×	×	×	×	×	×
		λ_{73}	×	×	×	×	×	t_{473}	×	×	t_{673}	×	×	×

Table A.8 Conflicting Trajectory Matrix for t_{672}

			Enter Lane (λ_{im})											
			i=2			i=2			i=2			i=2		
			λ_{21}	λ_{22}	λ_{23}	λ_{41}	λ_{42}	λ_{43}	λ_{61}	λ_{62}	λ_{63}	λ_{81}	λ_{82}	λ_{83}
Exit Lane (λ_{jn})	j=1	λ_{11}	×	×	×	t_{411}	×	×	t_{611}	×	×	×	×	×
		λ_{12}	×	×	×	×	×	×	×	t_{612}	×	×	×	×
		λ_{13}	×	×	×	×	×	×	×	×	t_{613}	×	×	t_{813}
	j=3	λ_{31}	×	×	×	×	×	×	t_{631}	×	×	t_{831}	×	×
		λ_{32}	×	×	×	×	×	×	×	×	×	×	t_{832}	×
		λ_{33}	×	×	t_{233}	×	×	×	×	×	×	×	×	t_{833}
	j=5	λ_{51}	t_{251}	×	×	×	×	×	×	×	×	t_{851}	×	×
		λ_{52}	×	t_{252}	×	×	×	×	×	×	×	×	×	×
		λ_{53}	×	×	t_{253}	×	×	t_{453}	×	×	×	×	×	×
	j=7	λ_{71}	t_{271}	×	×	t_{471}	×	×	×	×	×	×	×	×
		λ_{72}	×	×	×	×	t_{472}	×	×	×	×	×	×	×
		λ_{73}	×	×	×	×	×	t_{473}	×	×	t_{673}	×	×	×

Table A.9 Conflicting Trajectory Matrix for t_{673}

			Enter Lane (λ_{im})											
			i=2			*i*=2			*i*=2			*i*=2		
			λ_{21}	λ_{22}	λ_{23}	λ_{41}	λ_{42}	λ_{43}	λ_{61}	λ_{62}	λ_{63}	λ_{81}	λ_{82}	λ_{83}
Exit Lane (λ_{jn})	*j*=1	λ_{11}	×	×	×	t_{411}	×	×	t_{611}	×	×	×	×	×
		λ_{12}	×	×	×	×	×	×	×	t_{612}	×	×	×	×
		λ_{13}	×	×	×	×	×	×	×	×	t_{613}	×	×	t_{813}
	j=3	λ_{31}	×	×	×	×	×	×	t_{631}	×	×	t_{831}	×	×
		λ_{32}	×	×	×	×	×	×	×	×	×	×	t_{832}	×
		λ_{33}	×	×	t_{233}	×	×	×	×	×	×	×	×	t_{833}
	j=5	λ_{51}	t_{251}	×	×	×	×	×	×	×	×	t_{851}	×	×
		λ_{52}	×	t_{252}	×	×	×	×	×	×	×	×	×	×
		λ_{53}	×	×	t_{253}	×	×	t_{453}	×	×	×	×	×	×
	j=7	λ_{71}	t_{271}	×	×	t_{471}	×	×	×	×	×	×	×	×
		λ_{72}	×	×	×	×	t_{472}	×	×	×	×	×	×	×
		λ_{73}	×	×	×	×	×	t_{473}	×	×	t_{673}	×	×	×

Table A.10 Conflicting Trajectory Matrix for t_{671}

			Enter Lane (λ_{im})											
			i=2			*i*=2			*i*=2			*i*=2		
			λ_{21}	λ_{22}	λ_{23}	λ_{41}	λ_{42}	λ_{43}	λ_{61}	λ_{62}	λ_{63}	λ_{81}	λ_{82}	λ_{83}
Exit Lane (λ_{jn})	*j*=1	λ_{11}	×	×	×	t_{411}	×	×	t_{611}	×	×	×	×	×
		λ_{12}	×	×	×	×	×	×	×	t_{612}	×	×	×	×
		λ_{13}	×	×	×	×	×	×	×	×	t_{613}	×	×	t_{813}
	j=3	λ_{31}	×	×	×	×	×	×	t_{631}	×	×	t_{831}	×	×
		λ_{32}	×	×	×	×	×	×	×	×	×	×	t_{832}	×
		λ_{33}	×	×	t_{233}	×	×	×	×	×	×	×	×	t_{833}
	j=5	λ_{51}	t_{251}	×	×	×	×	×	×	×	×	t_{851}	×	×
		λ_{52}	×	t_{252}	×	×	×	×	×	×	×	×	×	×
		λ_{53}	×	×	t_{253}	×	×	t_{453}	×	×	×	×	×	×
	j=7	λ_{71}	t_{271}	×	×	t_{471}	×	×	×	×	×	×	×	×
		λ_{72}	×	×	×	×	t_{472}	×	×	×	×	×	×	×
		λ_{73}	×	×	×	×	×	t_{473}	×	×	t_{673}	×	×	×

Table A.11 Conflicting Trajectory Matrix for t_{813}

			Enter Lane (λ_{im})											
			i=2			*i*=2			*i*=2			*i*=2		
			λ_{21}	λ_{22}	λ_{23}	λ_{41}	λ_{42}	λ_{43}	λ_{61}	λ_{62}	λ_{63}	λ_{81}	λ_{82}	λ_{83}
Exit Lane (λ_{jn})	*j*=1	λ_{11}	×	×	×	t_{411}	×	×	t_{611}	×	×	×	×	×
		λ_{12}	×	×	×	×	×	×	×	t_{612}	×	×	×	×
		λ_{13}	×	×	×	×	×	×	×	×	t_{613}	×	×	t_{813}
	j=3	λ_{31}	×	×	×	×	×	×	t_{631}	×	×	t_{831}	×	×
		λ_{32}	×	×	×	×	×	×	×	×	×	×	t_{832}	×
		λ_{33}	×	×	t_{233}	×	×	×	×	×	×	×	×	t_{833}
	j=5	λ_{51}	t_{251}	×	×	×	×	×	×	×	×	t_{851}	×	×
		λ_{52}	×	t_{252}	×	×	×	×	×	×	×	×	×	×
		λ_{53}	×	×	t_{253}	×	×	t_{453}	×	×	×	×	×	×
	j=7	λ_{71}	t_{271}	×	×	t_{471}	×	×	×	×	×	×	×	×
		λ_{72}	×	×	×	×	t_{472}	×	×	×	×	×	×	×
		λ_{73}	×	×	×	×	×	t_{473}	×	×	t_{673}	×	×	×

Table A.12 Conflicting Trajectory Matrix for t_{831}

			Enter Lane (λ_{im})											
			i=2			*i*=2			*i*=2			*i*=2		
			λ_{21}	λ_{22}	λ_{23}	λ_{41}	λ_{42}	λ_{43}	λ_{61}	λ_{62}	λ_{63}	λ_{81}	λ_{82}	λ_{83}
Exit Lane (λ_{jn})	*j*=1	λ_{11}	×	×	×	t_{411}	×	×	t_{611}	×	×	×	×	×
		λ_{12}	×	×	×	×	×	×	×	t_{612}	×	×	×	×
		λ_{13}	×	×	×	×	×	×	×	×	t_{613}	×	×	t_{813}
	j=3	λ_{31}	×	×	×	×	×	×	t_{631}	×	×	t_{831}	×	×
		λ_{32}	×	×	×	×	×	×	×	×	×	×	t_{832}	×
		λ_{33}	×	×	t_{233}	×	×	×	×	×	×	×	×	t_{833}
	j=5	λ_{51}	t_{251}	×	×	×	×	×	×	×	×	t_{851}	×	×
		λ_{52}	×	t_{252}	×	×	×	×	×	×	×	×	×	×
		λ_{53}	×	×	t_{253}	×	×	t_{453}	×	×	×	×	×	×
	j=7	λ_{71}	t_{271}	×	×	t_{471}	×	×	×	×	×	×	×	×
		λ_{72}	×	×	×	×	t_{472}	×	×	×	×	×	×	×
		λ_{73}	×	×	×	×	×	t_{473}	×	×	t_{673}	×	×	×

Table A.13 Conflicting Trajectory Matrix for t_{832}

			Enter Lane (λ_{im})											
			i=2			i=2			i=2			i=2		
			λ_{21}	λ_{22}	λ_{23}	λ_{41}	λ_{42}	λ_{43}	λ_{61}	λ_{62}	λ_{63}	λ_{81}	λ_{82}	λ_{83}
Exit Lane (λ_{jn})	j=1	λ_{11}	×	×	×	t_{411}	×	×	t_{611}	×	×	×	×	×
		λ_{12}	×	×	×	×	×	×	×	t_{612}	×	×	×	×
		λ_{13}	×	×	×	×	×	×	×	×	t_{613}	×	×	t_{813}
	j=3	λ_{31}	×	×	×	×	×	×	t_{631}	×	×	t_{831}	×	×
		λ_{32}	×	×	×	×	×	×	×	×	×	×	t_{832}	×
		λ_{33}	×	×	t_{233}	×	×	×	×	×	×	×	×	t_{833}
	j=5	λ_{51}	t_{251}	×	×	×	×	×	×	×	×	t_{851}	×	×
		λ_{52}	×	t_{252}	×	×	×	×	×	×	×	×	×	×
		λ_{53}	×	×	t_{253}	×	×	t_{453}	×	×	×	×	×	×
	j=7	λ_{71}	t_{271}	×	×	t_{471}	×	×	×	×	×	×	×	×
		λ_{72}	×	×	×	×	t_{472}	×	×	×	×	×	×	×
		λ_{73}	×	×	×	×	×	t_{473}	×	×	t_{673}	×	×	×

Table A.14 Conflicting Trajectory Matrix for t_{833}

			Enter Lane (λ_{im})											
			i=2			i=2			i=2			i=2		
			λ_{21}	λ_{22}	λ_{23}	λ_{41}	λ_{42}	λ_{43}	λ_{61}	λ_{62}	λ_{63}	λ_{81}	λ_{82}	λ_{83}
Exit Lane (λ_{jn})	j=1	λ_{11}	×	×	×	t_{411}	×	×	t_{611}	×	×	×	×	×
		λ_{12}	×	×	×	×	×	×	×	t_{612}	×	×	×	×
		λ_{13}	×	×	×	×	×	×	×	×	t_{613}	×	×	t_{813}
	j=3	λ_{31}	×	×	×	×	×	×	t_{631}	×	×	t_{831}	×	×
		λ_{32}	×	×	×	×	×	×	×	×	×	×	t_{832}	×
		λ_{33}	×	×	t_{233}	×	×	×	×	×	×	×	×	t_{833}
	j=5	λ_{51}	t_{251}	×	×	×	×	×	×	×	×	t_{851}	×	×
		λ_{52}	×	t_{252}	×	×	×	×	×	×	×	×	×	×
		λ_{53}	×	×	t_{253}	×	×	t_{453}	×	×	×	×	×	×
	j=7	λ_{71}	t_{271}	×	×	t_{471}	×	×	×	×	×	×	×	×
		λ_{72}	×	×	×	×	t_{472}	×	×	×	×	×	×	×
		λ_{73}	×	×	×	×	×	t_{473}	×	×	t_{673}	×	×	×

Table A.15 Conflicting Trajectory Matrix for t_{851}

			Enter Lane (λ_{im})											
			i=2			i=2			i=2			i=2		
			λ_{21}	λ_{22}	λ_{23}	λ_{41}	λ_{42}	λ_{43}	λ_{61}	λ_{62}	λ_{63}	λ_{81}	λ_{82}	λ_{83}
Exit Lane (λ_{jn})	j=1	λ_{11}	×	×	×	t_{411}	×	×	t_{611}	×	×	×	×	×
		λ_{12}	×	×	×	×	×	×	×	t_{612}	×	×	×	×
		λ_{13}	×	×	×	×	×	×	×	×	t_{613}	×	×	t_{813}
	j=3	λ_{31}	×	×	×	×	×	×	t_{631}	×	×	t_{831}	×	×
		λ_{32}	×	×	×	×	×	×	×	×	×	×	t_{832}	×
		λ_{33}	×	×	t_{233}	×	×	×	×	×	×	×	×	t_{833}
	j=5	λ_{51}	t_{251}	×	×	×	×	×	×	×	×	t_{851}	×	×
		λ_{52}	×	t_{252}	×	×	×	×	×	×	×	×	×	×
		λ_{53}	×	×	t_{253}	×	×	t_{453}	×	×	×	×	×	×
	j=7	λ_{71}	t_{271}	×	×	t_{471}	×	×	×	×	×	×	×	×
		λ_{72}	×	×	×	×	t_{472}	×	×	×	×	×	×	×
		λ_{73}	×	×	×	×	×	t_{473}	×	×	t_{673}	×	×	×

REFERENCE

AASHTO, 2011. A policy on geometric design of highways and streets.

Abbas-Turki, A., Ahmane, M., Wu, J., El-Moudni, A., Miraoui, A., 2012. On the conflict with dioid algebra: Autonomous Intersection Management, in: 2012 7th IEEE Conference on Industrial Electronics and Applications (ICIEA). pp. 1018–1023. doi:10.1109/ICIEA.2012.6360872

Abdel-Aty, M.A., Keller, J., 2005. Exploring the overall and specific crash severity levels at signalized intersections. Accident Analysis and Prevention 37, 417–25. doi:10.1016/j.aap.2004.11.002

Abdelhameed, M.M., Abdelaziz, M., Hammad, S., Shehata, O.M., 2014. Development and evaluation of a multi-agent autonomous vehicles intersection control system, in: 2014 International Conference on Engineering and Technology. pp. 1–6.

Agbolosu-Amison, S.J., Yun, I., Park, B.B., 2012. Quantifying benefits of a dynamic gap-out feature at an actuated traffic signalized intersection under cooperative vehicle infrastructure system. KSCE Journal of Civil Engineering 16, 433–440. doi:10.1007/s12205-012-1495-7

Alonso, J., Milanés, V., Pérez, J., Onieva, E., González, C., de Pedro, T., 2011. Autonomous vehicle control systems for safe crossroads. Transportation Research Part C: Emerging Technologies 19, 1095–1110. doi:10.1016/j.trc.2011.06.002

Ammoun, S., Nashashibi, F., 2009. Real time trajectory prediction for collision risk estimation between vehicles, in: 2009 IEEE 5th International Conference on Intelligent Computer Communication and Processing. pp. 417–422. doi:10.1109/ICCP.2009.5284727

Au, T.-C., Shahidi, N., Stone, P., 2011. Enforcing liveness in autonomous traffic management., in: Proceedings of the 25th AAAI Conference of Artificial Intelligence. pp. 1317–1322.

Au, T., Zhang, S., Stone, P., 2015. Autonomous intersection management for semi-autonomous vehicles, in: Handbook of Transportation. pp. 88–104. doi:10.4324/9781315756684

Au, T.C., Fok, C.L., Vishwanath, S., Julien, C., Stone, P., 2012a. Evasion planning for autonomous vehicles at intersections. IEEE International Conference on Intelligent Robots and Systems 1541–1546. doi:10.1109/IROS.2012.6385936

Au, T.C., Quinlan, M., Stone, P., 2012b. Setpoint scheduling for autonomous vehicle controllers. Proceedings - IEEE International Conference on Robotics and Automation 2055–2060. doi:10.1109/ICRA.2012.6225232

Azimi, R., Bhatia, G., Rajkumar, R., Mudalige, P., 2014. STIP: Spatio-temporal intersection protocols for autonomous vehicles. 2014 ACM/IEEE International Conference on Cyber-Physical Systems, ICCPS 2014 1–12. doi:10.1109/ICCPS.2014.6843706

Bari, P., Fanti, M.P., Meloni, C., 2003. Real Time Optimization of Traffic Signal Control : Application to Coordinated Intersections, in: Systems, Man and Cybernetics, 2003. IEEE International Conference.

Bédard, M., Guyatt, G.H., Stones, M.J., Hirdes, J.P., 2002. The independent contribution of driver, crash, and vehicle characteristics to driver fatalities. Accident Analysis and

Prevention 34, 717–727. doi:10.1016/S0001-4575(01)00072-0

Bento, L.C., Parafita, R., Nunes, U., 2012. Intelligent traffic management at intersections supported by V2V and V2I communications. 2012 15th International IEEE Conference on Intelligent Transportation Systems 1495–1502. doi:10.1109/ITSC.2012.6338766

Bento, L.C., Parafita, R., Santos, S., Nunes, U., 2013. Intelligent traffic management at intersections: Legacy mode for vehicles not equipped with V2V and V2I communications. 16th International IEEE Conference on Intelligent Transportation Systems (ITSC 2013) 726–731. doi:10.1109/ITSC.2013.6728317

Carlino, D., Boyles, S.D., Stone, P., 2013. Auction-based autonomous intersection management. IEEE Conference on Intelligent Transportation Systems, Proceedings, ITSC 529–534. doi:10.1109/ITSC.2013.6728285

Carlino, D., Depinet, M., Khandelwal, P., Stone, P., 2012. Approximately orchestrated routing and transportation analyzer: Large-scale traffic simulation for autonomous vehicles. IEEE Conference on Intelligent Transportation Systems, Proceedings, ITSC 334–339. doi:10.1109/ITSC.2012.6338701

Centers for Disease Control and Prevention, 2010. Fatal Injury Reports, National and Regional [WWW Document]. Centers for Disease Control and Prevention. URL http://webappa.cdc.gov/sasweb/ncipc/mortrate10_us.html

Chang, H.-J., Park, G.-T., 2013. A study on traffic signal control at signalized intersections in vehicular ad hoc networks. Ad Hoc Networks 11, 2115–2124. doi:10.1016/j.adhoc.2012.02.013

Chen, C., Wu, Q., Zhang, G., Liu, X.C., Prevedouros, P.D., 2017. Extracting arterial access density impacts on safety performance based on clustering and computational analysis (In Press). Journal of Transportation Engineering, Part A: Systems.

Chen, C., Zhang, G., Qian, Z., Tarefder, R.A., Tian, Z., 2016. Investigating driver injury severity patterns in rollover crashes using support vector machine models. Accident Analysis and Prevention 90, 128–139. doi:10.1016/j.aap.2016.02.011

Chen, C., Zhang, G., Tarefder, R., Ma, J., Wei, H., Guan, H., 2015. A multinomial logit model-Bayesian network hybrid approach for driver injury severity analyses in rear-end crashes. Accident Analysis and Prevention 80, 76–88. doi:10.1016/j.aap.2015.03.036

Chen, H., Cao, L., Logan, D.B., 2012. Analysis of risk factors affecting the severity of intersection crashes by logistic regression. Traffic injury prevention 13, 300–7. doi:10.1080/15389588.2011.653841

Clement, S.J., Taylor, M.A.P., Yue, W.L., 2004. Simple platoon advancement: a model of automated vehicle movement at signalised intersections. Transportation Research Part C: Emerging Technologies 12, 293–320. doi:10.1016/j.trc.2004.07.012

Dresner, K., Stone, P., 2008. A multiagent approach to autonomous intersection management. Journal of Artificial Intelligence Research 31, 591–656. doi:10.1613/jair.2502

Dresner, K., Stone, P., 2005a. Turning the corner: Improved intersection control for autonomous vehicles. IEEE Intelligent Vehicles Symposium, Proceedings 2005, 423–428.

doi:10.1109/IVS.2005.1505140

Dresner, K., Stone, P., 2005b. Multiagent traffic management: An improved intersection control mechanism. In The Fourth International Joint Conference on Autonomous Agents and Multiagent Systems 471–477. doi:10.1109/AAMAS.2004.242421

Dresner, K., Stone, P., 2004. Multiagent traffic management: a reservation-based intersection control mechanism. Proceedings of the Third International Joint Conference on Autonomous Agents and Multiagent Systems, 2004. AAMAS 2004. 530–537. doi:10.1109/AAMAS.2004.242421

Durbin, D., 2015. Driverless car finishes the ultimate 3,400 mile U.S. road trip [WWW Document]. SKIFT. URL http://skift.com/2015/04/04/driverless-car-finishes-the-ultimate-3400-mile-u-s-road-trip/

Fajardo, D., Au, T.-C., Waller, S.T., Stone, P., Yang, D., 2012. Automated intersection control performance of future innovation versus current traffic signal control. Transportation Research Record: Journal of the Transportation Research Board 2259, 223–232. doi:10.3141/2259-21

Fang, Z., Li, Q., Li, Q., Han, L.D., Shaw, S.-L., 2013. A space–time efficiency model for optimizing intra-intersection vehicle–pedestrian evacuation movements. Transportation Research Part C: Emerging Technologies 31, 112–130. doi:10.1016/j.trc.2013.03.004

Federal Highway Administration, 2015. 2015 FHWA Vehicle to Infrastructure deployment guidance and products.

Federal Highway Administration, 2012. Focus on congestion felief [WWW Document]. U.S. Department of Transportation. URL http://www.fhwa.dot.gov/congestion/toolbox/service.htm

Federal Highway Administration, 2010. Highway statistic 2009 [WWW Document]. URL http://www.fhwa.dot.gov/policyinformation/statistics/2009/vm1.cfm

Federal Highway Administration, 2008. Signal Timing Manual, Federal Highway Administration.

Fok, C.-L., Hanna, M., Gee, S., Au, T.-C., Stone, P., Julien, C., Vishwanath, S., 2012. A platform for evaluating autonomous intersection management policies. 2012 IEEE/ACM Third International Conference on Cyber-Physical Systems 87–96. doi:10.1109/ICCPS.2012.17

Genders, W., Razavi, S.N., Asce, a M., 2015. Impact of connected vehicle on work zone network safety through dynamic route guidance. Journal of Computing in Civil Engineering 1–11. doi:10.1061/(ASCE)CP.1943-5487.0000490.

Glaser, S., Vanholme, B., Mammar, S., Gruyer, D., Nouvelière, L., 2010. Maneuver-based trajectory planning for highly autonomous vehicles on real road with traffic and driver interaction. IEEE Transactions on Intelligent Transportation Systems 11, 589–606. doi:10.1109/TITS.2010.2046037

Gordon, R., Reiss, R., Haenel, H., Case, E., French, R., Mohaddes, A., Wolcott, R., 2005. Traffic Control Systems Handbook. Federal Highway Administration, Washington D.C.

Gregoire, J. a, Bonnabel, S., de La Fortelle, A., 2014. Priority-based intersection management with kinodynamic constraints. 13th European Control Conference (ECC) 6. doi:10.1109/ECC.2014.6862377

Guberinic, S., Senborn, G., 1978. Optimal sequences of fixed time signal plans. Transportation Science 12.

Hu, W.H.W., Xiao, X.X.X., Xie, D., Tan, T.T.T., Maybank, S., 2004. Traffic accident prediction using 3-D model-based vehicle tracking. IEEE Transactions on Vehicular Technology 53, 677–694. doi:10.1109/TVT.2004.825772

Ilgin Guler, S., Menendez, M., Meier, L., 2014. Using connected vehicle technology to improve the efficiency of intersections. Transportation Research Part C: Emerging Technologies 46, 121–131. doi:10.1016/j.trc.2014.05.008

Jin, Q., Wu, G., Boriboonsomsin, K., Barth, M., 2012a. Advanced intersection management for connected vehicles using a multi-agent systems approach. 2012 Intelligent Vehicles Symposium 932–937. doi:10.1109/IVS.2012.6232287

Jin, Q., Wu, G., Boriboonsomsin, K., Barth, M., 2012b. Multi-agent intersection management for connected vehicles using an optimal scheduling approach. 2012 International Conference on Connected Vehicles and Expo (ICCVE) 185–190. doi:10.1109/ICCVE.2012.41

Kamal, M.A.S., Imura, J.I., Hayakawa, T., Ohata, A., Aihara, K., 2015. A vehicle-intersection coordination scheme for smooth flows of traffic without using traffic lights. IEEE Transactions on Intelligent Transportation Systems 16, 1136–1147. doi:10.1109/TITS.2014.2354380

Kiwi-W Consortium, 2000. Kiwi Format-Version 1.22 [WWW Document]. URL http://www.kiwi-w.org/format_english/format_kihon.html

Le Vine, S., Zolfaghari, A., Polak, J., 2015. Autonomous cars: The tension between occupant experience and intersection capacity. Transportation Research Part C: Emerging Technologies 52, 1–14. doi:10.1016/j.trc.2015.01.002

Lee, J., Abdulhai, B., Shalaby, A., Chung, E.-H., 2005. Real-time optimization for adaptive traffic signal control using genetic algorithms. Journal of Intelligent Transportation Systems 9, 111–122. doi:10.1080/15472450500183649

Lee, J., Park, B., 2012. Development and evaluation of a cooperative vehicle intersection control algorithm under the connected vehicles environment. IEEE Transactions on Intelligent Transportation Systems 13, 81–90. doi:10.1109/TITS.2011.2178836

Lee, J., Park, B., Malakorn, K., So, J., 2013. Sustainability assessments of cooperative vehicle intersection control at an urban corridor. Transportation Research Part C: Emerging Technologies 32, 193–206. doi:10.1016/j.trc.2012.09.004

Li, Z., Chitturi, M., Noyce, D., Ran, B., Chitturi, M. V, Noyce, D., 2013a. Development of next generation intersection control. Madison.

Li, Z., Chitturi, M. V., Zheng, D., Bill, A.R., Noyce, D.A., 2013b. A next-generation intersection control algorithm for autonomous vehicles, in: TRB 92nd Annual Meeting in Washington, D.C. Washington D.C.

Li, Z., Elefteriadou, L., Ranka, S., 2014. Signal control optimization for automated vehicles at isolated signalized intersections. Transportation Research Part C: Emerging Technologies 49, 1–18. doi:10.1016/j.trc.2014.10.001

Lord, D., Mannering, F., 2010. The statistical analysis of crash-frequency data: A review and assessment of methodological alternatives. Transportation Research Part A: Policy and Practice 44, 291–305. doi:10.1016/j.tra.2010.02.001

Lückel, J., Naumann, R., Rasche, R., Paderborn, U., Automatisierungstechnik, F.B., Paderborn, D., 1999. Systematic design of crosslinked mechatronic systems, exemplified by a decentralized intersection management, in: Control COnference (ECC). pp. 4531–4536.

Makarem, L., Gillet, D., 2013. Model predictive coordination of autonomous vehicles crossing intersections. IEEE Conference on Intelligent Transportation Systems, Proceedings, ITSC 1799–1804. doi:10.1109/ITSC.2013.6728489

Martínez-Barberá, H., Herrero-Pérez, D., 2014. Multilayer distributed intelligent control of an autonomous car. Transportation Research Part C: Emerging Technologies 39, 94–112. doi:10.1016/j.trc.2013.12.006

Moore, D.N., Schneider, W.H., Savolainen, P.T., Farzaneh, M., 2011. Mixed logit analysis of bicyclist injury severity resulting from motor vehicle crashes at intersection and non-intersection locations. Accident Analysis and Prevention 43, 621–30. doi:10.1016/j.aap.2010.09.015

Mundewadikar, R.S., Dorle, S.S., Keskar, A.G., Chakole, M.B., 2008. Intersection collision detection and warning protocol: design approach. First International Conference on Emerging Trends in Engineering and Technology 869–872. doi:10.1109/ICETET.2008.50

National Highway Traffic Safety Administration, 2015. Traffic Safety Facts 2015: A Compilation of Motor Vehicle Crash Data from the Fatality Analysis Reporting System and the General Estimates System. U.S. Department of Transportation DOT HS 812 384. doi:http://dx.doi.org/10.1016/j.annemergmed.2013.12.004

National Highway Traffic Safety Administration, 2010. Crash factors in intersection-related crashes: an on-scene perspective. doi:http://dx.doi.org/10.1037/e621942011-001

National Highway Traffic Safety Adminstriation, 2012. Traffic Safety Facts 2010 Data.

National Safety Council, 2011. Analysis of intersection fatal and nonfatal crashes from 2005 to 2009.

Naumann, R., Rasche, R., Tacken, J., 1998. Managing autonomous vehicles at intersections. IEEE Intelligent Systems and Their Applications 13, 82–86. doi:10.1109/5254.683216

Neuendorf, N., Bruns, T., 2004. The vehicle platoon controller in the decentralised, autonomous intersection management of vehicles. Proceedings of the IEEE International Conference on Mechatronics, 2004. ICM ’04. 375–380. doi:10.1109/ICMECH.2004.1364468

NHTSA, 2016. U.S. DOT advances deployment of Connected Vehicle Technology to prevent hundreds of thousands of crashes [WWW Document]. URL https://www.nhtsa.gov/press-releases/us-dot-advances-deployment-connected-vehicle-technology-prevent-hundreds-thousands (accessed 7.20.10).

Obeng, K., 2008. Injury severity, vehicle safety features, and intersection crashes. Traffic Injury Prevention 9, 268–76. doi:10.1080/15389580802040311

Onieva, E., Hernandez-Jayo, U., Osaba, E., Perallos, A., Zhang, X., 2015. A multi-objective evolutionary algorithm for the tuning of fuzzy rule bases for uncoordinated intersections in autonomous driving. Information Sciences 321, 14–30. doi:10.1016/j.ins.2015.05.036

Pavlic, T.P., Passino, K.M., 2009. Foraging theory for autonomous vehicle speed choice. Engineering Applications of Artificial Intelligence 22, 482–489. doi:10.1016/j.engappai.2008.10.017

Perronnet, F., Abbas-Turki, A., El Moudni, A., 2013. A sequenced-based protocol to manage autonomous vehicles at isolated intersections. IEEE Conference on Intelligent Transportation Systems, Proceedings, ITSC 1811–1816. doi:10.1109/ITSC.2013.6728491

Planung Transport Verkehr (PTV) AG, 2012. VISSIM - COM Interface Manual.

Poch, M., Mannering, F., 1996. Negative binomial analysis of intersection-accident frequency. Journal of Transportation Engineering 122, 105–113.

Quinlan, M., Au, T.C., Zhu, J., Stiurca, N., Stone, P., 2010. Bringing simulation to life: A mixed reality autonomous intersection. IEEE/RSJ 2010 International Conference on Intelligent Robots and Systems, IROS 2010 - Conference Proceedings 6083–6088. doi:10.1109/IROS.2010.5651993

Retting, R.A., Weinstein, H.B., Solomon, M.G., 2003. Analysis of motor-vehicle crashes at stop signs in four U.S. cities. Journal of Safety Research 34, 485–489. doi:10.1016/j.jsr.2003.05.001

Shahidi, N., Au, T.-C., Stone, P., 2011. Batch reservations in autonomous intersection management, in: 10th International Conference on Autonomous Agents and Multiagent Systems – Innovative Applications Track. Taipei.

Shi, H.H., Chen, H. jin, He, Q., 2015. Optimization algorithm of real-timing signal control for isolated intersections. Advanced Materials Research 1037–1037, 322–326. doi:10.4028/www.scientific.net/AMR.1037.322

Texas A&M Transportation Institute, 2013. 2012 Annual Urban Mobility Report.

Transportation Reserach Board of The National Academies, 2010. Highway Capacity Manual (HCM2010).

U.S. Department of Transportation, 2011. How Connected Vehicle Work.

VanMiddlesworth, M., Dresner, K., Stone, P., 2008. Replacing the stop sign: unmanaged intersection control for autonomous vehicles. International Conference on Autonomous Agents and Multiagent Systems 1413–1416.

Werneke, J., Vollrath, M., 2012. What does the driver look at? The influence of intersection characteristics on attention allocation and driving behavior. Accident Analysis and Prevention 45, 610–9. doi:10.1016/j.aap.2011.09.048

Wu, J., Abbas-turki, A., Moudni, A. El, 2010. Contextualized traffic controlling at isolated urban intersection. The 14th World Multi-Conference on Systemics, Cybernetics and Informatics:

WMSCI.

Wu, Q., Zhang, G., 2016. Formulating alcohol influenced driver injury severities in intersection-related crashes. Transport 1–12. doi:10.3846/16484142.2016.1144221

Wu, Q., Zhang, G., Ci, Y., Wu, L., Tarefder, R.A., Alcántara, A. “Dely,” 2015. Exploratory multinomial Logit model-based driver injury severity analyses for teenage and adult drivers in intersection-related crashes. Traffic Injury Prevention 2014–2015. doi:10.1080/15389588.2015.1100722

Wuthishuwong, C. a, Traechtler, A. a, 2013. Coordination of multiple autonomous intersections by using local neighborhood information. 2013 International Conference on Connected Vehicles and Expo (ICCVE) 48–53. doi:10.1109/ICCVE.2013.2

Wuthishuwong, C., Traechtler, A., 2013. Vehicle to infrastructure based safe trajectory planning for autonomous intersection management. 2013 13th International Conference on ITS Telecommunications, ITST 2013 175–180. doi:10.1109/ITST.2013.6685541

Yan, F., Wu, J., Dridi, M., 2014. A scheduling model and complexity proof for autonomous vehicle sequencing problem at isolated intersections, in: 2014 IEEE International Conference on Service Operations and Logistics, and Informatics (SOLI). pp. 78–83.

Zhang, T., Arrigoni, S., Garozzo, M., Yang, D.-G., Cheli, F., 2016. A lane-level road network model with global continuity. Transportation Research Part C: Emerging Technologies 71, 32–50. doi:10.1016/j.trc.2016.07.003

Zhang, Y., Fu, C., Cheng, S., 2014. Exploring driver injury severity at intersection : an ordered probit analysis. Advances in Mechanical Engineering.

Zhu, F., Ukkusuri, S. V., 2015. A linear programming formulation for autonomous intersection control within a dynamic traffic assignment and connected vehicle environment. Transportation Research Part C: Emerging Technologies 55, 363–378. doi:10.1016/j.trc.2015.01.006

Zohdy, I.H. a, Rakha, H. a. a, 2014. Intersection management via vehicle connectivity: the intersection cooperative adaptive cruise control system concept. Journal of Intelligent Transportation Systems PP, 37–41. doi:10.1080/15472450.2014.889918

Zohdy, I.H., Kamalanathsharma, R.K., Rakha, H., 2012. Intersection management for autonomous vehicles using iCACC. IEEE Conference on Intelligent Transportation Systems, Proceedings, ITSC 1109–1114. doi:10.1109/ITSC.2012.6338827